Master's thesis

NTNU
Norwegian University of Science and Technology
Faculty of Engineering
Department of Structural Engineering

Natalie Megan Malcolmson

Analysis of a post-tensioned slab with concentrated and distributed cables

Master's thesis in MTBYGG
Supervisor: Jan Arve Øverli
March 2023

NTNU
Norwegian University of
Science and Technology

Natalie Megan Malcolmson

Analysis of a post-tensioned slab with concentrated and distributed cables

Master's thesis in MTBYGG
Supervisor: Jan Arve Øverli
March 2023

Norwegian University of Science and Technology
Faculty of Engineering
Department of Structural Engineering

NTNU
Norwegian University of
Science and Technology

Preface

This master thesis marks my final milestone for my 5-year integrated master program for the study civil and environmental engineering at NTNU (Norges teknisk- og naturvitenskapelige universitet), at the department of structural engineering in Trondheim.

The purpose of this master thesis is to raise awareness and knowledge on the advantages of utilizing post-tensioning systems in flat slabs. This master thesis will describe in depth the different aspects of prestressing concrete and the calculation basis involved when dimensioning for a prestressed flat slab. To put the theory in practice, I was provided a building project from Verkís, which is an Icelandic consulting firm, based in Reykjavík. The building project is of an existing parking house, based in laugavegur 86-94. With the initial sketches of the building project, I have attempted at reconstructing the building with a post-tensioned flat slab. The design has been analyzed through the software ADAPT-Builder, which specializes in post-tensioning systems in slabs. Working with this topic in my masters has enabled me to have a better understanding of the benefits of prestressed slabs, in addition to strengthen my knowledge in how to perform analysis of- and calculate on post-tensioned flat slabs.

I want to personally thank my mentor Jan Arve Øverli, for guidance in executing this master thesis. Furthermore, I would also thank Joanne Webb from RISA Tech. for allowing me to borrow a license for the software ADAPT-Builder, so that I can perform a proper analysis of my design. Lastly, I would like to thank Magnús Skúlason at Verkís, for providing me with a building project so that I am able to have a practical application of this topic in my master thesis.

Abstract

This report addresses the advantages of utilizing tensioning systems within a slab. It will describe the mechanics behind the tensioning systems, what equipment is used, the different types of losses in relation to tensioning and much more. It will also address the calculation principles that are in line with the appropriate standards. This will give the reader a better understanding as to how to appropriately calculate on a slab with tensioning systems.

The report will also provide an appropriate example on a post-tensioned system within a slab. This is to prove the stated benefits of tensioned systems, and to give the reader a practical understanding of how the execution of tensioned systems within a slab can be performed. The example is a project originally provided by Verkís, an Icelandic consulting firm for building engineers. The project was adjusted to fit with the theme of the master, thereby redesigning it to a slab with uniform thickness.

The project was executed in a software called ADAPT-Builder. The report will therefore also give appropriate explanations as to how it can be modelled and checked for within the program. It will also give explanations as to why the calculations in the program would deviate from the hand-calculations if present.

The results will show that the solution of my design is in line with certain benefits that are stated for the tensioning systems within a slab. This is for instance the ability to have larger span lengths and low deflection. Since this is the first time that I have tried at modelling and calculating for a structure with tensioning systems, I realize there is also room for improvement within my design. The report therefore also addresses the different areas for improvement, and how that would underline the benefits of tensioned systems within slab further.

Sammendrag

Denne rapporten tar for seg de ulike fordelene av å bruke spennarmering i et flatdekke. Rapporten vil forklare de ulike mekanismene, hvilke utstyr som er relevant, ulike former for tap i forbindelse med spennarmering og mye mer. Oppgaven vil også ta for seg de ulike beregningsprosedyrene som er relevant fra de ulike standardene. Dette vil gi leseren en bedre forståelse for hvordan man kan beregne på et spennarmert flatdekke på riktig måte.

Rapporten vil også gi et passende eksempel på et etteroppspent flatdekke. Hensikten er å understreke de nevnte fordelene ved å benytte seg av spennarmering, og å gi leseren en bedre praktisk forståelse av hvordan en kan utføre spennarmering i et flatdekke. Eksempelet stammer fra et prosjekt som var gitt av Verkís, et islandsk konsulentfirma for bygg ingeniører. Prosjektet var justert slik at det passer med temaet av masteren, ved å endre modellen til å ha et flatdekke med uniform tykkelse.

Prosjektet var utført I et program som heter ADAPT-Builder. Rapporten vil derfor også gi forklaringer til hvordan man kan modellere og sjekke for beregninger i programmet. Dersom håndberegningene og beregningene fra programmet avviker, er det gitt mulige forklaringer til hva som kan være årsaken for dette.

Resultatene vil vise at løsningen på eksempelet bekrefter enkelte av de nevnte fordelene for spennarmering i flatdekke. Dette er blant annet egenskapen til å ha lengre spennvidder og lav nedbøyning. Ettersom dette er første forsøk på å modellere og beregne for en konstruksjon med spennarmering, innser jeg også at det finnes rom for forbedringer innenfor mitt design. Rapporten vil derfor også gjennomgå de ulike aspektene ved mitt design som kunne vært forbedret, og hvordan det ville ha fremhevet fordelene med spennarmering i flatdekke enda mer.

Innhold

1 Introduction

The purpose of this master task is to raise awareness and knowledge on the advantages of utilizing post-tensioning systems in flat slabs. Post-tensioning systems are becoming more popular, as it both has environmental and mechanical benefits in comparison to the use of only regular reinforcement. To put the theoretical knowledge in practice, I decided to do an analysis of a PT-reinforced flat slab. The original plan sketches for the building, loading and coverage was given to me by Verkís, an Icelandic consulting firm based in Reykjavík. By designing a solution for a PT-reinforced flat slab, I am able to compare my solution to what is considered common practice for non-stressed slabs, and also prove the beneficial statements given when using PT-reinforcement. The in-depth analysis also gives me the opportunity to give proper guidance on how it is possible to design and calculate for PT-reinforced slabs, and what is perceived as practical choices when executing a typical design of PT flat slabs. Lastly, the analysis is performed in ADAPT-Builder. This is an optimal program for analyzing PT reinforced slabs. The master will therefore also give insight to the software, how it works and how to perform the analysis in the software. It will therefore also provide you information in how to utilize an appropriate specialized software for PT slabs.

The 2nd chapter will explain the theoretical views on the different types of prestressing. Why is it considered advantageous in comparison to non-stressed, how does the prestressing function and what types of prestressing exists. It will also explain the practical execution of the prestressing. What choice of concrete is recommended, what types of layout of the prestressing is utilized and what equipment are relevant for prestressing practices. The 3rd chapter contains the general calculation principles that should be followed when designing for a PT slab. This includes both recommendations given by professors at NTNU, and relevant criteria by EC2 which needs to be followed. The 4th chapter is the explanation of the building project and the execution of the PT slab in ADAPT-Builder. It will therefore explain the reasoning for the choice of design, and explain the results from ADAPT-Builder to that of my hand calculated ones. Lastly 5th and 6th chapter concludes and discusses the premises on how the program works, and how my solution has proven to be beneficial in comparison to non-stressed slabs. In addition, it also explains further optimizations to my solution, which would highlight the benefits of utilizing PT over regular reinforcement even further. The appendix gives the hand calculation, various reports from ADAPT-Builder and a summary of the geometry from the initial building project provided by Verkís.

2. Theory

The purpose of this section is to give an introduction of the important aspects within prestressed concrete. This is to provide the reader with necessary background information to understand why stressed concrete is dimensioned and calculated accordingly to chapter 2; “Calculation & dimensioning principles”. Furthermore, this chapter will give an overview over different available practices within prestressed concrete, why and how it is applied on different building projects. All the theory described below is in accord with the European standard EC2. Any explanations of common practices or choices is in accord with the typical Norwegian practices.

2.1 Concrete

Concrete is commonly strong in compression but weak in tension. The tensile strength is approximately 10% of its compressive strength. Hence, it is common to reinforce concrete with steel so the reinforcement will carry the tension that is developed due to the applied loadings (Bhatt, 2011).

For constructions with tensioned reinforcement, it is common to utilize concrete types with a higher strength as they have better deformational properties. Having better deformational properties is an important aspect for prestressed members, as it influences how much of the prestress force is retained in the long term (Bhatt, 2011). Furthermore, higher strength concrete is required as prestressing introduces early compression stresses within the concrete that it must sustain, in comparison to non-stressed members.

2.2 Prestressing

Prestressed concrete can be defined as compressed concrete, affected by applied stress from reinforcement. The purpose of such a process is to eliminate the consequences of the external forces applied onto a concrete element. These pressures within the compressed concrete are the responsive behavior to when tensioned reinforcement is introduced within the concrete element. Since the reinforcement is in tension, it will attempt to stabilize back into no stress, thereby afflicting the connected concrete with compression. This is both due to the presence of friction between concrete and tensioned reinforcement and mainly due to the fastenings at each end of the tensioned reinforcement (Sørensen, 2013).

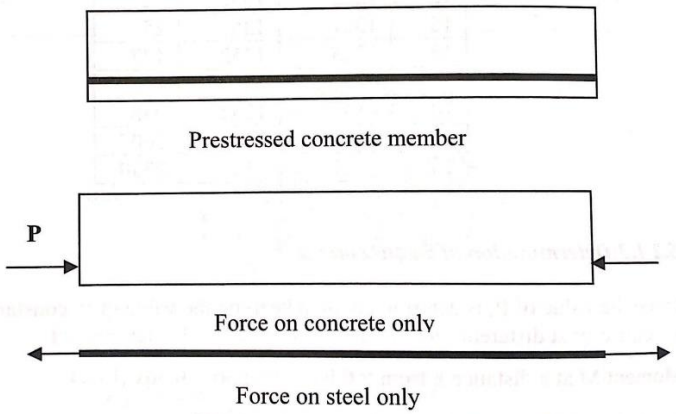

Figure 2.1: *Loading due to tensioning of reinforcement (Bhatt, 2011)*

The biggest asset by introducing tensioned reinforcement, is how it lowers the predicted deflection of element due to the presence of its external forces. It will also subsequently lower the tensile stress within the concrete, which is beneficial as concrete has a high compression strength and low tensile strength. Idealistically, the reinforcement would be positioned in similar pattern to predicted moment diagram by the external loading on the element. This is since the point at maximum momentum will also be the point of highest tensile stress within the concrete profile. When the stressed reinforcement profile is positioned with an eccentricity to the gravity line, it causes a moment within the concrete that, if designed correctly, will be in opposite direction to the moments caused by external forces, thereby leading to less deflections and less tension within the concrete member. This is defined as load-balancing, where the loading from the tendons counteracts the loading from self-weight and live load (Sørensen, 2013).

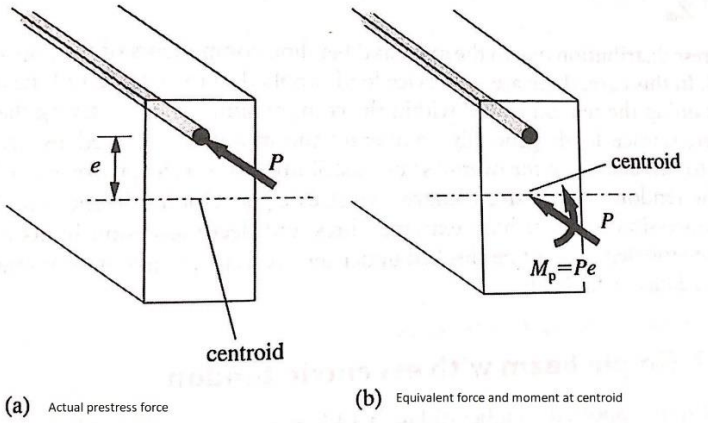

Figure 1.2: *Equivalent loading at center of gravity axis for concrete (Obrien, Dixon, & Shiels, 2012)*

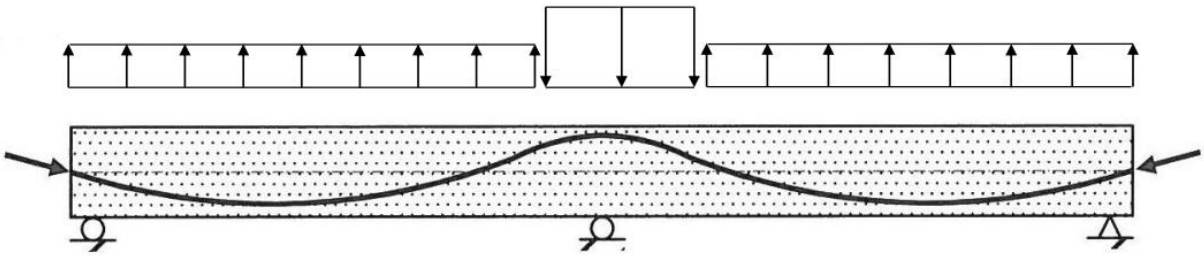

Figure 2.3: *Tendon profile and its equivalent loads to counteract predicted moment-diagram generated by external loading (Øverli, 2022)*

Figure 2.3 illustrates a possible tendon profile and its equivalent load from prestressing. This is a valid tendon profile for a beam that is expected to have loading which will produce moment in opposite direction, thereby eliminating the moment and stresses applied on the beam. This is for instance, deadweight. However, in practice it is more common to orient the tendons as static over field segments, and parabolic over supports. This is since it is deemed easier to assemble, and secondly it has proven to have a favorable effect all things considered (Trygstad, Generelt om spennarmeringens fortrinn, 2022). In essence, such an assembly manages to reduce the moments over the supports, which is in most cases the area with the critical moment loading over its construction element (Øverli, 2022).

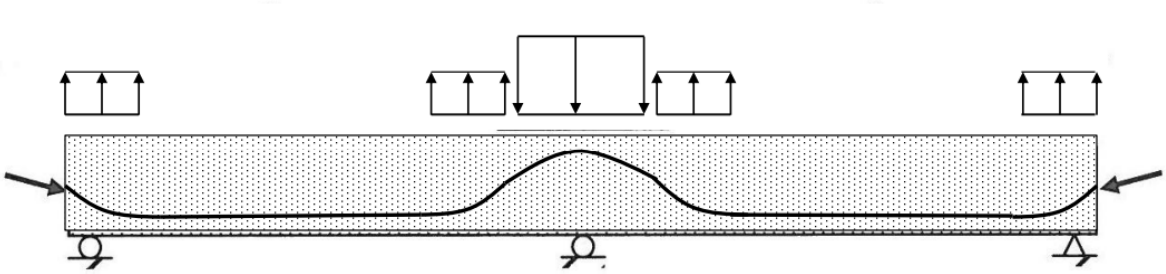

Figure 2.4: *Practical assembly of tendon profile (Øverli, 2022)*

However, producing a stressed reinforcement profile mimicking the moment-diagram of the member can be difficult to accomplish accurately for all different processes of stressed members. For pre-tensioning, the reinforcement is stressed without the use of ducts, and the level of tension stress within each wire makes it hard to create any form of profile than a straight profile. However, this practice is achievable and more common for post-tensioned concrete. Since the reinforcement is placed within strong ducts, it is possible to manufacture ducts that will mimic the pattern of deflection, forcing the tensioned reinforcement into same profile as the ducts. It is therefore a common practice for post-tensioned members.

Another advantage of utilizing tensioned reinforcement is how the decrease in deflection leads also to less cracks (Sørensen, 2013). This is advantageous in terms of durability, as the presence of cracks can expose reinforcement to possible corrosive chemicals. Especially in the case of car parks, crack-free slabs limit the damage due to seepage of water with de-icing salts from melting snow (Bhatt, 2011). Furthermore, prestressing members have shown to increase capacity of member within shear, torsion and punching shear (Øverli, 2022). Lastly, introducing tensioning in reinforcement leads to reduced amount of reinforcement necessary to be in accord with Eurocode criteria. This is advantageous in relation to the economical aspect of a building project (Trygstad, Generelt om spennarmeringens fortrinn, 2022).

2.3 Tensioned Reinforcement

When designing a structure with tensioned tendons, it is highly necessary to utilize reinforcement with higher strength than commonly used for un-tensioned reinforcement. The main reason for this is how the tensioned reinforcement will over time loose its tensions due to short-term and long-term effects such as creep, shrinkage and relaxation (Sørensen, 2013). The loss of tension becomes less of importance if the choice of tendons has a high strength. The production of tensioned tendons is therefore produced with the aim of having a high strength. This is often achieved by cold-drawn high strength wires or high-strength alloy steel bars. High strength steel wires are by far the most used material for prestressing and will therefore be addressed here.

High strength steel wires do not generally have sufficient strength to be used singly for prestressing purposes. Tensioned wires are produced each as one thread of 4-5mm diameter. Each wire will subsequently be intertwined to form a strand. Most manufacturers provide strands which constitutes about 7 wires, but 5-wired strands and 19-wired strands is also available. For post-tensioned concrete, it is common to utilize multiple strands further intertwined, forming what we denote as a cable or tendon. A complete tendon can consist of how many strands are needed to carry the desired tension level (Obrien, Dixon, & Shiels, 2012).

Figure 2.5A: *A strand consisting of 7 wires intertwined (Obrien, Dixon, & Shiels, 2012)*

Figure 2.5B: *Anchorage and duct for post-tensioned system to support a tendon consisting of 19 strands (Trygstad, Generelt om spennarmeringens fortrinn, 2022)*

We have two main categories within tensioned reinforcement, denoted as pre-tensioned- and post-tensioned reinforcement. The difference between the two is whether the tensioning of the reinforcement is applied before or after the casting of the concrete (Sørensen, 2013).

2.3.1 Prestressing Equipment

The tensioning of steel reinforcement is achieved for prestressed members by mechanical jacking using hydraulic jacks. The force applied from the jack is recalculated as hydraulic pressure and monitored on the equipment (Kalland, 2022). Since pretensioned members often utilize strands over tendons, each strand is stressed individually using smaller jacks. However, in post-tensioned members, as it consists of several strands within each duct, common practice is to use a bigger jack that can stress multiple strands simultaneously (Obrien, Dixon, & Shiels, 2012).

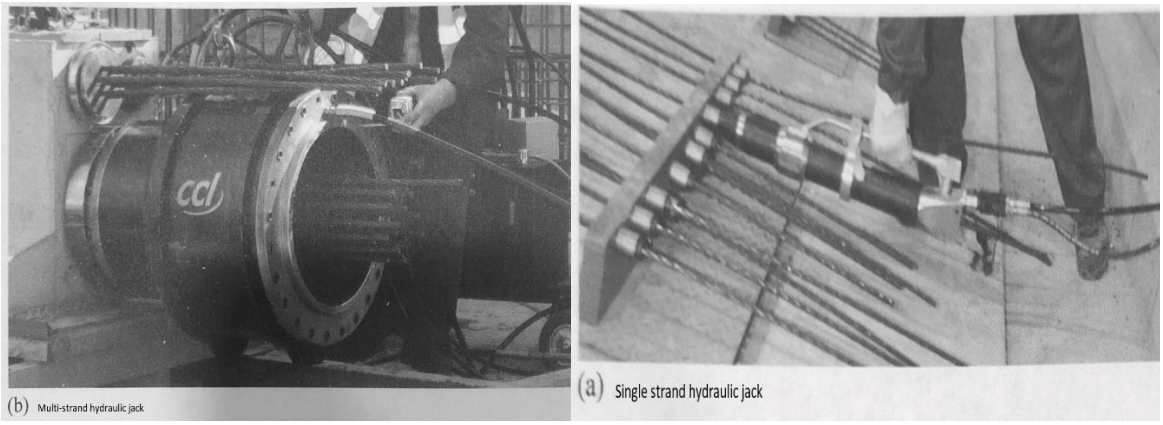

Figure 2.6: *multi-strand hydraulic jack & single-strand jack (Obrien, Dixon, & Shiels, 2012)*

Both post-tensioning and pre-tensioning processes require at certain phases, a support-system to hold- and strain strands in tension. Commonly used anchorage system for pre-tensioned members is the wedge grip, with the purpose of holding the strands in tension before the release. This is also a system applied onto post-tensioning members, where the cables are stressed from this end only. At the passive end, the cables are anchored using “basket-type dead-end” anchors. It is also possible for post-tensioned members to have buried anchors. This requires that the cables are placed before the concrete is casted. When utilizing one active anchor end and one passive end for post-tensioned members, it is often typical that such members have cables with length less than 50 m and flat tendon profiles. In other cases, it is more common to have two active ends, in other words, two anchors at each end that applies stress to the cables (Bhatt, 2011).

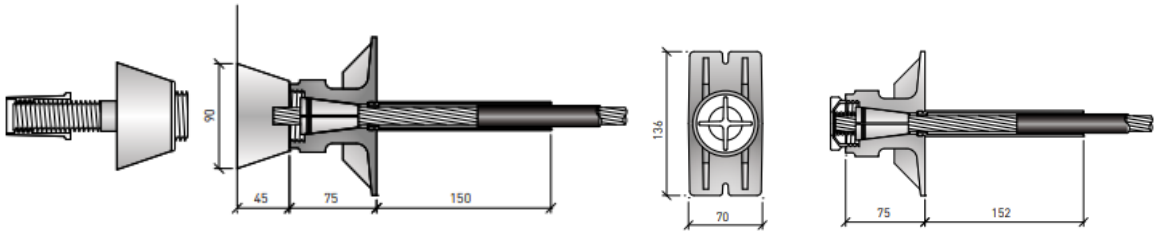

Figure 2.7: *Anchorage system for a smaller number of strands (Spennteknikk, 2022)*

Active anchorage

Passive anchorage

Ducts utilized for post-tensioned members are either metal ducts of 0.25 mm wall thickness or corrugated high density polyethylene (HDPE) ducts of about 3-6 mm wall thickness. It is important that the duct is strong enough to withstand pressure during grouting and prevent distortion during casting of concrete. For post-tensioning, the cables within the ducts can either be pushed through the ducts or pulled through using a winch (Bhatt, 2011). For particularly longer construction members, it will be a question how to enable prestressing for cables through construction joints. This is where we introduce couplers.

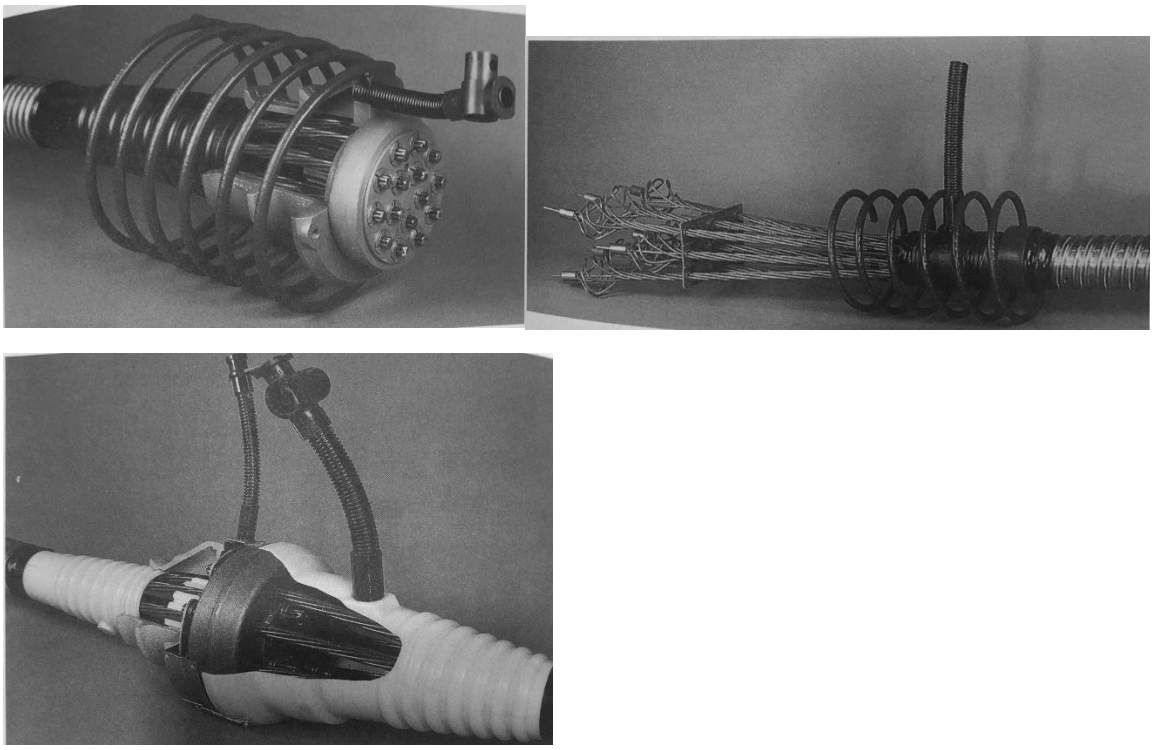

Figure 2.8: *Equipment for Post-tensioned system (Bhatt, 2011)*

Top left; Active end anchorage

Bottom left; coupler

Right; passive end anchorage.

2.3.2 Pre-Tensioned Reinforcement

Pre-tensioned concrete elements are largely produced in factories as it requires utilization of quite advanced machineries. The pre-tensioning process involves roughly three basic stages. Steel strands will firstly be placed in a casting bed and subsequently stresses to its desired level and thereby anchored between its two supports. Next stage involves the casting of the concrete onto the casting bed, allowing the concrete to set over a certain time. When the concrete has attained sufficient compressive strength, the strands are released from the supports (Obrien, Dixon, & Shiels, 2012). As the strands are released, they will attempt to contract to neutralize the tension stress, thereby compressing the casted concrete. This is functional as the strands are directly casted inside the concrete, forming an adequate bond between concrete to reinforcement. Furthermore, as the strands are stretched, they will reduce in diameter. As the strands are cut and the concrete has stiffened, the strands will try to regain its original diameter, thereby introducing additional frictional forces. This is denoted as the Hoyer effect (Bhatt, 2011). As a result of this, there is no need for anchoring the ends of the concrete members after the concrete has stiffened and strands are cut.

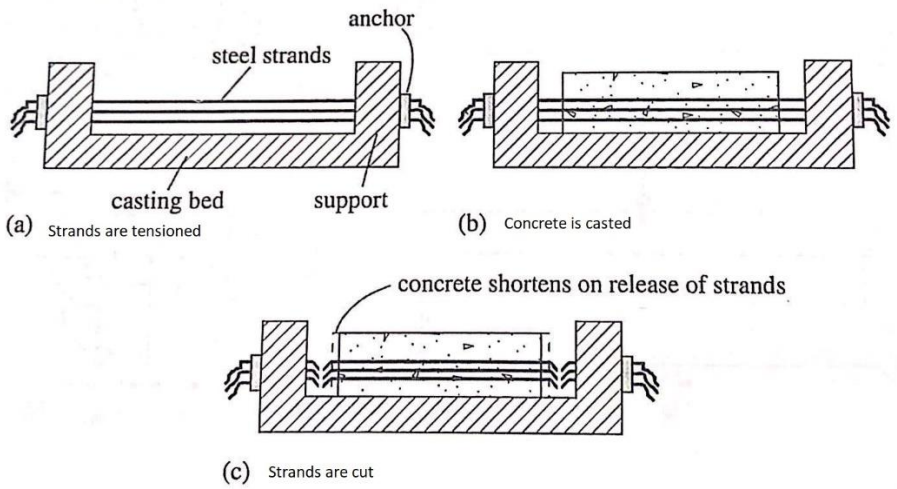

Figure 2.2: *pre-tensioning process (Obrien, Dixon, & Shiels, 2012)*

As mentioned before, this process makes it difficult to create a tendon profile for the strands, so the tendon profile is often in a straight line. If all the strands are tensioned with the same stress, the member can experience serious cracking at the top face by supports. This applies for instance a simply supported member with a uniform loading. A possible solution would be to wrap some of the strands in plastic tubing towards the supports, so the bond between steel and concrete is prevented, thereby making those strands inactive over its covered length. This method is denoted as debonding or blanketing of cables. In this way, we vary the total prestressing force over the different cross sections (Bhatt, 2011).

In some cases, pre-tensioned slabs are designed with a certain tendon profile, by pulling down the strands at specific points. We denote this process as deflecting, draping or harping of strands. Although this is a less preferred method than debonding (Bhatt, 2011).

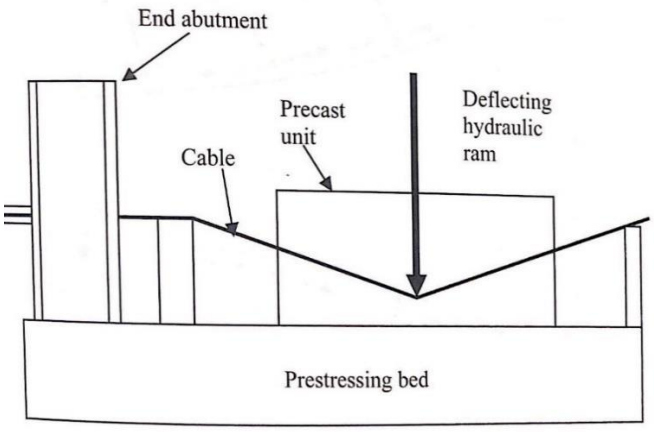

Figure 2.3: *Harping/Draping of strands (Bhatt, 2011)*

2.3.3 Post-Tensioned Reinforcement

Post-tensioning of members is the most common method to utilize in situations where concrete needs to be casted in-situ as it does not require a casting bed. To tension the reinforcement after casting the concrete, it is necessary to firstly cast the concrete around a hollow duct. After the concrete has set, a tendon consisting of several strands will be pushed through the duct. The tendon will subsequently be jacked from either one or both ends using hydraulic jacks, thereby functioning in same manner as the pre-tensioned reinforcement. Unlike pre-tensioned reinforcement, the strands will not be cut by the supports but rather anchored at ends.

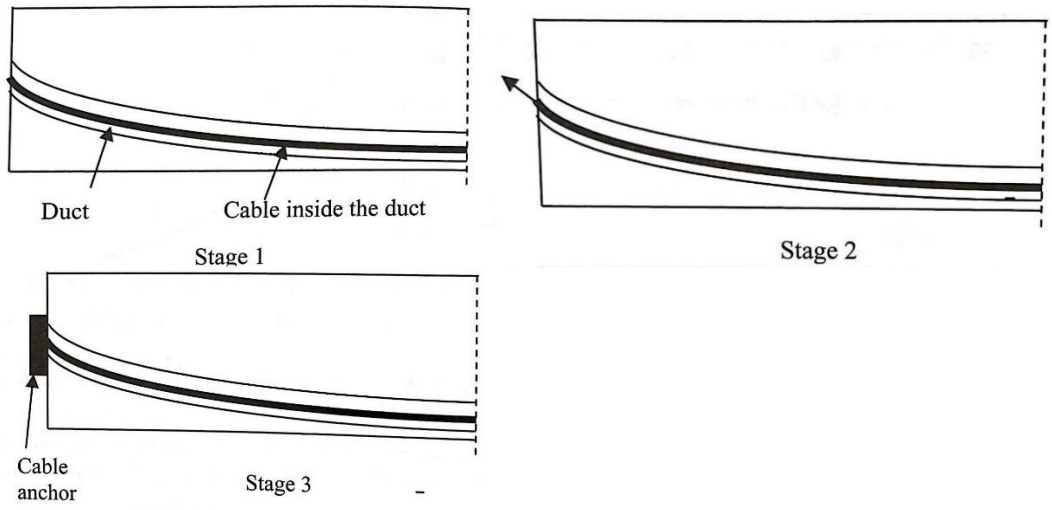

Figure 2.4: *simplified procedure for post-tensioned system (Bhatt, 2011)*

Ducts can be filled with grout which forms a bond between the strands and the concrete. Grouted post-tensioned members are often denoted as bonded construction compared to an un-grouted duct. This will provide a connection between the strands to the concrete, so the concrete compression is not solely based upon the pressure from the anchorages. Furthermore, grout is utilized as means to prevent corrosion of the strands. The variety of the tendon profile within the concrete members will also help to establish a higher friction between concrete to reinforcement (Obrien, Dixon, & Shiels, 2012). This means that if a segment of the cable is damaged, the loss of capacity is kept locally to the damaged segment. Bonded systems are typical in bridges and beams (Kalland, 2022).

There is also the possibility of manufacturing post-tensioned members without grout, denoted as unbonded systems. In these systems, cables are encased in a greased plastic tube. The advantage of an unbonded system is the time management, as the grouting procedure is quite time consuming. In

this case, the tendons are kept in tension only by the end anchorages. In essence, damaging a segment leads to loss of full tension throughout that cable (Kalland, 2022). The unbonded system is extensively used in the construction of prestressing slabs (Bhatt, 2011).

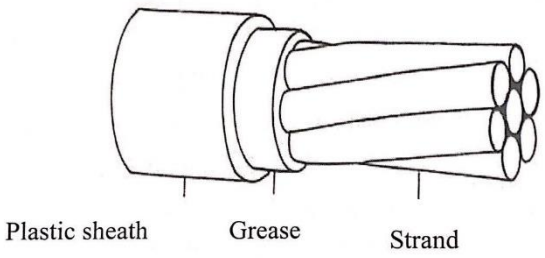

Figure 2.5A: *Unbonded cable* (Bhatt, 2011)

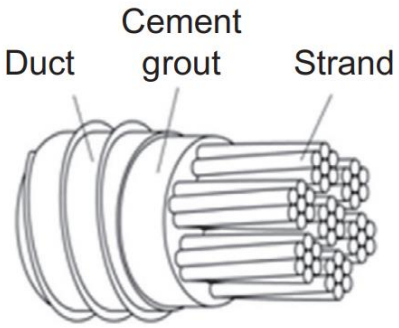

Figure 2.12B: *Bonded cable* (Balázs, Farkas, & Kovács, 2016)

2.4 Tension losses

There are many reasons as to why the applied tension in the tendons is not of same magnitude that can be observed within the member. Nor is the tension level uniform along the length of the member. Since it is so common to expect a loss of tension, it is vital to consider a certain loss of tension so the calculations can be conservative with respect to the losses. In this way, we can either adjust initial prestress force with regards to some of the expected losses or ensure a more realistic analysis of the member. In the case where tension losses are not considered, it will influence the capacity of the construction and stresses within the concrete, in addition to cracks and deformations within serviceability limit state (Øverli, 2022).

Since tension losses are inevitable, it is important to assess the different types of tension losses that can take place. We can divide the different types within two main categories: immediate losses and time-dependent losses. The division between the two lies in whether the type of tension loss happens during the prestressing process or over a longer period.

2.4.1 Immediate losses

Friction loss:

Friction losses occurs more commonly in post-tensioned members where the tendons are lying within ducts. We can denote two main causes for friction losses:

1. Friction loss due to the curvature of the tendon profile

2. Friction loss due to deviation of initial curvature of ducts denoted as “wobble”

When we jack tendons with a prestressing force, the tendons will tighten but simultaneously resist the jacking force due to the friction of the curvature along the tendon’s length. Roughly speaking, we consider the magnitude of tension loss due to friction greater when the curvature is greater (Sørensen, 2013). We can therefore find a direct correlation between the distance from jack and the change in angle. Thus, in a situation where the tendons have multiple curvatures between stressed jack to the point of evaluation, the corresponding loss is greater as the changes in angle are additive (Obrien, Dixon, & Shiels, 2012).

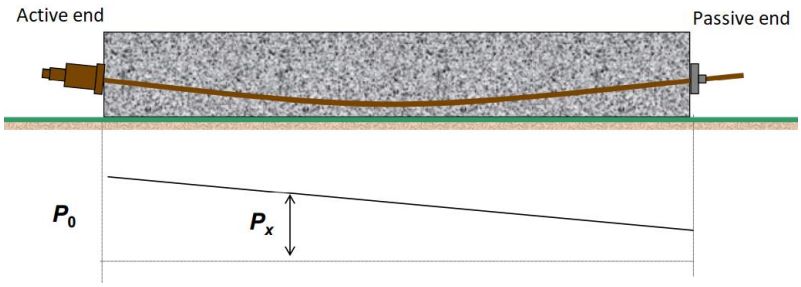

Figure 2.13: *simplification of tension loss due to curvature along length of tendon (Øverli, 2022)*

In theory, the change in prestressing force will diminish if length of tendon is infinite due to friction loss based on curvature of tendon. Remedies to this is therefore to apply active anchorages on both ends on a tendon. Alternatively, adjust the prestress force based on knowledge of the predicted loss, and subsequently slack the prestress force. It is also possible to increase number of prestressing tendons, which will have the same means of adjusting the prestressed force such as in previous mentioned remedy (Øverli, 2022).

Unintentional wobble arises due to flaws in the assembly of the duct system within the slabs. A common flaw is that ducts and anchorages dispositions due to the pressure of casting concrete. Furthermore, it can be assumed that the cables will be dispositioned due to workers tripping on the cables on worksite (Kalland, 2022). Unintentional wobble is therefore considered through a constant k that depends on amongst other things: workmanship and degree of vibration, during the production of the prestressed slab. For post-tensioned tendons in unbonded systems, the friction losses are notably smaller.

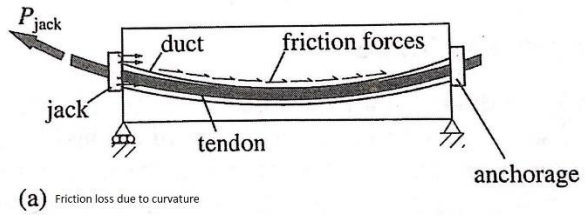

Figure 2.14A: *Friction loss due to curvature* (Obrien, Dixon, & Shiels, 2012)

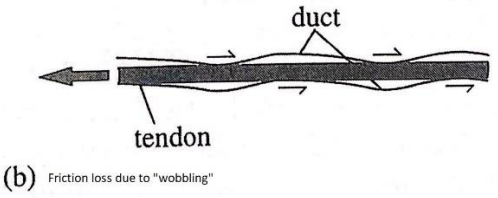

Figure 2.14B: *Friction loss due to "wobbling" (Obrien, Dixon, & Shiels, 2012)*

Draw-in loss:

Draw-in loss is the expected loss for post-tensioned members when strands go from being stressed by the jack to being held by the anchorages. Since strands are stressed in tension, it will naturally try to contract, and by releasing the jack sustaining the tension, a natural slippage of strands happens before the strands are anchored. The slippage leads to a loss of initial prestress force by jacking. For bonded post-tensioned members, the friction between ducts and tendons will prevent the loss of stress to proceed along the strand's entire length. This leads to a somewhat local loss of stress around the area of the anchorages (Obrien, Dixon, & Shiels, 2012).

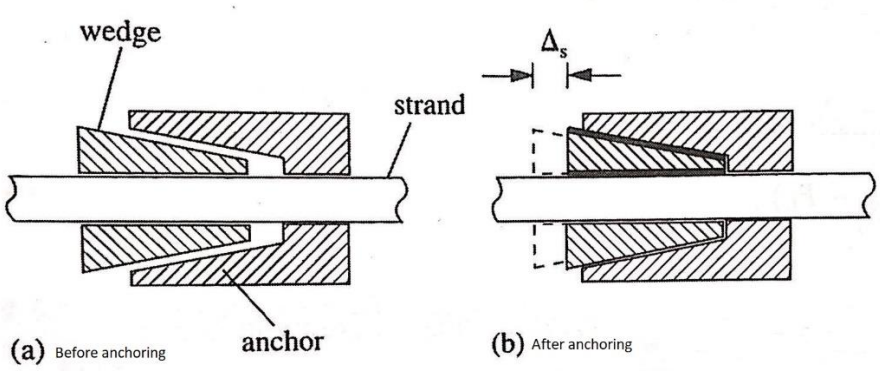

Figure 2.6: *Illustration of tension loss due to shortening* Δ_S *(Obrien, Dixon, & Shiels, 2012)*

Elastic deformation loss due to temperature change:

This type of loss is particularly applicable for pre-tensioned members. As the pre-tensioned process stress the strands before the casting of concrete, the steel will experience a change of temperature. This is in relation with the number of chemical reactions that concrete undergoes as it is hardening to its optimal strength, thereby also heating the connected strands within the member. The expansion due to heat development often occurs at a point in the hardening stage of concrete where the bond between steel and concrete is yet to be set. This leads to a loss in stress as the strands can deform due to temperature change, thereby lessening the initial prestress force. In the later stage of the

casting, temperature of concrete will reduce as a response to less chemical reactions within the concrete. But at the point of heat reduction, the bond is set and the change in stress leads to a permanent prestress loss (Sørensen, 2013).

Elastic deformation loss due to stressing tendons:

As the tension within cables are transferred into compressive stresses onto the concrete member, it is logical to assume that the concrete member undergoes an elastic deformation. The compression of the concrete member reduces the length of the member, which in return may slack the strands and therefore lead to a loss of prestress force. This loss is considered an immediate loss as the magnitude of the jacking force applied is never, at any point in time, similar to the prestress force applied to the concrete by the cables (Obrien, Dixon, & Shiels, 2012).

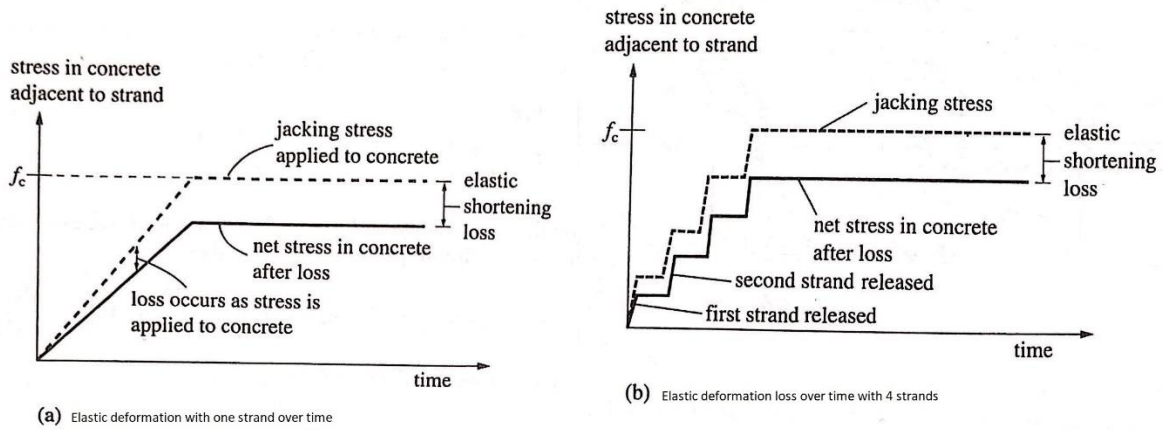

Figure 2.7: *Elastic deformation loss due to transfer of stresses (Obrien, Dixon, & Shiels, 2012)*

Elastic deformation losses are important to evaluate for pre-tensioned members but not for post-tensioned members in which all strands are strained simultaneously. This is because the post-tensioning process can restress the tendons to compensate for the loss of tension due to the shortening of concrete. In the case of pre-tensioned members, the bonding between stressed strands and concrete is already set by the time the loss applies (Obrien, Dixon, & Shiels, 2012). However, if the post-tensioning system stresses strands individually, elastic deformation losses occur. Stressing an individual strand to compensate for elastic deformation loss, and subsequently stressing another leads to loss of prestress in initial strand since the stressing of second strand causes additional shortening of concrete member, thereby causing slacking of initial strand.

2.4.2 Time-dependent losses

Creep:

Like any other material, when applying loading onto a member, the member will experience an instant deflection. What separates concrete from other materials is that over time, this displacement gradually increases with time. This is what we call a long-term effect denoted as creep. It is the case that the displacement of the member can reach a value as large as three to four times than that of immediate elastic deformation. Creep can be defined as the increase of strain under constant stress. This is a non-reversible deformation, which means that part of the deflection during stress will be permanent deflection during unloading scenarios as well. The effect creep has on the concrete's strain is tied to its content. A general rule states that an increase in water/cement ratio or an increase in cement content increases creep. However, increasing aggregate content has opposite effect (Bhatt, 2011).

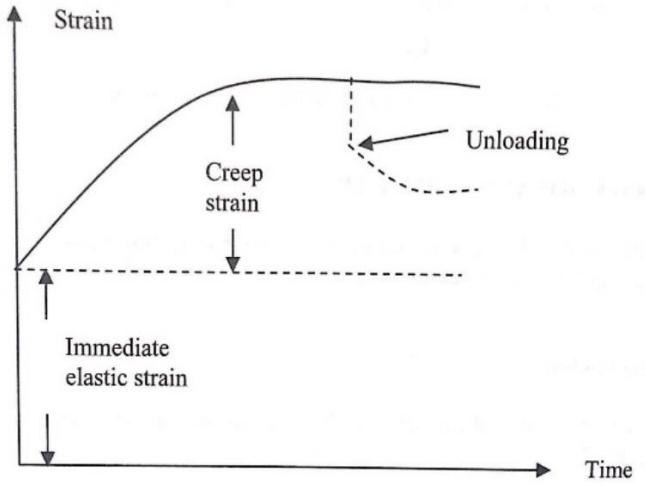

Figure 2.8: *Strain development over time, permanent strain after unloading (Bhatt, 2011)*

Shrinkage:

When it comes to shrinkage, we have three different types of shrinkage, denoted plastic shrinkage, autogenous shrinkage, and drying shrinkage. Plastic shrinkage occurs when concrete is in fresh phase. In other words, during the early stiffening in its mold. Plastic shrinkage occurs when water evaporates from the concrete's surface faster than the time water within the concrete can replace the evaporation. This will result in an under-pressure of water which will subsequently lead to contraction of surrounding particles (Jacobsen, 2022).

Autogenous shrinkage is the concrete's self-induced shrinkage and is highly dependent on the concrete's content. In essence, the chemical reaction results in a loss of volume as the reactants fills a greater volume than its reaction product (Jacobsen, 2022).

Drying shrinkage occurs in the phase where the concrete is hardened. This is related to the humidity of the air in which the concrete lies. In the case of dry air, the water content within the concrete will be removed by time by evaporation. This will initially start at the exposed surface and work inwards on the concrete element. In essence, it has the same reaction as the plastic shrinkage, whereas under-pressure and capillary stresses causes the concrete to contract (Jacobsen, 2022).

Relaxation:

In similar pattern as concrete, steel reinforcement exhibits relaxation. If the strain is maintained constant, which is the case for stressed reinforcement, the stress required to maintain this strain reduces over time. This means the stressed tendons within prestressed members undergoes a loss of prestress force over time.

Time-dependent losses due to creep, shrinkage of concrete and relaxation of the steel reinforcement can be as high as 25% of the initial stress applied (Bhatt, 2011).

2.4.3 Losses in relation to pre- & post-tensioned systems:

Pre-tensioning systems suffer immediate losses from elastic shortening or elastic deformation of the concrete. For post-tensioning systems, sources for immediate losses originates from elastic deformation, draw-in losses at anchorages and friction losses in the presence of ducts. However, both post- and pretensioned systems suffer from the same time-depending losses: relaxation of steel, creep and shrinkage of concrete (Obrien, Dixon, & Shiels, 2012).

2.5 Slabs

2.5.1 Flat slabs

There are several types of slabs in concrete dimensioning. What they have in common is that they are all regarded as a concrete plate. What separates flat slabs from other types of slabs is the existence of columns supporting the plate without the presence of beams (Norsk betongforening, 2022).

Typical design of a flat slabs contains a maximum span length up to $7{,}2\ m$ between each column. Designing a flat slab with larger spans have in some cases caused too large deflections. Then the matter of the overall thickness of slab becomes important to establish appropriate deflections during SLS (NTNU - Department of structural engineering, 2021). It is recommended a thickness of the slab equivalent to $\frac{L}{25}$ for designing a flat slab with normal live loads and spans under $7{,}2\ m$. For situations

where the spans are much smaller than $7{,}2\ m$, the minimum slab thickness of $\frac{L}{30}$ is an appropriate dimension (NTNU - Department of structural engineering, 2021). When there is high loading, it should be considered to have higher thickness of slab than these recommended values, as deflection varies both with loading and dimensions of constructions. A flat slab is characterized by having a uniform thickness. The advantage of a flat slab is that the formwork of producing a flat slab in contrast to other types is simple (Bhatt, 2011).

2.5.2 Drop panel & column capitals

Depending on the design, loading and geometric dimensions of the columns and flat slab, enhancement of the columns might be necessary. Because the load transfers from the slab down through the columns, the shear stresses around the column tend to be very high (Bhatt, 2011). If it is needed to have a rather thinner thickness to the flat slab, it might be necessary to include larger thickness around the connection of the columns to the flat slab. This is to provide sufficient capacity for punching shear resistance. An alternative is to have an addition of reinforcement locally around columns without any enhancements. Enhancements of slabs are commonly the 3 following; column head, drop panel or drop panel with column head.

Drop panel is an addition of thickness of the flat slab around the area of the columns. Column head, also denoted as capital, is an extension of the cross section of the columns connecting to the flat slab. Column head and drop panel provide the same functions, to increase local shear capacity around the columns. Sometimes it is necessary to introduce enhancement purely since the necessary amount of reinforcement locally around columns exceeds the available thickness spacing of the slab, thereby forcing to introduce enhancements locally around columns to reduce needed reinforcement and give a larger area for the layout of reinforcement. Alternatively, it is needed to increase the uniform thickness of the slab.

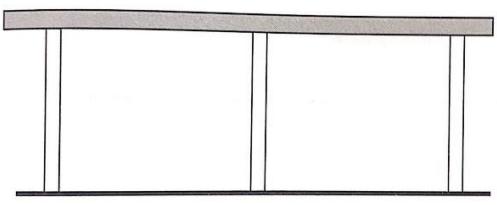

Figure 2.9A: *Flatslab without enhancements* (Sørensen, 2013)

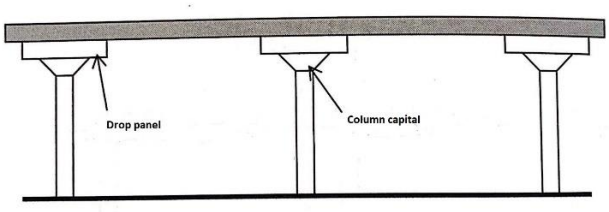

Figure 2.18B*: Flatslab with drop panel & column capital* (Sørensen, 2013)

2.5.3 Tensioned flat slabs

Since tensioned reinforcement contributes to eliminate deflections caused by external forces, it is a valid option within the construction of flat slabs. When designing a flat slab with tensioned reinforcement, we enable the construction to have larger spans between each column as deflection often is a deciding factor that restricts the dimensioning of the structure. This means we could design a flat slab with fewer columns or have more room in choosing the layout of the columns. Another advantage is how prestressed slabs enables the possibility of designing a slab with smaller thickness than otherwise, as deflection is originally lower due to presence of prestressing.

There are several ways to design the layout of the pre-/post-stressed tendons, each with their own advantages. For practical reasons, laying tendons as fully banded in both directions is the simplest approach (Sørensen, 2013). However, the common practice is to design the layout of tendons as fully banded in one direction and evenly distributed in another. Apart from previous mentioned layout, this layout generally minimizes the amount of weaving of tendons and is a simplified laying procedure in comparison to others (Bhatt, 2011). It is further common to lay the fully banded tendons first, then weave the evenly distributed tendons subsequently (Trygstad, Generelt om spennarmeringens fortrinn, 2022).

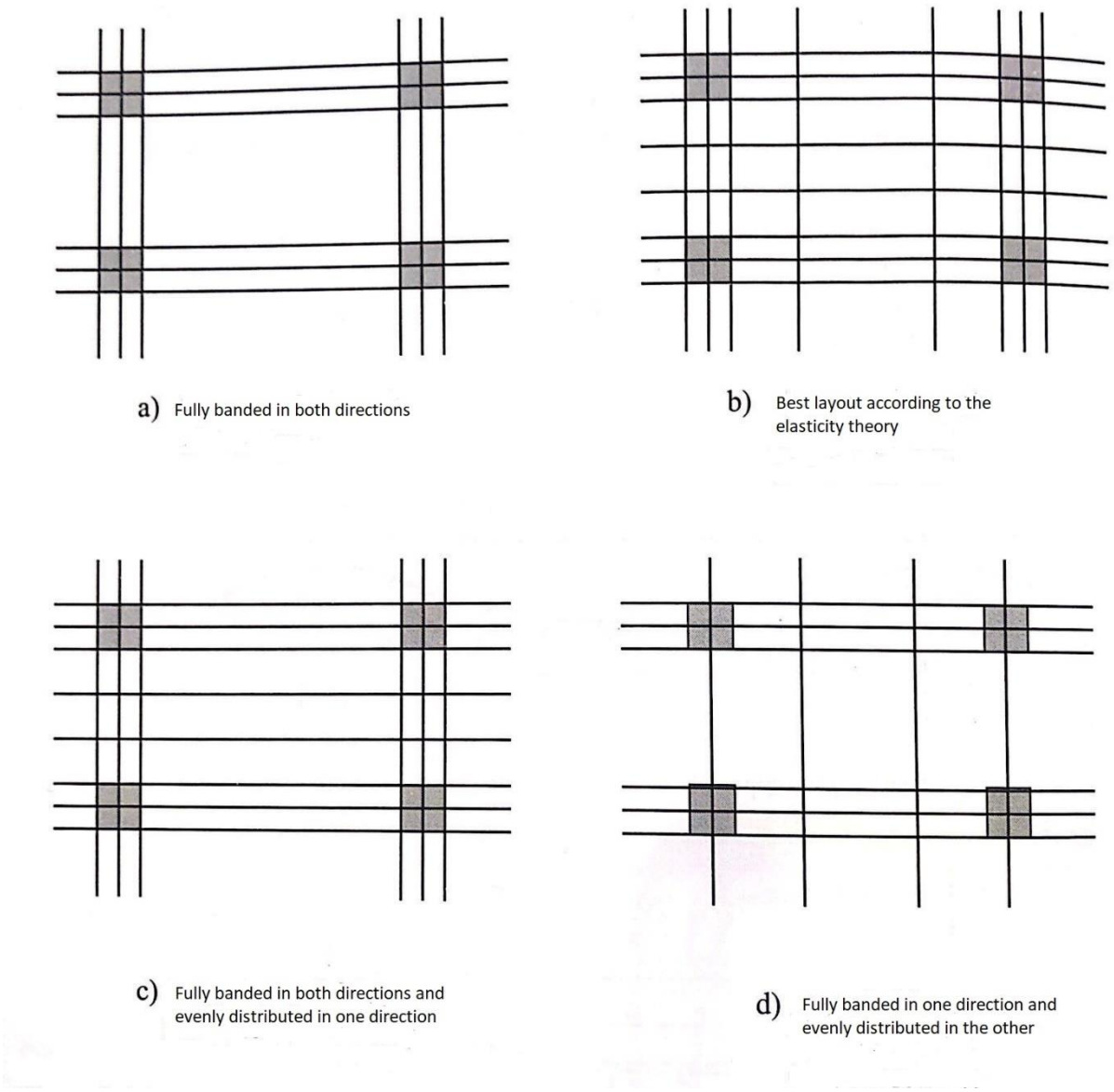

Figure 2.10: *Layout of tendons in flat slabs (Sørensen, 2013)*

It is worth noting that reinforcement layout such as $a)$ and $d)$ enables the opportunity to have bigger gaps within the slab in contrast to the others. In the case where it is very distributed reinforcement layout, there would be a need to scan through the slab to assess where it is possible to create gaps for stairs and other purposes (Trygstad, Generelt om spennarmeringens fortrinn, 2022).

2.5.4 "Waffle" slab & One-way ribbed slab

Waffle slab is another type of slab with distribution of supported columns. Unlike flat slabs, waffle slabs contain an addition of underlying beams in two directions. Hence, the underside is reminiscent of a Belgian waffle, thereby denoted as a waffle slab. The One-way ribbed slab is constructed as a waffle slab, only with beams in one prominent direction. The purpose of this design is to lower the dead-weight of the slab, by allowing in average, a thinner thickness than utilized for flat slabs.

However, due to the complexity of construction, this construction form is not so common as the flat slab (Bhatt, 2011).

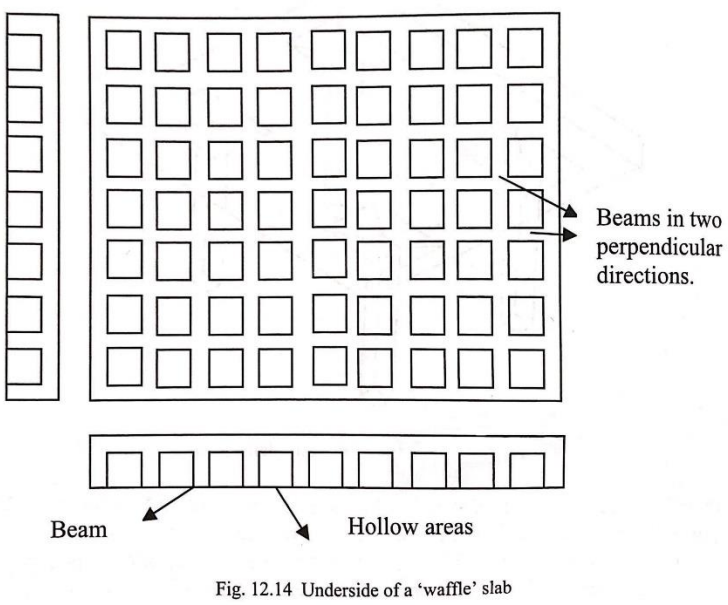

Fig. 12.14 Underside of a 'waffle' slab

Figure 2.11: *waffle slab (Bhatt, 2011)*

2.6 Environmental aspects to tensioned constructions

Introducing tensioned constructions has also certain environmental advantages in comparison to unstressed constructions. In the case for tensioned flat slabs, tensioned reinforcement will allow the slab to utilize a smaller thickness, thereby reducing the amount of concrete needed for a building project. Reducing the amount of concrete will thereby reduce amount of produced cement, leading to less CO2- emissions for the building project. Including prestressed reinforcement has in some cases given reductions in CO2- emissions up to 45% (Trygstad, Generelt om spennarmeringens fortrinn, 2022).

3. Calculation- & dimensioning principles

The purpose of this section is to provide further knowledge in how to calculate for a prestressed slab with post-tensioning. In other words, calculations that are in line with the task for this master thesis. The statements below are in accord with the guidelines given in Eurocodes and national annex for Norwegian practices.

3.1 Characteristics for prestressing steel

For stressed steel, the characteristic strength f_{yk} is replaced by $f_{p0,1k}$ where it is considered a $0{,}1\%$ deviance from the typical linear elastic strain. This is the maximum strength stressed steel can have before it becomes plastic. Furthermore, f_{pk} denoted the characteristic strength within the plastic area before fraction for steel. Since stressed steel is often produced as high strength steel wires, it is common that $f_{p0,1k} = 1500 - 1800\ Mpa$, which is 3 times higher in comparison to regular reinforcement (Sørensen, 2013).

To ensure the calculations are within a safe approximation, characteristic strength $f_{p0,1k}$ is replaced by a design strength f_{pd}, such that $f_{pd} < f_{p0,1k}$. We define the design strength as: $f_{pd} = \frac{f_{p0,1k}}{\gamma_s}$ where γ_s is the material factor given as 1.15

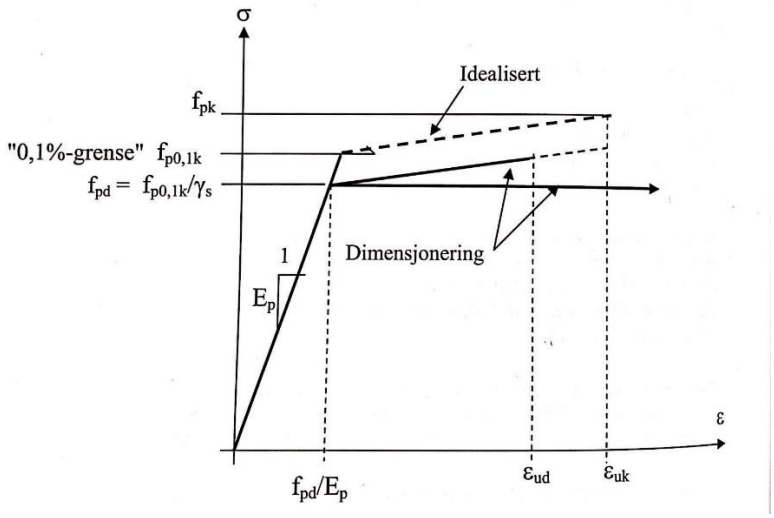

Figure 3.1: *Idealized stress-strain relationship for prestressing steel (Sørensen, 2013)*

Following the linear relationship between stress and Youngs modulus, given by Hooke's law, gives that E_p is also higher in comparison to regular reinforcement.

Eurocode 2, 3.3.6 gives:

$$E_p = 2{,}05 * 10^5\ Mpa \quad \text{for steel wires}$$

$$E_p = 1{,}95 * 10^5\ Mpa \quad \text{for steel strands}$$

Lastly, ε_{uk} and ε_{ud} denoted the maximum characteristic and design strain before fracture, respectively. What the magnitude of the characteristic strengths and strain is, depends on the producent of the prestressed steel and type of prestressed steel utilized in construction.

3.2 Upper limitations to prestress force

As previously mentioned, the applied jacking force P_{jack} is never consistent with the actual prestress force within the concrete element, due to tension losses. Regardless, it is important to gather knowledge of the applied jacking force, to deduct the actual prestress force with respect to tension losses.

3.2.1 Maximum jacking force

Eurocode 2 gives a limitation to the magnitude of prestress force that can be applied onto a concrete element.

Eurocode 2, 5.10.2.1 (1) gives:

$$P_{max} = A_p * \sigma_{p,max} \tag{3.1}$$

$$\sigma_{p,max} = min\{0{,}8f_{pk}, 0{,}9f_{p0,1k}\} \tag{3.2}$$

In situations where it can be proven that the jacking force can be measured accurately within $\pm 5\%$ by the hydraulic jack, $\sigma_{p,max}$ can be altered.

Eurocode 2, 5.10.2.1 (2) gives:

$$\sigma_{p,max} = 0{,}95f_{p0,1k} \tag{3.3}$$

In most cases, P_{jack} equals the limitation given by EC2, so prestress is utilized at full potential ($P_{jack} = P_{max}$).

3.2.2 Maximum initial prestress force

Initial prestress force P_{m0}, is defined as the maximum prestress force concrete can experience immediately as the strands are anchored/cut, thereby compressing concrete with a prestress force based on the applied jacking force. As this process already poses immediate tension losses; $P_{jack} \neq P_{m0}$. This is defined as an upper limit to the actual initial prestress force P_0, given by Eurocode 2.

Eurocode 2, 5.10.3 gives:

$$P_{m0} = A_p * \sigma_{pm0} \tag{3.4}$$

$$\sigma_{pm0} = \min\{0{,}75 f_{pk}, 0{,}85 f_{p0{,}1k}\} \tag{3.5}$$

3.3 Loss of prestress force due to tension losses

P_0 defines the resulting prestress force after immediate losses. ε_{p0} defines the resulting strain after immediate losses. Furthermore, P_0' defines the effective resulting prestress force, which includes the contributions of both immediate and time-dependent losses. ε_{p0}' defines the effective strain which includes all tension losses.

3.3.1 Draw-in loss

Eurocode 2, clause 5.10.5.3 (2) specifies that the amount of slippage, $\Delta_{låS}$, is dependent upon the equipment and situation, and is therefore often provided by an organization, with a value that is within the agreement of building practices. The length that is affected by the draw-in loss is dependent on the friction loss within the cable. As previously mentioned, the larger curvature gives a higher friction within the cable, and subsequently, it follows that it influences the impact draw-in loss has on the cable. By assuming that the value of friction loss follows a linear curve from active end to passive end, it is possible to deduct a slope of the correlation:

$$a = \frac{\Delta P_\mu}{L} \tag{3.6}$$

By assuming an inverted slope for the draw-in loss, it is possible to deduct an approximation to what part of cable is affected by this type of loss:

$$l_{låS} = \sqrt{\frac{\Delta_{låS} E_p A_p}{a}} \tag{3.7}$$

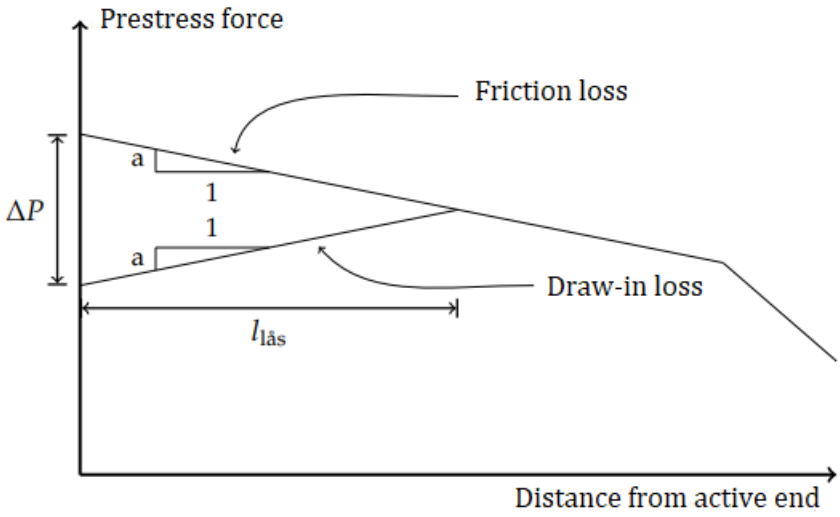

Figure 3.2: *Linear correlation between prestress loss and distance between active end for friction loss. Corresponding inverted relationship for draw-in losses (Collins & Mitchell, 1991)*

The affected length by draw-in loss can be greater or smaller than the length of the cable. If it is greater, the loss is present at passive end in addition to the active end. If this is the case, the resulting loss of prestress due to draw-in is as such:

$$\Delta P_{lås,active} = \frac{\Delta_{lås} E_p A_p}{L} + aL \qquad (3.8A)$$

$$\Delta P_{lås,passive} = \frac{\Delta_{lås} E_p A_p}{L} - aL \qquad (3.8B)$$

If the affected length is smaller than the length of the cable, the draw-in loss is only present at the active end. Hence, this formula becomes applicable:

$$\Delta P_{lås,active} = 2al_{lås} \qquad (3.8C)$$

3.3.2 Friction loss

Friction loss can be calculated through the formula in EC2, 5.10.5.2 (1):

$$\Delta P_{\mu}(x) = P_{max}(1 - e^{-\mu(\theta + kx)}) \qquad (3.9)$$

Where k is as previously mentioned, dependent upon the workmanship and assembly of ducts. Furthermore, μ expresses the friction present between duct to the tendons. θ is the sum of the changes of angle from active jacking end to point x.

3.3.3 Elastic deformation loss due to stressing tendons

Immediate elastic deformation can be calculated through the formula in EC2, 5.10.5.1 (2):

$$\Delta P_{el} = A_p * E_p * \Sigma[\frac{j*\Delta\sigma_c(t)}{E_{cm}(t)}] \qquad (3.10)$$

Where $\Delta\sigma_c(t)$ expresses the change in stress with regards to the gravity center for the tendon at time t. This can be found through formula:

$$\Delta\sigma_c(t) = -\frac{P_0}{A_t} - \frac{P_0(e-y_t)(y-y_t)}{I_t} \qquad (3.11)$$

Where A_t denotes the transformed cross-section, $A_t = A_c + (\eta - 1)A_p$. A_c and A_p is the cross-sectional area of concrete and stressed tendons, respectively. η can be found through $\eta = \frac{E_p}{E_{cm}}$. Furthermore, y_t introduces the concept of a new gravity center of concrete, when stressed tendons are considered as a part of the cross-section. y_t is expressed through $y_t = \frac{(\eta-1)A_p*e}{A_t}$, and denotes the difference between center of gravity considering concrete alone, to the new center of gravity considering both elements. e denotes the distance between center of gravity considering concrete alone, to the center of gravity considering tendons alone. Lastly, the transformed second moment of area is calculated as such: $I_t = \frac{bh^3}{12} + bh * y_t^2 + (\eta - 1)A_p * (e - y_t)^2$.

The formula for $\Delta\sigma_c(t)$ follows the directions illustrated in figure below. Such that positive values of stress are tension and negative values are pressure stresses.

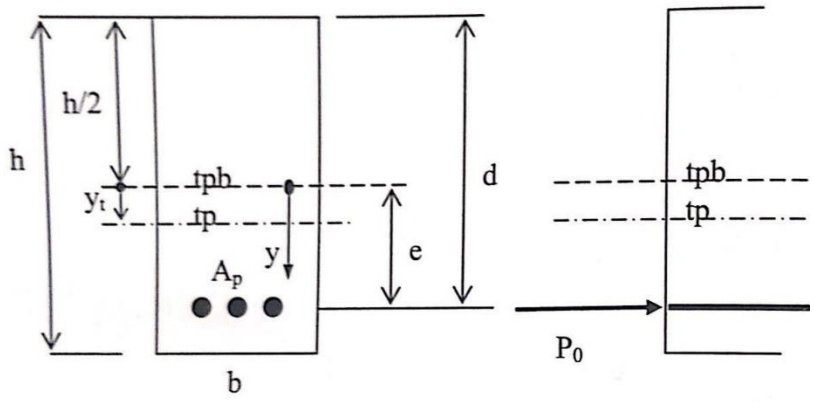

Figure 3.3: *Concrete cross-section (Sørensen, 2013)*

3.3.4 Time-dependent losses

As previously mentioned, shrinkage, creep and relaxation are three processes that contributes to the time-dependent losses. Since these three processes are always present within every concrete element, Eurocode 2 has deducted a formula that contains the contributions of all three components, denoted as ΔP_{c+s+r}.

Eurocode 2, 5.10.6 (2) gives:

$$\Delta P_{c+s+r} = A_p \frac{\varepsilon_{cs} E_p + 0{,}8\Delta\sigma_{pr} + \frac{E_p}{E_{cm}}\varphi(t,t_0)\sigma_{c,QP}}{1+\frac{E_p}{E_{cm}}\frac{A_p}{A_c}\left(1+\frac{A_c}{I_c}z_{cp}^2\right)[1+0{,}8\varphi(t,t_0)]} \quad (3.12)$$

z_{cp} is the distance between the center of gravity for concrete and prestressed tendons. $\sigma_{c,QP}$ is the stress in the concrete at the level of the prestressed tendons due to self-weight and prestressing.

Shrinkage:

ε_{cs} describes the strain due to presence of shrinkage which constitutes of two contributions, autogeneous shrinkage strain and drying shrinkage. In other words, $\varepsilon_{cs} = \varepsilon_{ca} + \varepsilon_{cd}$. The contribution from the autogeneous shrinkage can be found through Eurocode 2, 3.1.4 (6):

$$\varepsilon_{ca}(t) = \beta_{as}(t)\varepsilon_{ca}(\infty) \quad (3.13)$$

$$\beta_{as}(t) = 1 - e^{(-0{,}2t^{0{,}5})} \quad (3.14)$$

$$\varepsilon_{ca}(\infty) = 2{,}5(f_{ck} - 10)10^{-6} \quad (3.15)$$

t denotes the time since firstly casted until current time, measured in days.

The contribution from the drying shrinkage can be found through the same clause in Eurocode 2:

$$\varepsilon_{cd}(t) = \beta_{ds}(t, t_s)k_h\varepsilon_{cd,0} \quad (3.16)$$

$$\beta_{ds}(t, t_s) = \frac{(t-t_s)}{(t-t_s)+0{,}04\sqrt{h_0^3}} \quad (3.17)$$

And the subsequent k_h and $\varepsilon_{cd,0}$ are constants which can be found through tables in the standard.

Creep:

$\varphi(t, t_0)$ is a term related to the presence of creep. The value of this component is dependent upon, of amongst other things, the moisture conditions in the surroundings and the concrete composition. This is therefore a term that considers all the variables that influences the presence of creep. t_0

describes the initial age of concrete when the loading is applied. A common way to find $\varphi(t, t_0)$ is through graphs (look figure below).

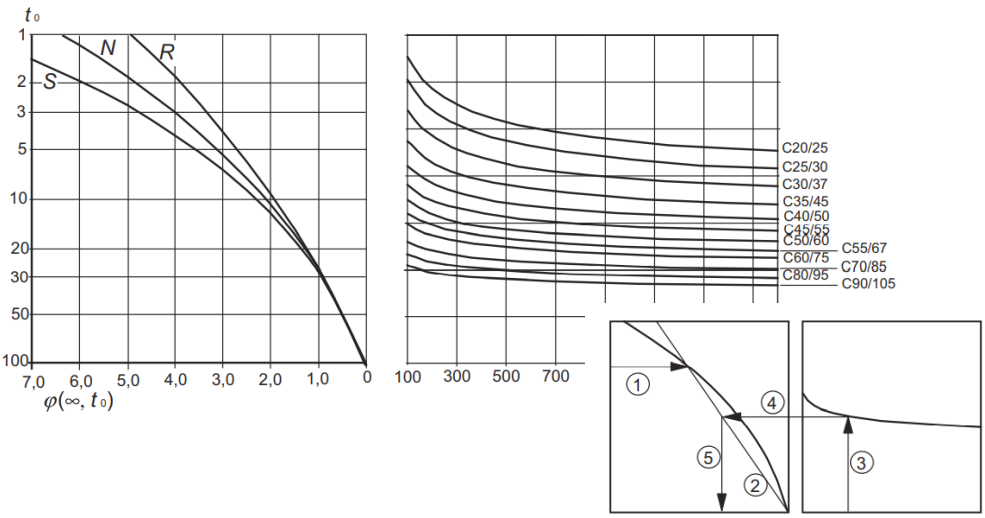

Figure 3.4: *Procedure to find the appropriate creep coefficient (Standard Online AS, 2021)*

Alternatively, $\varphi(t, t_0)$ can be calculated through formulas given in EC2, B.1(1):

$$\varphi(t, t_0) = \varphi_0 * \beta_c(t, t_0) \qquad (3.18)$$

$$\beta_c(t, t_0) = [\frac{t - t_0}{\beta_H + t - t_0}]^{0,3} \qquad (3.19)$$

$$\varphi_0 = \varphi_{RH} * \beta(f_{cm}) * \beta(t_0) \qquad (3.20)$$

φ_0 is defined as the expected creep coefficient. In other words, this component constitutes of the different variables to the process of creep. φ_{RH} is a factor that takes relative humidity into consideration. $\beta(f_{cm})$ considers the concrete strength in relation to creep. $\beta(t_0)$ evaluates the effect of the initial age of concrete when loading is applied. $\beta_c(t, t_0)$ addresses the development of creep over time after loading is applied. Formulas to express these terms are also stated in Eurocode 2, section B.1.

Relaxation:

$\Delta\sigma_{pr}$ is the absolute change of tension due to the presence of relaxation. The level of relaxation present as a time-dependent loss is highly influenced by the type of reinforcement steel present within the concrete. We therefore categorize the relaxation into three classes, which depends on the production procedure of the steel. The different classes explain how highly influenced the concrete is

by relaxation. The value of this component can be deducted through formulas given in Eurocode 2, clause 3.3.2 (7):

$$\frac{\Delta\sigma_{pr}}{\sigma_{pi}} = 5{,}39\rho_{1000}e^{6{,}7\mu}\left(\frac{t}{1000}\right)^{0{,}75(1-\mu)}10^{-5} \qquad \text{for class 1} \qquad (3.21A)$$

$$\frac{\Delta\sigma_{pr}}{\sigma_{pi}} = 0{,}66\rho_{1000}e^{9{,}1\mu}\left(\frac{t}{1000}\right)^{0{,}75(1-\mu)}10^{-5} \qquad \text{for class 2} \qquad (3.21B)$$

$$\frac{\Delta\sigma_{pr}}{\sigma_{pi}} = 1{,}98\rho_{1000}e^{8\mu}\left(\frac{t}{1000}\right)^{0{,}75(1-\mu)}10^{-5} \qquad \text{for class 3} \qquad (3.21C)$$

t is here defined as time in hours after stressing the tendons. For post-tensioned systems, σ_{pi} defines the initial prestress. ρ_{1000} denotes the percentage-wise loss of relaxation 1000 hours after stressing the tendons. μ is a ratio relating the initial prestress to the characteristic strength of prestressed tendons, $\mu = \frac{\sigma_{pi}}{f_{pk}}$.

3.4 Equivalent loading of prestressing

The jacking force applied is in equilibrium with the internal forces applied onto the concrete. How the tendon profile is assembled affects if the concrete experiences shear forces, normal forces, and moment. Since hydraulic jacks apply normal stresses to the tendon, the external jacking force are normal to the angle of the tendon where it is stressed.

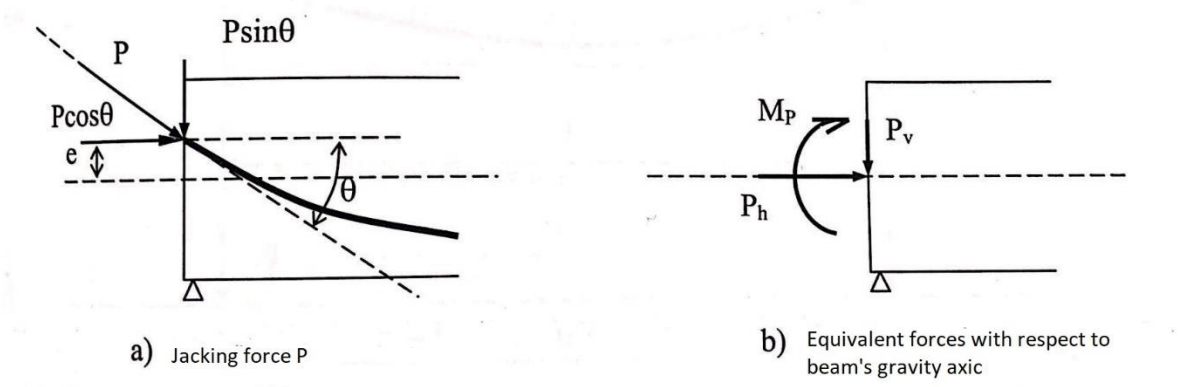

Figure 3.5: *Forces at anchorages, jacking force P decomposed (Sørensen, 2013)*

In cases where the tendons are deflected and eccentric to the gravity line of concrete, the jacking force applied can be decomposed to a normal force P_h, vertical force P_v and momentum M_p. This is achieved by geometry and equilibrium along gravity line of concrete:

$$P_h = P * \cos\theta$$

$$P_v = P * \sin\theta$$

$$M_p = P_h * e = P * \cos\theta * e$$

In practice, the slope of tendon is very small compared to tendon's length. It can therefore be assumed that:

$$\sin\theta \approx \theta$$

$$\cos\theta \approx 1$$

Which leads to the simplifications of the jacking force P to:

$$P_h = P * \cos\theta \approx P$$

$$P_v = P * \sin\theta \approx P * \theta$$

$$M_p = P * \cos\theta * e \approx P * e$$

Depending upon the assembly of the tendon profile, we can have equivalent forces along the tendon's length. This can vary from distributed loading with a range of intensities to point loadings. We can divide as followed:

1. Straight tendon profiles give no vertical forces along tendon's length.
2. Tendon profiles with harped points along tendon's length gives concentrated vertical forces K
3. Tendon profiles with curvatures leads to distributed vertical forces $q(x)$ along its length x

In theory, a stressed tendon will try to straighten to minimize length of tendon, thereby reduce the afflicted stress. This will in turn pressure the concrete at points where it deviates from a straight line. Hence, depending on the tendon profile, vertical forces from tendon pushing on the concrete arises throughout beams length.

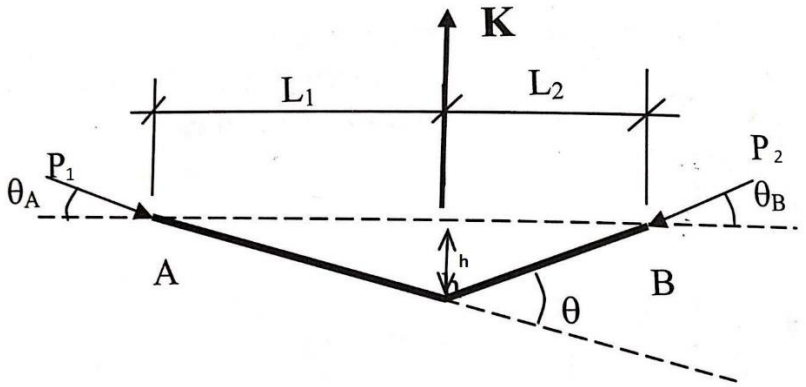

Figure 3.6: *Tendon profile harped at one point (Sørensen, 2013)*

In the case for harped tendon profiles, equilibrium establishes the magnitude of concentrated force. Decomposing jacking force into P_v & P_h gives following equilibrium equation for K:

$$\Sigma R_v = 0 \Rightarrow P_{v1} + P_{v2} = K$$

$$P * \theta_A + P * \theta_B = K$$

$$P\left(\frac{h}{L_1} + \frac{h}{L_2}\right) = K$$

For a tendon profile with curvature, we can assume that equivalent distributed force equals to $q(x) = P * \frac{d^2y}{dx^2}$, where $y(x)$ is a function describing the tendon profile along the beam's length. For a parabolic curvature, $q(x)$ will therefore be constant along the beam's length.

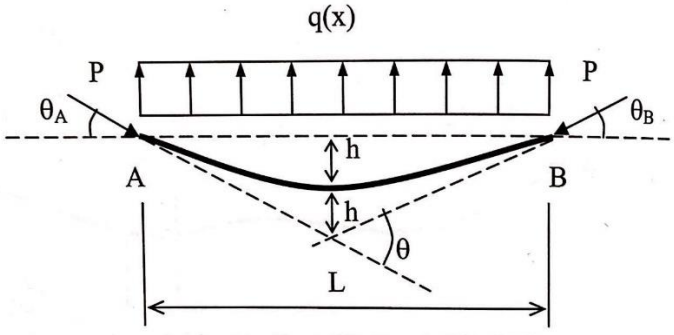

Figure 3.7: *Parabolic tendon profile (Sørensen, 2013)*

Following the previous procedure gives that the resulting force $K = q_0 * L = P(\theta_A + \theta_B)$, such that:

$$q_0 = \frac{P}{L_{tot}}\left(\frac{2h}{L_1} + \frac{2h}{L_2}\right)$$

If $L_1 = L_2 = \frac{L}{2}$: $q_0 = \frac{P}{L}\left(\frac{4h}{L} + \frac{4h}{L}\right) = \frac{8Ph}{L^2}$

3.4.1 Statically determined constructions

The equivalent forces from prestressing tendon with a certain tendon profile creates compression, shear and moment along the beam's length.

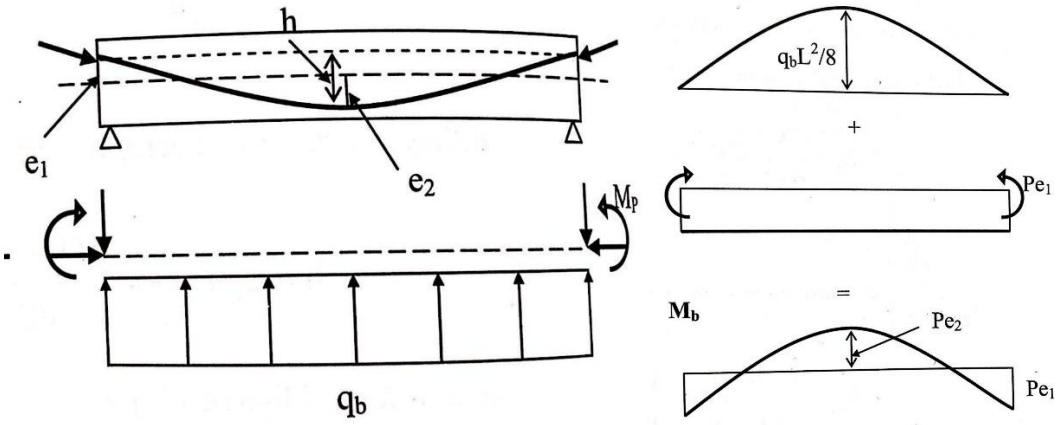

Figure 3.8: *Tendon profile with end-eccentricities and corresponding moment diagram (Sørensen, 2013)*

In this case, a constant moment due to the eccentricity of the jacking force leads to a static $M_p = P * e_1$. In addition, the corresponding distributed force $q_b = \frac{8Ph}{L^2}$ will lead to a parabolic moment-diagram, with max intensity of $\frac{q_b L^2}{8} \Rightarrow \frac{8Ph}{L^2} * \frac{L^2}{8} = Ph$. Due to the initial eccentricity, $h = e_1 + e_2$. By adding the two moment-diagrams, we observe that the corresponding moment diagram follows the eccentricity along the beam's length. This observation is true for all statically determined constructions, such that the total moment from prestressing is simply $M = P * e$. We denote this as primary moment.

3.4.2 Statically indetermined constructions

For statically indetermined constructions, moment consists of both primary moment and secondary moment/parasitic moment.

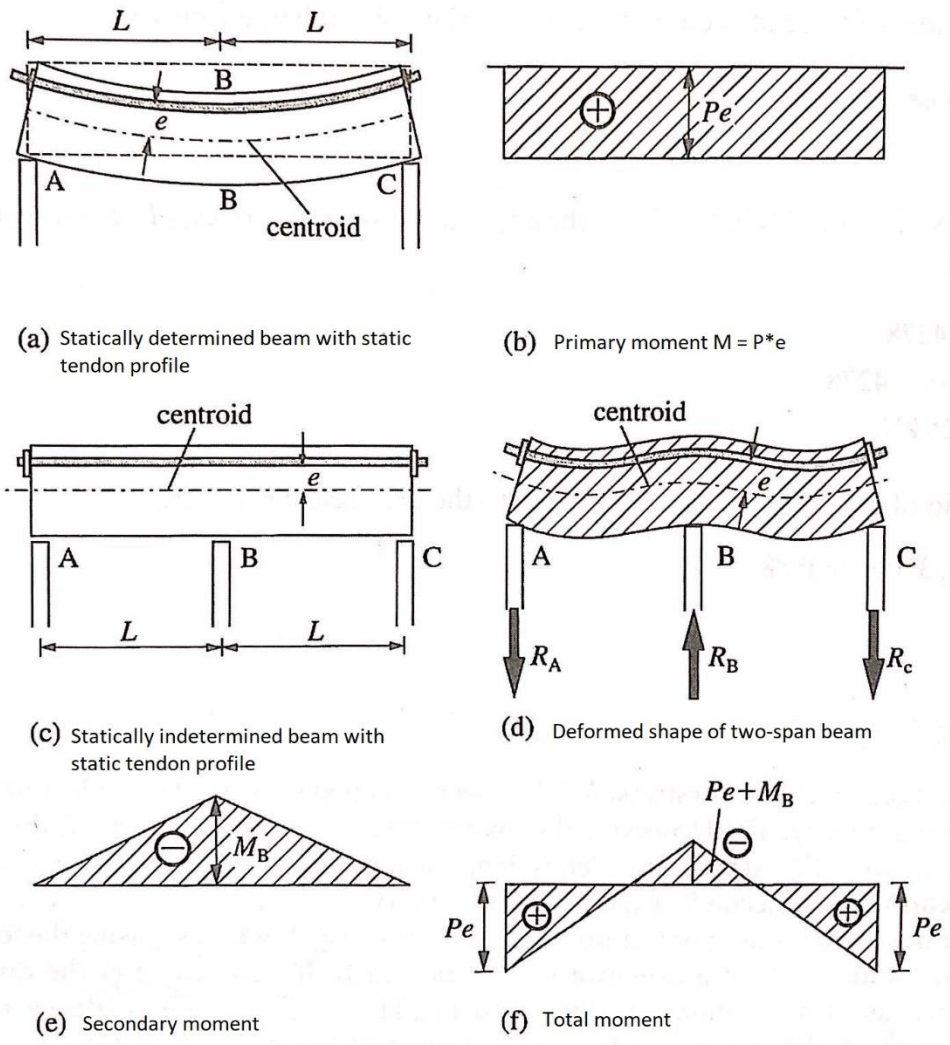

Figure 3.9: *Statically indetermined structure and its equivalent moment diagram consisting of both primary and secondary moment diagram (Obrien, Dixon, & Shiels, 2012)*

Taking the example from above, the primary moment leads to a static moment consisting of $M_p = P * e$. However, this would cause the statically indetermined beam to have maximum upward deflection at center of beam's length. Because of the presence of the support B, this is inconsistent with a realistic deflection of the beam. As a result, a force representing the existence of support B, is withholding the deflection at this point, causing the secondary moment. The total moment-diagram due to the prestressing force is therefore a sum of primary moment and parasitic moment/secondary moment.

3.5 How to account for prestressing in calculations

There are two ways in how to account for prestressing through the calculation procedure. In principle, the prestressing force can either be viewed upon as an external loading in addition to

dead-weight and live load. Alternatively, it can be addressed as an internal resistance, as the concrete element is modified. For ultimate limit state (ULS), the prestress force can be regarded as either of the two previously mentioned options. In the case where the stressed reinforcement lies within the compression zone of the cross-section, it is common to regard the prestress force as an external load, and when it lies within the tensioned zone of cross-section, it is regarded as an internal force (Sørensen, 2013). However, it is mostly common to regard it as an internal resistance for the moment capacity check (Kanstad, Kontroll i bruks- og bruddgrensetilstand, 2022). The reasoning for this is that we often design the tendon profile so that, in the presence of other loadings such as live load and self-weight, the stressed tendon is within the tensioned zone. Meanwhile, for serviceability limit state (SLS), it is required to view the prestress force as an external force (Øverli, 2022).

3.5.1 External load

If the prestressing force is addressed as an external force, the design prestressed force needs to be multiplicated with a load factor as per usual for loadings in ultimate limit states. What load factor is used, is dependent upon if the prestressing is behaving in a favorable condition for the construction or not.

Eurocode 2, NA 2.4.2.2 (1) gives:

$\gamma_p = 1{,}1$ If unfavorable condition

$\gamma_p = 0{,}9$ If favorable condition

In the case where the prestressing tendon is applied at a segment where the concrete is in pressure, this will provide as an unfavorable condition, since the prestressing force will ultimately further contribute to higher pressure. As the prestressing tendon is placed at a segment where the concrete experiences tension, the prestress force will counteract the stresses, thereby functioning as a favorable condition. This is based upon the previous mentions that if a tendon profile deviates from the gravity line of concrete, it will create a moment with regards to the axis, thereby either contributing to excess stress or counteracting the existing stress from other applied loadings.

The external prestress force is regarded as following:

$$P_0' = \varepsilon_{p0}' * E_p * A_p \qquad (3.22)$$

Where E_p denotes the young modulus for the prestress reinforcement

A_p denotes the cross-sectional area of the prestressing

ε'_{p0} describes the effective strain difference due to the presence of tension losses

P'_0 is denoted effective jacking force, which is the magnitude of force applied onto concrete considering the presence of all tension losses

3.5.2 Internal Resistance

If the prestress force is regarded as an internal force within the concrete element, thereby modifying the qualities of the concrete, it will act as a contribution to the different capacities. The internal force, S_p, is determined through the total strain present in the stressed reinforcement.

The internal force due to prestressing reinforcement, S_p, can be calculated as follows for unbonded post-tensioned systems:

$$S_p = (\varepsilon'_{p0} E_p A_p + \Delta\sigma_{p,ULS}) \frac{1}{\gamma_s} = (0{,}8\varepsilon_{p0} E_p A_p + 100 \frac{N}{mm^2}) \frac{1}{\gamma_s} \quad (3.23)$$

Where the additional $\Delta\sigma_{p,ULS} = 100 \frac{N}{mm^2}$ is a rough, conservative estimate given in EC2, 5.10.8(2). The purpose of this addition is to take into consideration the changes that happens when the concrete element is deformed due to external loading. The first term, $\varepsilon'_{p0} E_p A_p$considers the effect the tension losses have to the resulting prestress force.

3.6 Flat slabs

There are several different methods in how to calculate and analyze flat slabs in an appropriate manner. However, the most common approach is defined as the equivalent frame analysis. Since we will utilize ADAPT-builder for this project, which also uses the finite element method, both methods will be addressed below.

3.6.1 Equivalent frame analysis

Eurocode 2, Annex I.1.2 gives recommendations in how to calculate on a flat slab with the use of equivalent frames as the applicable method. Here it is explained how the common approach is to part both directions into equivalent frames. In other words, for a flat slab with loading, the loading will be parted by the equivalent frames in the slab. Each frame consists of a width corresponding to half of the span width on both sides of the columns. In this way, we ensure that all the area of slab with loading is converted into equivalent frames that withstands each a part of the total distributed loading applied.

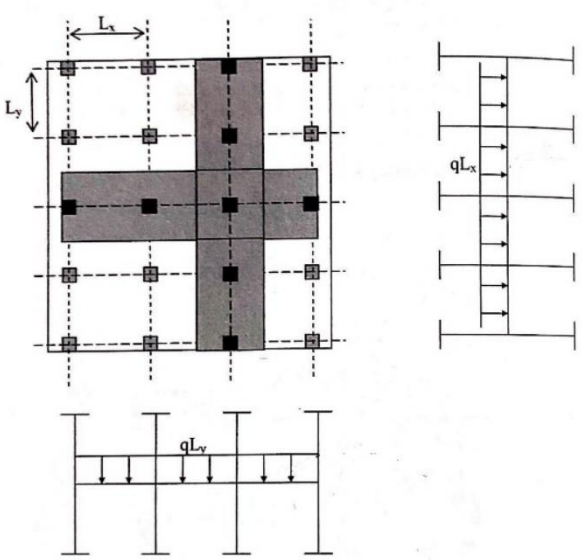

Figure 3.10: *Equivalent frames and corresponding equivalent loading onto each frame based on width of each span in the slab (Sørensen, 2013)*

M_s and M_f corresponds to the dimensioning moments found within the equivalent frames in both directions, where M_s defines the maximum moment at support and M_f defines the maximum field moment. The applied loading will have to provide the worst possible scenario for the slab, which equals the highest dimensioning moment. The live load will therefore be placed partwise onto different fields, such that it will provide higher moment for M_s and M_f in both directions.

After the moment M_s and M_f is calculated for the equivalent frames, the corresponding distributed moment across the width of each frame is thereby found by dividing on the width of the frame. Eurocode 2, Table I.1 specifies how the resulting moment should be distributed across the frame.

Furthermore, NB33 provides a possible solution for the distribution of moment that is in line with Eurocode 2 as shown in figure below.

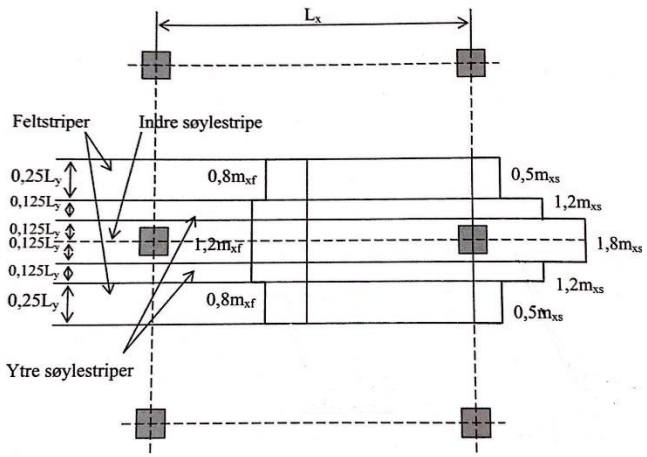

Figure 3.11: *Distribution of moment based on a possible solution provided in NB33 (Sørensen, 2013)*

In the presence of prestressing slabs, concentrated stressed tendons is considered as a frame with width as described above. However, equally distributed stressed tendons in one direction will be treated as a one-way slab. This means that the frames for distributed stressed tendons will each have 1m width (Kanstad, Verifikasjon av resultater, håndregning. , 2022). When calculating the moment-capacity utilizing the equivalent frame method, the width is $\frac{L}{4}$ and 1 m for concentrated and distributed tendons, respectively.

3.6.2 Finite element method

ADAPT-builder utilizes finite element method to deduct the corresponding dimensioning forces within the construction. Finite element method is a way to solve a complex construction, by simplifying the construction into a set of elements with nodes. The solution is therefore an approximation to the actual solution but within a reasonable margin if handled correctly. In other words, choosing correct element type that can represent the response to the loading correctly, and ensuring the solution will converge to the correct solution as you increase the number of nodes or number of elements. The behavior of each element is limited to the number of nodes. For instance, two nodes at the edge of element will only enable the edge of the element to have a linear displacement field in the according direction. We denote the description of the displacement field for an element as the form function. In addition, how much the displacement of the node will occur when applied with loading is dependent on the stiffness of the structure, denoted as the stiffness

matrix. The resulting set of equations based on finite number of nodes and the equivalent stiffnesses, will provide you with information of stress, strain and displacement at the point of the nodes.

3.7 Ultimate limit state

Common ultimate limit state checks for flat slabs that are stressed are check of moment capacity and the shear punching check locally around the columns.

3.7.1 Moment-capacity check

Previously, it has been addressed that the prestress force in the moment capacity check will be regarded as an internal resistance, such that any generated moment from the existence of prestress within the slab is not regarded as a part of the external loading when checking external loading against the moment capacity. However, this is not valid for indeterminate structural systems. Since the secondary moment is not directly linked to the presence of prestressed tendons, but a response to the system being indeterminate, the secondary moment will be regarded as external loading, even though this moment arises when we have prestressed systems.

The check against moment capacity is:

$$M_{ed} \prec M_{Rd} \qquad (3.24)$$

where the designed external loading is found as:

$$M_{ed} = \gamma_g M_g + \gamma_q M_q + \gamma_p M_1 \quad (3.25)$$

This is applicable for a loading case with self-weight $[g]$, live load $[q]$ and secondary moment $[1]$ (Kanstad, Kontroll i bruks- og bruddgrensetilstand, 2022). $\gamma_{[x]}$ references to the corresponding load factors for the different loadings in accord with ULS, thereby converting the characteristic moments in the equation, into design moment.

As the prestress force is regarded as an internal resistance, the equivalent contribution from prestress is now a part of the total generated moment capacity for the concrete element.

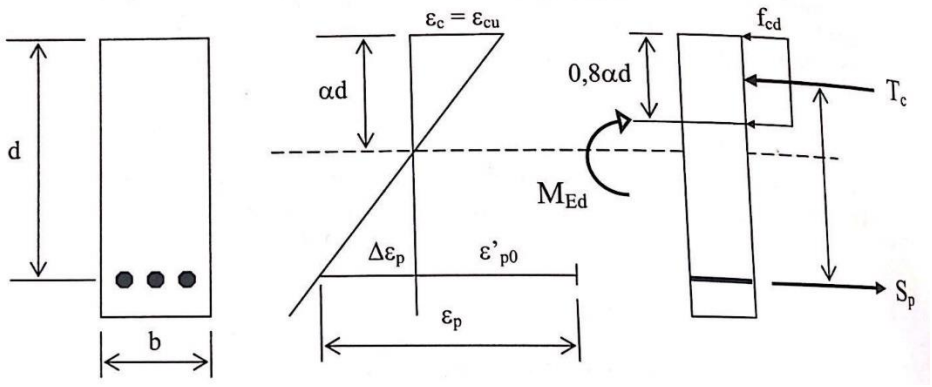

Figure 3.12: *Basis behind generating formula for moment-capacity when Sp is regarded as an internal force (Sørensen, 2013)*

We consider the moment capacity as:

$$M_{Rd} = T_c z = 0{,}8\alpha(1 - 0{,}4\alpha) f_{cd} b d_m^2 \qquad (3.26)$$

In theory, to utilize the proper formula for α, which contains the contribution from the presence of stressed, and un-stressed reinforcement, we must understand the state of the reinforcement at the critical cross-section. We define the term α_b which provides the exact state where tendons transition into plastic state and the concrete reaches its maximum concrete compression limit:

$$\alpha_b = \frac{\varepsilon_{cu}}{\Delta\varepsilon_p + \varepsilon_{cu}} = \frac{\varepsilon_{cu}}{\frac{f_{pd}}{E_p} - \varepsilon'_{p0} + \varepsilon_{cu}} \qquad (3.27)$$

This will in turn provide the needed reinforcement $A_{p,balanced}$ to reach this state:

$$A_{p,balanced} = 0{,}8\alpha_b b d_m \frac{f_{cd}}{f_{pd}} - A_s \frac{f_{yd}}{f_{pd}} \qquad (3.28)$$

Now, comparing the balanced reinforcement to current stressed reinforcement, will provide us with the information if our reinforcement is elastic, $A_p > A_{p,balanced}$, or plastic $A_p < A_{p,balanced}$.

For under-reinforced systems $A_p < A_{p,balanced}$:

$$\alpha = \frac{S_p + f_{yd} A_s}{0{,}8 f_{cd} b d_m} \qquad (3.29)$$

Most commonly, we design the system as under-reinforced, as it will provide a more ductile fraction response than brittle. This will provide visual cues in advance before fraction, thereby acting as a safety measurement. It can be assumed that the formula for under-reinforced systems can be used without checking if $A_p < A_{p,balanced}$, since it is often the case (Kanstad, Kontroll i bruks- og bruddgrensetilstand, 2022).

3.7.2 Shear punching check

The different procedures to check with regards to the shear punching is provided by Eurocode 2, 6.4.3(2), as follows:

A) At the edge of the columns the shear force should be limited to

$$\nu_{Ed} \leq \nu_{Rd,max} \tag{3.30}$$

B) Shear reinforcement is not necessary in situations when

$$\nu_{Ed} \leq \nu_{Rd,c} \tag{3.31}$$

C) If the situation is such that $V_{Ed} > V_{Rd,c}$, the dimensioning shear force exceeds the capacity of the concrete slab without any shear reinforcement. Hence, an additional procedure follows, given in Eurocode 2, 6.4.5 (1), such that the result will be as follows:

$$\nu_{Rd,cs} \geq \nu_{Ed} \tag{3.32}$$

$V_{Rd,max}$ represents the maximum shear capacity.

$V_{Rd,c}$ represents the shear capacity for a slab without any shear reinforcement.

$V_{Rd,cs}$ represents the shear capacity for a slab with shear reinforcement included.

Dimensioning shear stress υ_{Ed}

Shear force V_{Ed} can arise because of concentrated load on a local area, or support forces. For flat slabs, it is therefore an important check, as the columns contribute with locally concentrated support forces. The concentrated force will distribute as shear stress within the slab, thereby risking shear cracking failure locally around the column. The dimensioning shear stress ν_{Ed} is therefore defined as the distributed dimensioning shear force V_{Ed} around the column in question.

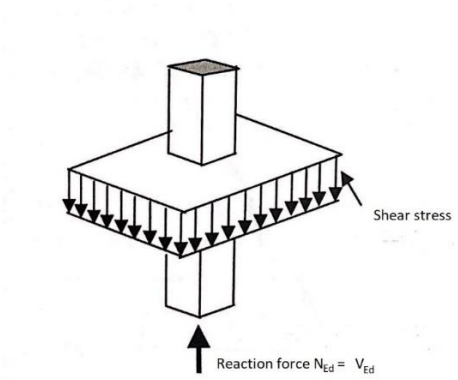

Figure 3.13: *Shear distribution locally around column because of concentrated force (Sørensen, 2013)*

In practice, there is a presence of moment transfer from the slab onto the column in a flat slab. The resulting moment force M_{Ed} is balanced by distributed bending moment m, torsion m_{xy} and shear forces v_x and v_y. This affects the distribution of shear stress and must be accounted for in the calculations. In the case where concentrated forces contributes with moment in both directions, in addition to shear force, Eurocode 2, clause 6.4.3 (2) defines:

$$v_{Ed} = \beta \frac{V_{Ed}}{u_i d} \qquad (3.33)$$

u_i represents the local circumference around the column in question. This circumference is located either at the most critical section regarding shear punching failure u_1 or at the face of the column u_0. Eurocode 2 define that the typical shear cracking pattern locally around the column happens at an angle of approximately $\theta = 26{,}6°$ of the edge surface of the column. Hence, it is deducted that the critical section in question against shear punching u_1 is at a distance $2d$ from edge surfaces of the column.

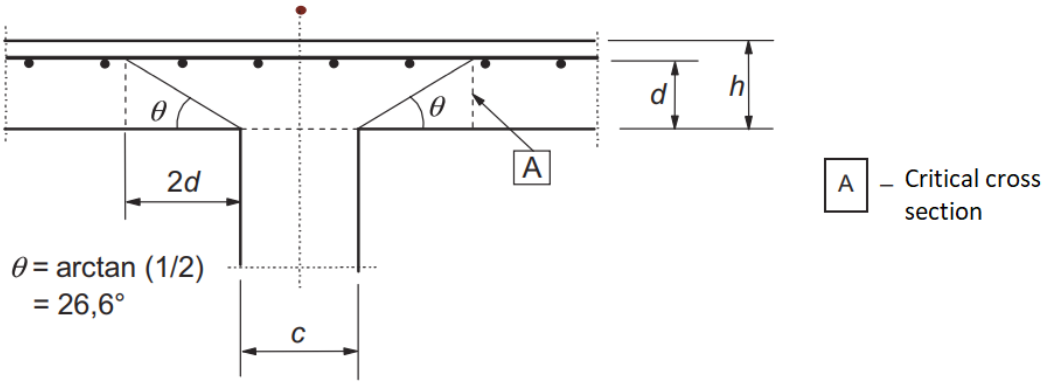

Figure 3.14: *Section to control for shear punching failure (Sørensen, 2013)*

Depending on the shape of the column, the formulas for the circumference around critical section varies. For internal circular-, and rectangular columns, typical circumference for the cracking pattern is as follows:

$$u_1^{circular} = \pi(\mathrm{D} * 4\mathrm{d}) \qquad (3.34A)$$

$$u_1^{Rectangular} = 4\pi d + 2c_1 + 2c_2 \qquad (3.34B)$$

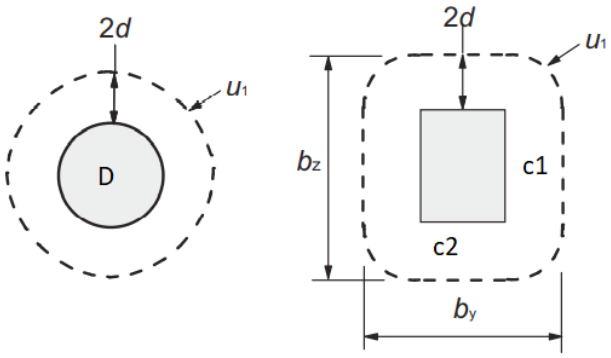

Figure 3.15: *Sketch of the critical control perimeter based on shape of column (Sørensen, 2013)*

For columns that are located at the edge or corner of a slab, the cracking pattern locally around the column are altered. In this case, a different set of equations for u_1 follows, where the perimeter will be smaller due to absent slab surrounding the column. As a result, edge columns and corner columns are often more critical in relation to shear punching.

β represents the total contribution M_{Ed} have on the total shear stress along the critical perimeter u_1. Eurocode 2, clause 6.4.3 (3) defines β to be as follows for circular-, and rectangular columns:

$$\beta = 1 + 0{,}6\pi \frac{M_{Ed}}{V_{Ed}} \frac{1}{D+4d} \qquad \text{for circular columns} \qquad (3.35A)$$

$$\beta = 1 + k \frac{M_{Ed}}{V_{Ed}} * \frac{u_1}{w_1} \qquad \text{for rectangular columns} \qquad (3.35B)$$

k is a factor that represents the amount of moment M_{Ed} that is balanced by shear stress v_x and v_y, in comparison to moment m and torsion m_{xy} (Sørensen, 2013). This varies between $0{,}45 - 0{,}8$ depending on the geometry of the rectangular column in question.

w_1 represents the distribution of the moment M_{Ed} into shear stress. Eurocode 2, clause 6.4.3(3) gives:

$$w_1 = \frac{c_1^2}{2} + c_1 c_2 + 4c_2 d + 16d^2 + 2\pi d c_1 \qquad (3.36)$$

For a rectangular column with moment M_{Ed} in one direction. Here, c_1 is the dimension of the column that is parallel with the bending moment and c_2 angular with the direction of the bending moment.

For situations where there is dimensioning moment along both directions, the calculation of an appropriate β value can be quite difficult. Hence, a simplification of correct β value can be found in Eurocode 2, Figure 6.21N. This is sufficient provided that the columns are not withstanding horizontal

loading, thereby functioning as a part of the horizontal stability of the construction (Kanstad, Kontroll i bruks- og bruddgrensetilstand, 2022).

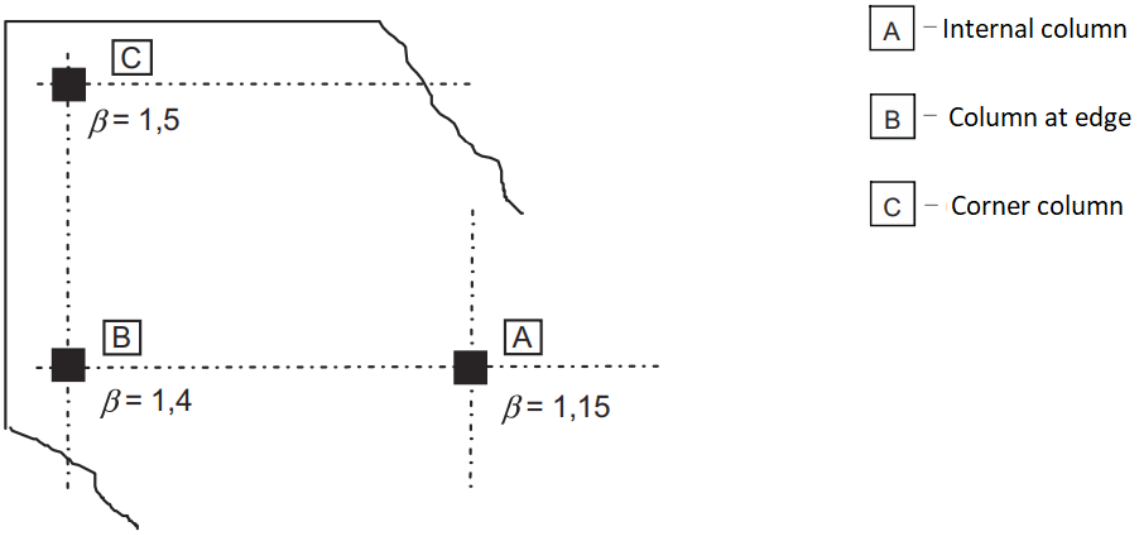

Figure 3.16: *Simplification of correct beta value depending on type of column in slab (Standard Online AS, 2021)*

Maximum shear capacity $v_{Rd,max}$

Eurocode 2, NA 6.4.5(3) gives following:

$$v_{Rd,max} = 0{,}4 v f_{cd} \qquad (3.37)$$

Where $v = 0{,}6(1 - \frac{f_{ck}}{250})$ as determined by Eurocode 2, clause NA.6.2.2(6). v is a factor representing the reduction in strength as a response to cracks given by shear force. The maximum shear capacity must be checked against the shear stress along the face of the column, thereby providing the subsequent equation:

$$v_{Ed} = \beta \frac{V_{Ed}}{u_0 d} \leq v_{Rd,max} \qquad (3.38)$$

Where the perimeter along the face of the column u_0 depends on the shape of the column, in addition to the location on the slab. In other words, if the column in question is an internal column, corner column or column at the edge of slab.

Shear capacity without shear reinforcement $v_{Rd,c}$

Eurocode 2, clause 6.4.4 (1) provides the formula for the shear capacity as follows:

$$v_{Rd,c} = C_{Rd,c} k (100 \rho_l f_{ck})^{\frac{1}{3}} + k_1 \sigma_{cp} \geq (v_{min} + k_1 \sigma_{cp}) \qquad (3.39A)$$

$$\rho_l = \sqrt{\rho_{ly} * \rho_{lz}} \leq 0{,}02 \qquad (3.39B)$$

$$\sigma_{cp} = \frac{\sigma_{cy}+\sigma_{cz}}{2} = \frac{1}{2}\left(\frac{N_{Ed,y}}{A_{c,y}} + \frac{N_{Ed,z}}{A_{c,z}}\right) \qquad (3.39C)$$

$$k_1 = 0{,}1$$

ρ_l is related to all the tensioned reinforcement that is set with the concrete. In other words, for post-tensioned systems with ungrouted ducts, this reinforcement is neglected in this calculation.

σ_{cp} gives the average normal stress in both directions at the critical perimeter. $N_{Ed,y}$ and $N_{Ed,z}$ are forces in relation to the jacking of the slab in the equivalent directions. We can assume the normal force N_{Ed} is defined to be $N_{Ed} = 0{,}85\gamma_p P_{max}$ (Kanstad, Kontroll i bruks- og bruddgrensetilstand, 2022). As the presence of this normal force N_{Ed} contributes to a higher shear capacity for the slab, it is a favorable situation, such that $\gamma_p = 0{,}9$. $A_{c,y}$ and $A_{c,z}$ are the corresponding areas that the normal force is distributed along the slab. For evenly distributed tensioned reinforcement, the area is simply the length between the cables and the thickness. Meanwhile, for concentrated tensioned reinforcement, the normal stress is concentrated over the area this reinforcement is placed and distributed at an angle $45°$ to the spanwidth $\frac{L}{2}$ (Kanstad, Kontroll i bruks- og bruddgrensetilstand, 2022). This is illustrated in Figure 3.17.

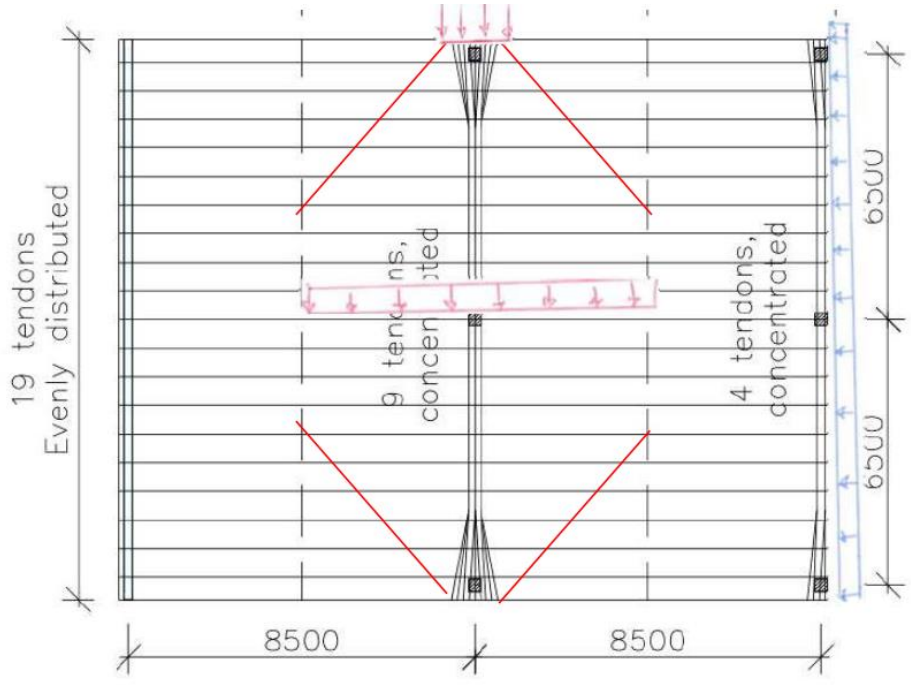

,

Figure 3.17: *Distribution of normal force onto slab for a slab with concentrated stressed tendons in one direction and equally distributed stressed reinforcement in the other (Kanstad, Kontroll i bruks- og bruddgrensetilstand, 2022).*

ν_{min} is provided by Eurocode 2, clause NA 6.4.4(1) as follows:

$$\nu_{min} = 0{,}035 k^{\frac{2}{3}} f_{ck}^{\frac{1}{2}} \tag{3.40}$$

The shear stress in question, ν_{Ed} is provided at the critical control perimeter which is at the distance 2d from the column.

Shear capacity with shear reinforcement $\nu_{Rd,cs}$

Eurocode 2, clause 6.4.5 (1) provides the appropriate formula for $\nu_{Rd,cs}$:

$$\nu_{Rd,cs} = 0{,}75\nu_{Rd,c} + 1{,}5\frac{d}{S_r} A_{sw} f_{ywd,ef} \frac{1}{u_1 d} \sin\alpha \leq \nu_{Rd,c} k_{max} \tag{3.41}$$

This is a calculation that will provide the information of the necessary reinforcement needed to provide sufficient safety precautions for shear punching around local column. $\nu_{Rd,c}$ provides the initial contribution to capacity around column without shear reinforcement, where both the mixture of concrete slab itself and the prestressing plays a role in the capacity. The second part of the formula refers to the contribution the shear reinforcement will play in the total capacity. Since both S_r and A_{sw} will be unknown terms in the calculation, it is common to decide S_r to deduct what the necessary reinforcement will be per perimeter. Such that:

$$A_{sw} = (\nu_{Rd,c} k_{max} - 0{,}75\nu_{Rd,c}) S_r u_1 \frac{1}{1{,}5 f_{ywd,ef} \sin\alpha} \tag{3.42}$$

A_{sw} is defined as the area of shear reinforcement along the circumference of one section around the column

S_r is the radial distance between each segment of shear reinforcement around the column

α is the angle between the shear reinforcement and the plane of the slab. For vertical links, $\alpha = 90°$.

$f_{ywd,ef}$ is defined as the effective dimensioning strength of the shear reinforcement under the influence of concentrated loads. This is determined through $f_{ywd,ef} = 250 + 0{,}25d \leq f_{ywd}$.

k_{max} is a factor that limits how much the capacity can be with the use of shear reinforcement included. Eurocode 2, clause NA.6.4.5(1) gives that k_{max} is 1,5 or 1,8 depending on the type of shear reinforcement used in the design.

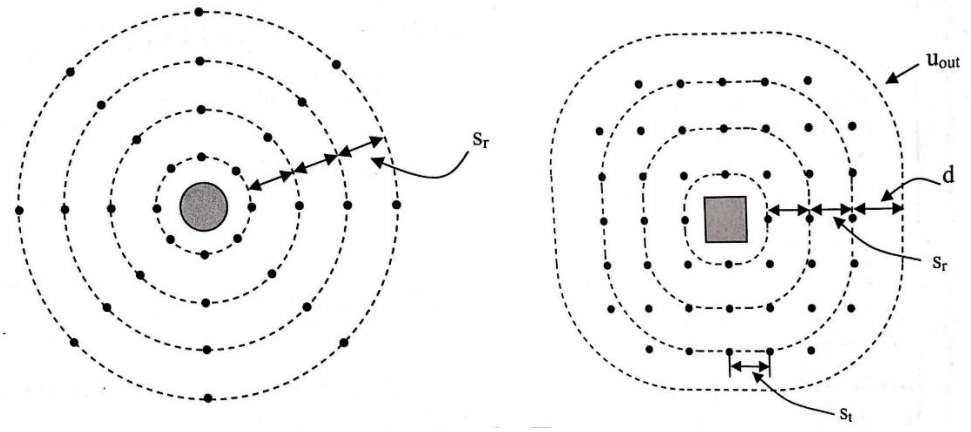

Figure 3.18: *Layout of shear reinforcement (Sørensen, 2013)*

circular pattern

rectangular pattern

In practice, it is possible to lay the shear reinforcement in these two patterns as shown in the Figure 3.18. Although it is worth mentioning there are certain set of rules involved when performing the layout of the shear reinforcement.

3.8 Serviceability limit state

3.8.1 Rules set for limitations of stresses

With the presence of prestressing forces, the prestressing and other loadings at the time of jacking or the transition from jacking to concrete pressure should be limited.

Eurocode 2, clause 5.10.2.2 gives:

$$\sigma_{c,pressure} \leq 0{,}6 f_{ck}(t) \qquad (3.43)$$

Furthermore, Eurocode 2, clause 7.1 (2) states that for the different calculations within serviceability limit state, the concrete should be assumed to be in an uncracked state. In other words, it needs to be ensured that the concrete stress is lower than the mean value of its strength in tension:

$$\sigma_{c,tension} \leq f_{ctm} \qquad (3.44)$$

3.8.2 State I: Uncracked cross-section

If $\sigma_{c,tension} \leq f_{ctm}$, we have an uncracked cross-section. We can assume during the hand-calculations that the contribution from reinforcement is neglected in the calculation, as this simplifies the calculation and only leads to a maximum of 10% deviance in correct solutions (Kanstad, Kontroll i

bruks- og bruddgrensetilstand, 2022). This means that the reinforcement does not relocate the center of gravity as explained previously, and the stress in concrete is simplified to being:

$$\sigma_c(t) = -\frac{P_0}{A_c} - \frac{M}{I}y \qquad (3.45)$$

Where M defines the total moment, which constitutes of M_{g+q} and M_p.

$I = \frac{bh^2}{12}$ as we do not longer calculate the cross-section as a transformed cross-section due to the neglect of reinforcement.

A_c is the area of the concrete.

P_0 is the prestress force without the time-dependent effects (P_0')

3.8.3 State II: Cracked cross-section

If $\sigma_{c,tension} \geq f_{ctm}$, we have a cracked cross-section. This means that the strength in tension for the concrete is exceeded, such that the concrete element cannot withstand tension. For this situation, the prestressed reinforcement needs to be considered as regular reinforcement, thereby calculating as a cracked cross-section with regular reinforcement (Kanstad, Kontroll i bruks- og bruddgrensetilstand, 2022).

3.8.4 Critical moment of cracking

The critical moment of cracking M_{cr}, defines the necessary moment for the cross-section to go from state I to state II. In other words, at the point where $\sigma_{c,tension} = f_{ctm}$. It is possible to find this critical moment by reformulating the formula for stress in state I, and equal it to the mean tension strength in concrete, f_{ctm}. This gives:

$$f_{ctm} = -\frac{P_0}{A_c} - \frac{M_{cr}}{I}y \Leftrightarrow M_{cr} = -f_{ctm}\frac{I}{y} - \frac{P_0}{A_c}\frac{I}{y} \qquad (3.46)$$

3.8.5 Limitation to deflection of flat slab

According to Eurocode 2, clause 7.4.1 (4), the general functionality of the slab may be considered reduced for a load combination with approximate permanent loads, if the corresponding deflection is:

$$\delta_{deflection} > \frac{L}{250} \qquad (3.47)$$

Where L denotes the span length at the area where the value of deflection is extracted. However, in practice, this limitation is often based on what is sought after in the current building project, not necessarily what is provided in the Eurocode 2.

4 Modelling and Analysis

4.1 Building Project

The building project provided by Verkís is of an existing parking house in Reykjavík town, more specifically in Laugavegur 86-94. This parking house is constructed with a post-tensioning system, although in a different manner than what will be analyzed in this thesis. The slab consists of prefabricated concrete elements supported by structural beams with post-tensioning. Because of the existence of these huge structural beams, it allows for long spans such that the entire floor is only held by a single row of thick circular columns. Since the design deviates from the scope of this thesis; post-tensioning system of a flat slab, a part of the task will be to reconstruct and design another solution of the parking cellar. In other words, the number of columns will increase as we reconstruct the design by eliminating structural beams and prefabricated concrete elements with a flat slab with post-tensioned system with uniform thickness. In addition, simplifications of the original sketches of the building project will be done as this analysis is of a preliminary design, so the amount of reinforcement will be a conservative result, which is the usual procedure within preliminary designs.

The original sketches show a system of prefabricated waffle slab elements that are categorized by a numbering system, whereas each number indicates an element with different geometry. This is either by a different geometric size of the element, or a different placement of cavities within each element that forms the element to be of a waffle slab design. Furthermore, the original solution of the parking house also consists of 14 structural beams. These beams are categorized from “Biti B1” to “Biti B8”. The division comes from change in geometry and layout of the post-tensioning reinforcement within the beams. Lastly, due to the presence of these structural beams underneath the slab, it allows for a row consisting of 5 massive circular columns to support the entire slab. Two additional columns are placed at each end of a wall separating the parking space and the drive-in to the parking house.

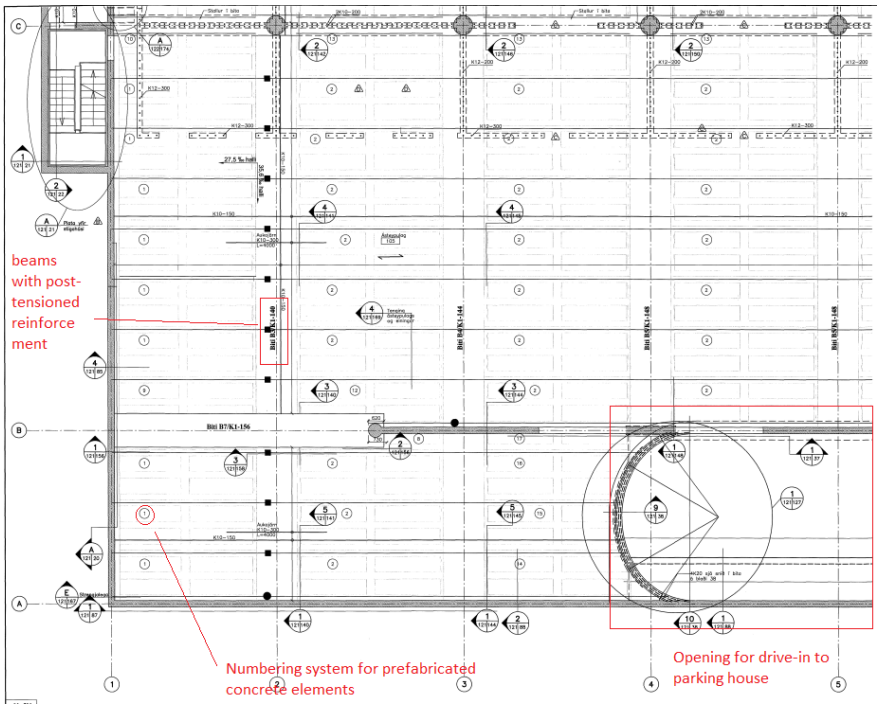

Figure 4.1: *A segment of the original sketches provided by Verkís, illustrating the overall layout of one floor of the parking house*

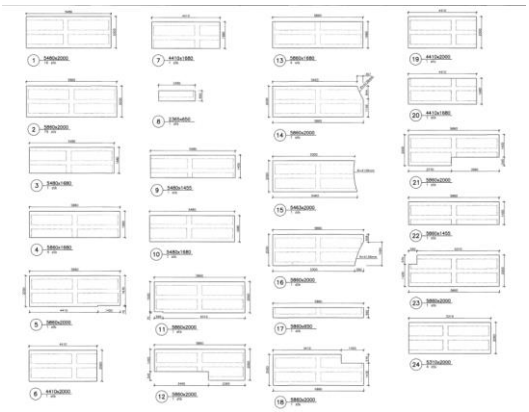

Figure 4.2: *List of prefabricated elements and its geometry provided by Verkís*

A sketch consisting of all necessary geometric dimensions and layout of the parking house is provided below with remarks.

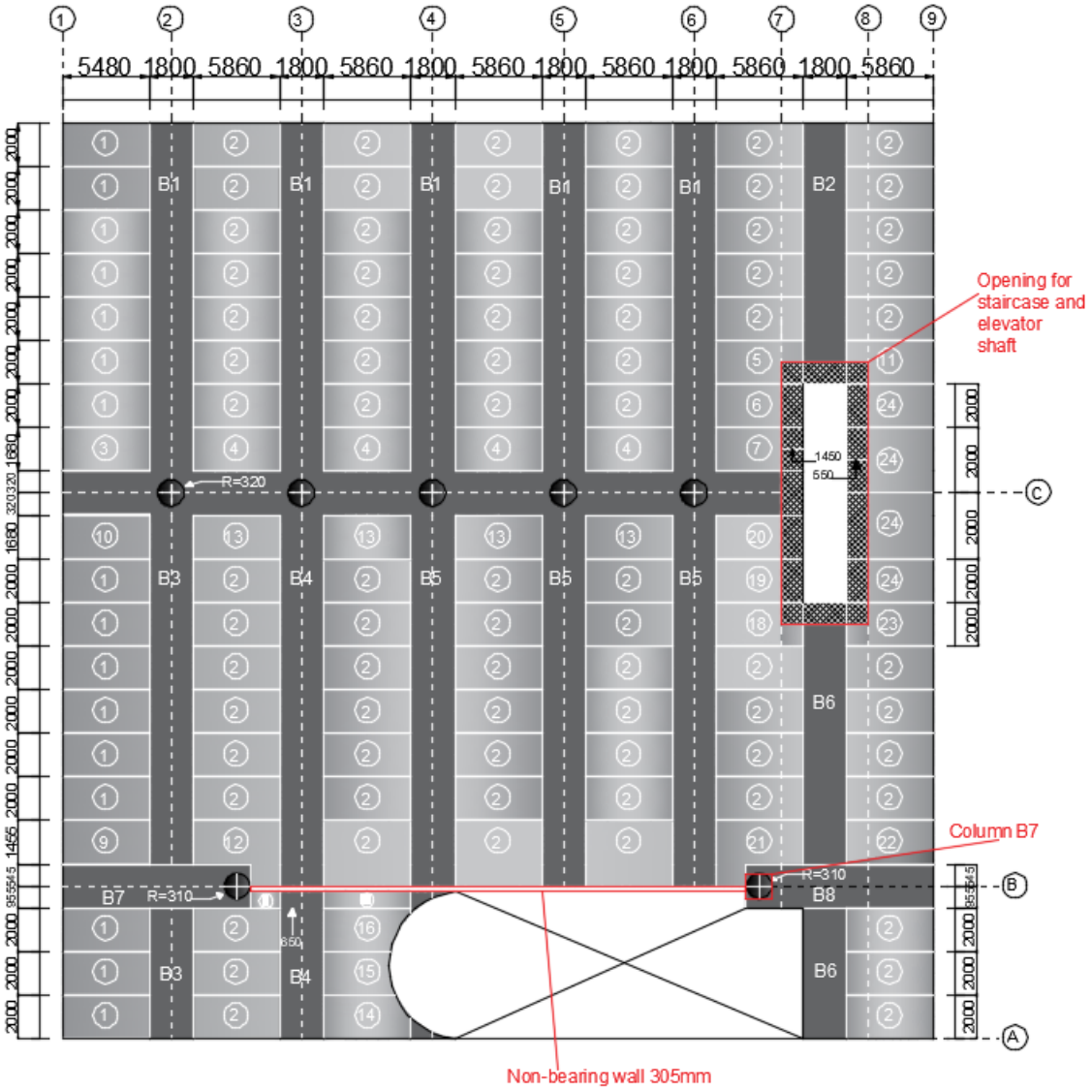

Figure 4.3: *sketch with geometric dimensions of the complete parking lot. Executed in AutoCAD*

As seen from the sketch in Figure 4.3, there is two openings. One opening is a room for staircase and elevator shaft, meanwhile the other is the opening for cars to drive into the parking lot. Additionally, there are 12 vertical beams separating the prefabricated elements, all marked with labels “B1-B6”. Furthermore, 3 vertical beams are also illustrated, whereas one of them remains unlabeled as it is not a structural beam with post-tensioned reinforcement. The positioning of the columns is marked with a circle and is labelled after its positioning in the sketch. Lastly, a wall is highlighted, which separates the drive-in area to the parking space for cars within the floor. The edge of the floor is supported by walls which can be assumed to be of same thickness as the wall highlighted. By combining the geometric dimensions, the total area is shown to be approximately $51{,}440x38{,}955m^2$, neglecting the various openings for staircase and drive-in. Tables that refers to

the numbering systems of columns, banded beams and prefabricated elements are given in the appendix.

4.2 Simplifications & reconstructed design of parking house

The original building project will be reconstructed for us to do an analysis of a post-tensioning system within a flat slab. In other words, the beams containing PT reinforcement and the prefabricated waffle slab elements will be replaced by a concrete slab with uniform thickness. Furthermore, several columns will also be added for the parking house to have a representative flat slab.

Prab Bhatt in her book "*Prestressed concrete design to Eurocodes*" gives recommendations for dimensions of different types of slabs, which is listed below in Table 4.

Table 4.1: *Recommendations for thickness and span length of different slabs (Bhatt, 2011)*

Slab Type	**Slab Span** $[m]$	**Slab depth** $[m]$	**Beam depth** $[m]$	**Span/Depth ratio, slab, beam**
Solid flat slab	6	200		30
	8	250		32
Solid flat slab with drop panels	8	225		36
	12	300		40
One-way slab with band beams	6	150	300	40,20
	8	200	375	40,21
	12	300	550	40,22
Ribbed slab	6	300		27
	8	450		27
	12	575		26

Hence, considering the area $51{,}440x38{,}955\ m^2$ disposable for the design, along with the recommendations given in Table 4.1, a new sketch is provided (Figure 4.4). As the sketch illustrates, the length consisting of $51{,}440\ m$, is divided into 6 span lengths of $8{,}5\ m$ and $8{,}6m$. Furthermore, the width of slab which equals to $38{,}955\ m$ is divided into 5 span lengths of $7{,}791\ m$. For convenience, these span lengths will be rounded up in analysis, such that the 5 span lengths will be $7{,}8\ m$. Hence, the total area as input in ADAPT-Builder will be $51{,}5x39\ m^2$. The influence this rounding will have to the analysis is that the amount of reinforcement, deflection, and amount of concrete, such as slab thickness will slightly increase, so we ensure we will have a conservative analysis.

The choice for thickness that is according to the recommendations given, is taken by iterating the recommended slab depth for solid flat slab with drop panels. Such that, for a maximum span length of $8{,}6m$, recommended slab thickness will be equal to approximately $t = 236\ mm$. However, considering the amount of load, concrete type and coverage which will be specified below, this is not sufficient. The efficiency of each tendon is dependent upon the eccentricity it is allowed to have over columns and fields. Such that, a thicker slab depth will provide each tendon to create more uplift. Since each of the tendons in my analysis is restricted by a relatively big coverage limit, the recommended value of slab thickness will lead to a need for excessive number of cables for the limitations to be in check. In addition, since the concrete type specified is not one of the high-strength concrete types, the limitations to the value of concrete stresses in tension is also restricted. Lastly, the loading is excessive, in that the dead load is more than what is typically considered. It has therefore been deducted that a slab depth of $t = 320\ mm$ will be reasonable given the limitations. This slab depth is more likely to lead to a reasonable number of post-tensioned reinforcement necessary, as it enables each tendon to have more efficiency in terms of uplift.

Initially it was modelled in ADAPT-Builder with rectangular columns of size $400x400mm^2$. This was later changed to rectangular columns of size $550x550mm^2$. We have to keep in mind the equivalent frame method in order to understand the reasoning for this change. It has been previously mentioned that the distributed cables has a width of 1m when it comes to the loading width and when calculating the appropriate moment capacity. It will be explained later that ADAPT-Builder will divide the slab into tributary regions and design cuts. The tributary regions divide the loading and the width of each design cut that ADAPT-Builder bases its moment capacity off. It will also be shown that these tributary regions have a width of $\frac{L}{2}$, such that each calculated moment capacity in ADAPT-Builder is based on a cross-section corresponding that width. For distributed cables, this is not an accurate representation. Furthermore, ADAPT-Builder will provide a possible solution in terms of extra base reinforcement so that the moment capacity is sufficient for each design cut. It is then possible to manufacture a manual design cut of 1m width in the critical areas. Here, it was shown that the loading was much higher since the moment concentrates over the columns. This led to that moment capacity for the manufactured design cuts of 1m width was not sufficient. When the cross-section now has a loading width of 1m, the dimensioning moments over the columns was much higher than dividing the moment in each strip on the loading width of $\frac{L}{2}$. Hence, to have reasonable moments for the distributed cables, increasing the size of the columns was an efficient change in the design.

In addition to the reconstructed design of the parking house, simplifications will be done to the initial parking house. Firstly, we will neglect openings for the elevator shaft, staircase, and the drive-in. Since it is an analysis in the preliminary design phase, neglecting the openings will result in a conservative choice for amount of reinforcement. This is, as mentioned previously, advantageous in early phases of designing. Furthermore, details such as slight slope in the original building project will be neglected.

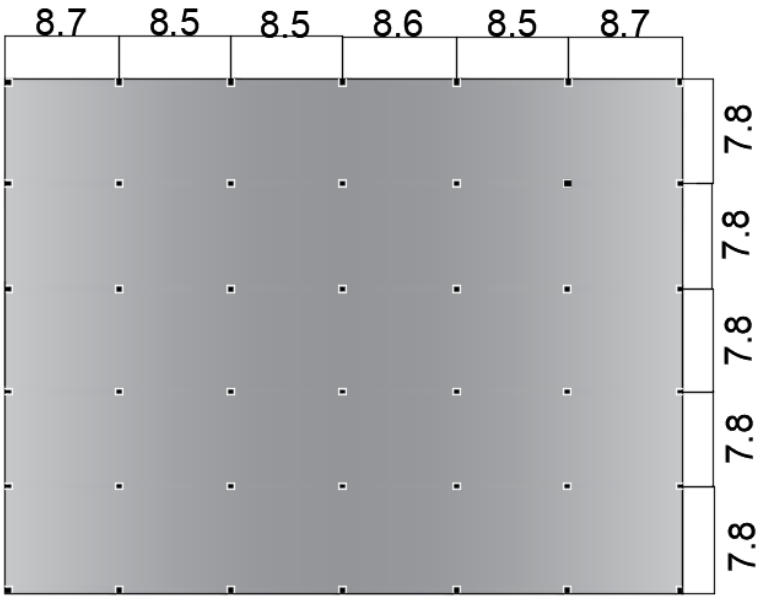

Figure 4.4: *sketch of the revised design of parking house based on recommendations. Executed in AutoCAD*

4.3 Categorization of model in ADAPT-Builder

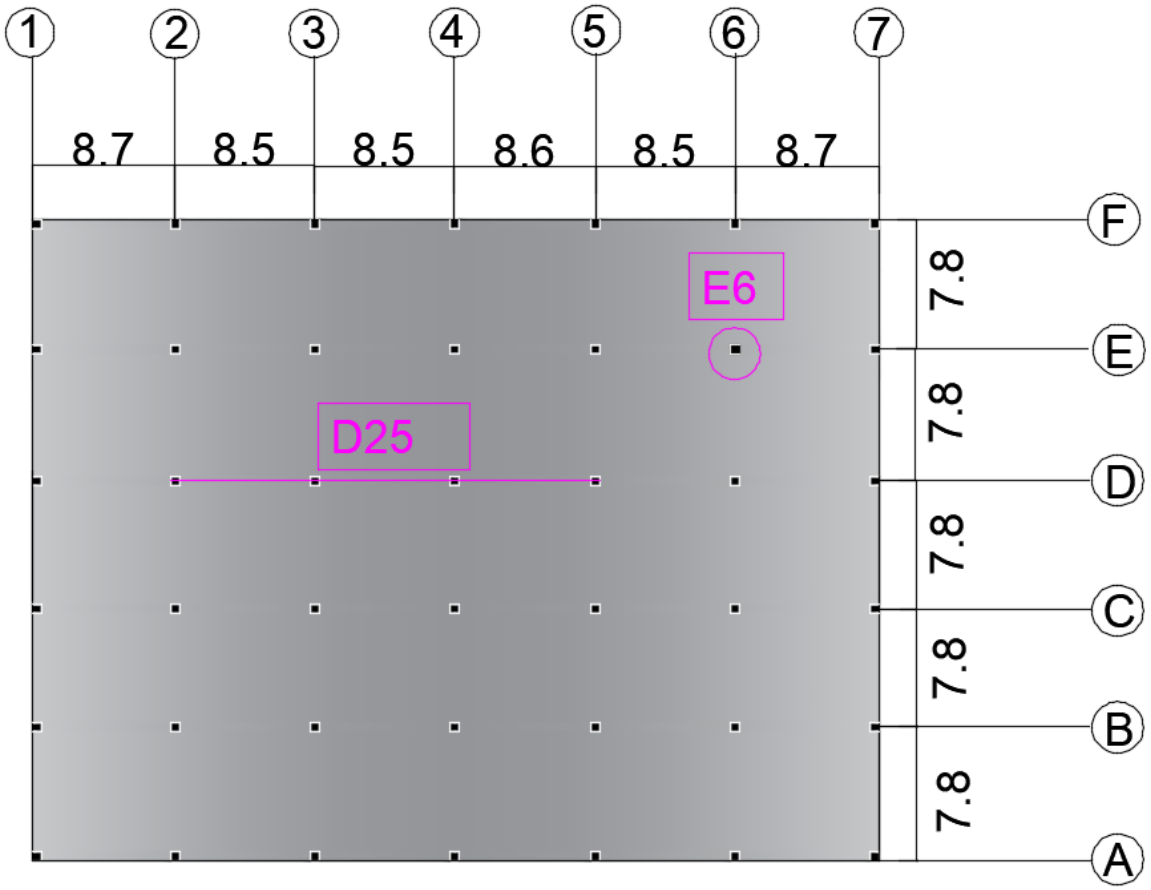

Figur 4.5: *sketch of layout of slab showing gridlines and categorization system. Executed in AutoCAD*

For the reader to have appropriate understanding during this section, it was deemed necessary to produce another sketch of the modelled slab in ADAPT-Builder. The gridlines as shown in the sketch is in accord with the model in ADAPT-Builder. To understand which column is referred to, each column is named after the position it is in based on the gridlines, as shown by the purple circle on the sketch. Field or areas are subsequently named by the gridlines it lays within. Hence, for the purple line in the sketch, this crosses gridline 2 to gridline 5, and follows gridline D.

4.4 Material properties

The original sketches of the parking hall that is executed as a slab with post-tensioned beams has utilized a B35 (C35/45) concrete type. Hence, I will perform the analysis with the B35 concrete type as specified in the project.

Table 4.2: Material properties for the design of parking house [B35]

Material properties for concrete type B35	
Exposure class	XD3
Resistance class	M40
f_{ck}	$35\frac{N}{mm^2}$
f_{cd}	$19{,}83\frac{N}{mm^2}$
f_{ctm}	$3{,}2\frac{N}{mm^2}$
E_{cm}	$34\ Gpa$
ε_{cu}	$3{,}5\ ‰$
h	$275\ mm$
C_{nom}	$60\ mm$

The post-tensioning system will be of the product CCL XU2-15. XU is the initials representing an unbonded post-tensioned system and comprises of a single strand anchored at both ends. This type of unbonded system is commonly used in slabs, and hence is a reasonable choice for the design of post-tensioned flat slab for the parking house (CCL Scandinavia, u.d.). CCL XU2-15 system contains single strands with nominal diameter of 15 mm. The material properties for CCL XU2-15 are provided by CCL as a PDF-file and crucial properties are listed below in Table 4.3.

Table 4.3: Material properties for the design of parking house [CCL XU2-15] (European Technical Assessment, 2020)

Material properties for CCL XU2-15	
A_p	$150\ mm^2$
f_{pk}	$1860\ Mpa$
$f_{p0,1k}$	$1640\ Mpa$
f_{pd}	$1426\ Mpa$
E_p	$195\ 000\ Mpa$
Seating loss $\Delta_{lås}$	$6\ mm$
Friction coefficient μ	$0{,}07\ rad^{-1}$
Wobble factor k	$0{,}001\ \frac{rad}{m^{-1}}$

4.5 Loading

The loading is taken from the description given for the building project. The values are specified underneath in Table 4.4. A concrete type that is reinforced is considered to have a density of approximately $25\frac{KN}{m^3}$. The self-weight of the slab is automatically taken into consideration in the software, in contrast to the other mentioned loadings.

Table 4.4: Loading onto the slab

Loading type	Magnitude $[\frac{KN}{m^2}]$	ψ_0	ψ_1	ψ_2
Dead Load	6			
Live Load	2.5	0.7	0.7	0.6
Self-weight	8			

To understand the origin of the live load and axle load described in the project, it is necessary to define the category type of the building. Table 6.7 in Eurocode 1 (NS EN 1991) gives:

Table 4.5: Traffic- and parking areas in buildings, EC1-1-1 (Standard Norge, 2019)

Categories for traffic areas	Specific use	Examples
F	Traffic and parking areas for lightweight vehicles ($\leq 30\ KN$ gross weight and ≤ 8 seats not considering driver seat)	Garage Parking areas, parking house
G	Traffic- and parking areas for middle to big vehicles ($> 30\ KN, \leq 160\ KN$ gross weight on two axles)	Areas for delivering Areas for arrival of fire trucks ($\leq 160\ KN$ total weight

Furthermore, Table 6.8 in Eurocode 1 (NS EN 1991) gives the designated loading based on category type as follows:

Table 4.6: Live loads on garages and traffic areas, EC1-1-1 (Standard Norge, 2019)

Categories for traffic areas	$\boldsymbol{q_k}\ [\frac{KN}{m^2}]$	$\boldsymbol{Q_k}\ [KN]$
Category F Gross weight: $\leq 30\ KN$	1,5-2,5	10-20
Category G Gross weight: $30\ KN\ < gross\ vehicle\ weight\ \leq 160\ KN$	5	40-90

The building falls within the category F, which is the appropriate category for a parking house. Hence, the live load should be within the span of $1{,}5 - 2{,}5\ \frac{KN}{m^2}$. Here, the national annex recommends $2{,}5\ \frac{KN}{m^2}$. Furthermore, point loads are given which relates to the weight of the vehicles being comprised to pressure points onto the slab from the wheels. Section 6.3.3.2, figure 6.2 in EC1-1-1

gives a proper description of the dimensions of how these point loads are to be applied onto the slab.

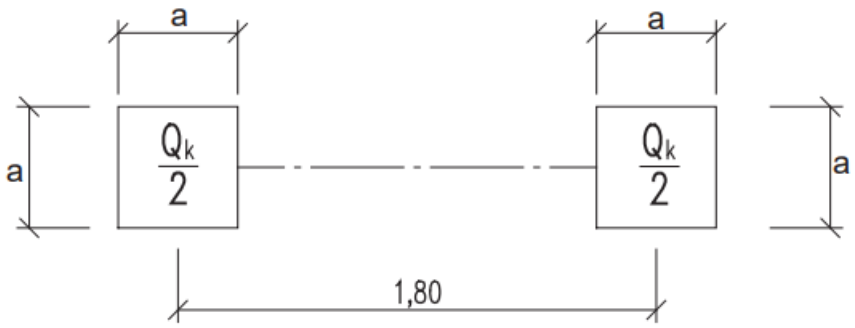

Figure 4.6: *Description of axle load onto slab (Standard Norge, 2019)*

Here, for a category F, the area on which the point load is distributed is $0{,}1x0{,}1m^2$, with a distance of $1{,}8m$. It has been chosen to neglect these point loads during the analysis in ADAPT-Builder.

Table A1.1, in EC0 gives associated ψ factors for the live load which are to be used for the different load combinations:

Table 4.7: *Section of Table A1.1, EC0, describing the attributed ψ factors for live load (Standard Norge, 2016)*

Load	ψ_0	ψ_1	ψ_2
Categories for live load in buildings (look NS EN 1991-1-1)			
Category A: Indoor living areas	0.7	0.5	0.3
Category B: Office areas	0.7	0.5	0.3
Category C: Areas where people gather	0.7	0.7	0.6
Category D: Business areas	0.7	0.7	0.6
Category E: Storage areas	1.0	0.9	0.8
Category F: Traffic areas, gross weight $\leq 30\ KN$	0.7	0.7	0.6
Category G: Traffic areas, gross weight $30\ KN - 160\ KN$	0.7	0.5	0.3
Category H: Roof	0	0	0

The live load is placed in a pattern onto the slab that will result in the most unfavorable condition of loading onto slab for ULS state. This will ensure that a design that is in accord with the ULS-design checks will be able to withstand the worst possible scenario of loading situations. Prab Bhatt in her book "*Prestressed concrete design to eurocodes*" gives recommendations of loading patterns, which has been modelled accordingly. These patterned loadings are created to generate the highest moment within the field between the supports.

However, three additional loading patterns has been created which does not involve the typical loading patterns illustrated in the book. This is recommended patterned load by my mentor, Jan Arve Øverli. The purpose of these patterned loadings is to create the highest moment at the supports. This is also supported by the results from ADAPT-Builder, as will be shown later. Illustrations of the different loading patterns in ADAPT-Builder for the live load is given below. Here, the first four loading patterns are as recommended by Prab Bhatt, and the last three is then the patterned loading recommended by Jan Arve Øverli. In the figures, the green colored areas highlight where the loading is applied.

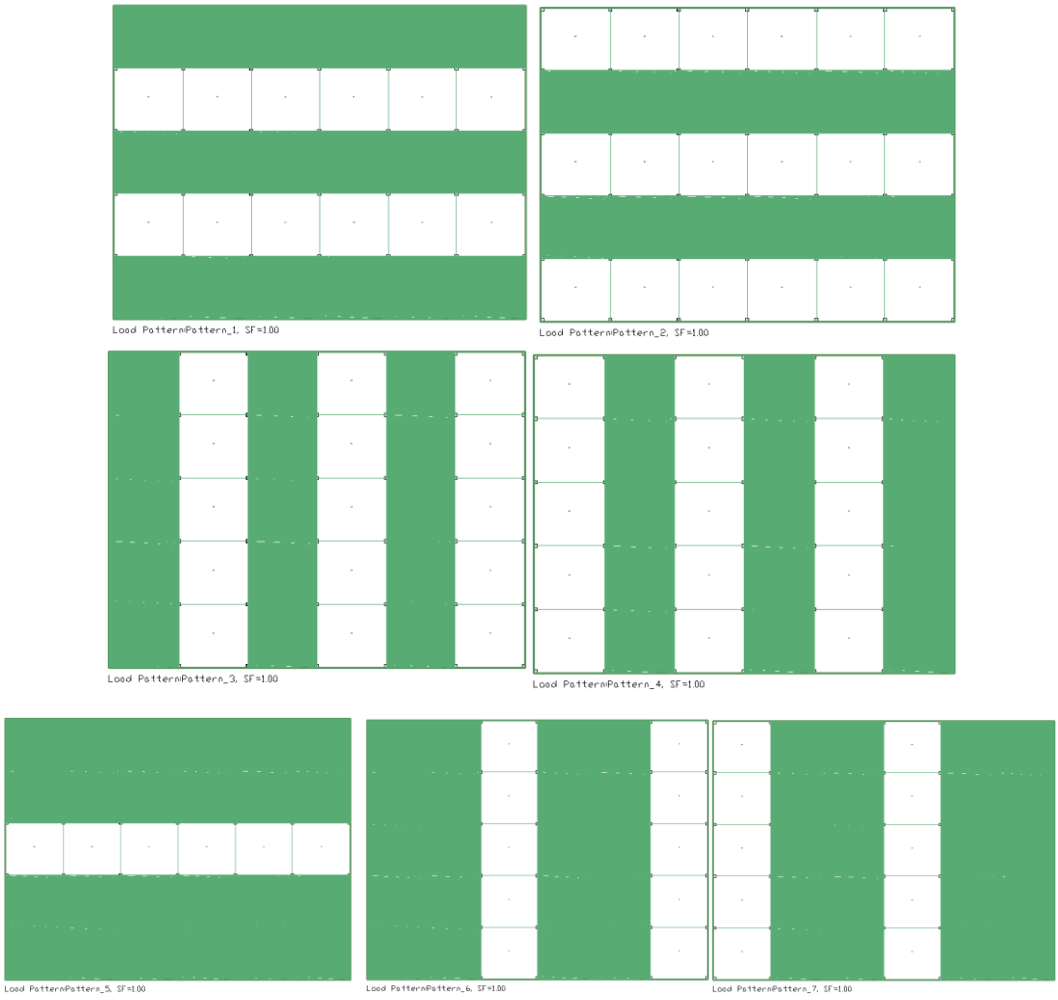

Figure 4.7: *Load patterns for live load programmed in ADAPT-Builder*

Load combinations generated within ADAPT-Builder is in accord with the table NA.A1.2(B), EC0 which gives these equivalent load factors for the ULS load combinations given in table 11. Here, it is also accounted for the presence of prestressing, which also corresponds with a loading factor as mentioned in the chapter of calculation principles. Furthermore, for the SLS load combinations, the load factors are in accord with section 6.5.3, EC0, for the quasi-permanent load combination. As mentioned in chapter of calculation principles, for ULS-state the prestressing is considered as an internal force, where the parasitic moment is an additional contribution to the load combination for indeterminate structures. However, for SLS-state, it is recommended to consider prestressing force as an external force.

Table 4.8: *Load factors for the different load combinations modelled in ADAPT-Builder*

Load combinations	G_k	q_k	M_1	**P**
ULS – unfavorable prestress [EQ.6.10A]	1,35	1,05	1,1	-
ULS – favorable prestress [EQ.6.10A]	1,35	1,05	0,9	-
ULS – unfavorable prestress [EQ.6.10B]	1,2	1,5	1,1	-
ULS – favorable prestress [EQ.6.10B]	1,2	1,5	0,9	-
SLS	1	0,6	-	1

Label	Analysis/Design option	Deflection Load T...	Age at Loading (da...	Observation d...	Load Combination
SLS - shortterm	CRACKED DEFLECTION	Sustained	7		Self + Dead + Live + Pres
ULS - unfavorable - full 6-10A	STRENGTH				1.35 x Self + 1.35 x Dead + 1.05 x Live + 1.1 x Hype
ULS - favorable - full 6-10A	STRENGTH				1.35 x Self + 1.35 x Dead + 1.05 x Live + 0.9 x Hype
ULS - unfavorable - pattern 1 6-10A	STRENGTH				1.35 x Self + 1.35 x Dead + 1.05 x Patt + 1.1 x Hype
ULS - favorable - pattern 1 6-10A	STRENGTH				1.35 x Self + 1.35 x Dead + 1.05 x Patt + 0.9 x Hype
ULS - unfavorable - pattern 2 6-10A	STRENGTH				1.35 x Self + 1.35 x Dead + 1.05 x Patt + 1.1 x Hype
ULS - favorable - pattern 2 6-10A	STRENGTH				1.35 x Self + 1.35 x Dead + 1.05 x Patt + 0.9 x Hype
ULS - unfavorable - pattern 3 6-10A	STRENGTH				1.35 x Self + 1.35 x Dead + 1.05 x Patt + 1.1 x Hype
ULS - favorable - pattern 3 6-10A	STRENGTH				1.35 x Self + 1.35 x Dead + 1.05 x Patt + 0.9 x Hype
ULS - unfavorable - pattern 4 6-10A	STRENGTH				1.35 x Self + 1.35 x Dead + 1.05 x Patt + 1.1 x Hype
ULS - favorable - pattern 4 6-10A	STRENGTH				1.35 x Self + 1.35 x Dead + 1.05 x Patt + 0.9 x Hype
ULS - unfavorable - full 6-10B	STRENGTH				1.2 x Self + 1.2 x Dead + 1.5 x Live + 1.1 x Hype
ULS - favorable - full 6-10B	STRENGTH				1.2 x Self + 1.2 x Dead + 1.5 x Live + 0.9 x Hype
ULS - unfavorable - pattern 1 6-10B	STRENGTH				1.2 x Self + 1.2 x Dead + 1.5 x Patt + 1.1 x Hype
ULS -favorable - pattern 1 6-10B	STRENGTH				1.2 x Self + 1.2 x Dead + 1.5 x Patt + 0.9 x Hype
ULS - unfavorable - pattern 2 6-10B	STRENGTH				1.2 x Self + 1.2 x Dead + 1.5 x Patt + 1.1 x Hype
ULS - favorable - pattern 2 6-10B	STRENGTH				1.2 x Self + 1.2 x Dead + 1.5 x Patt + 0.9 x Hype
ULS - unfavorable - pattern 3 6-10B	STRENGTH				1.2 x Self + 1.2 x Dead + 1.5 x Patt + 1.1 x Hype
ULS - favorable - pattern 3 6-10B	STRENGTH				1.2 x Self + 1.2 x Dead + 1.5 x Patt + 0.9 x Hype
ULS - unfavorable - pattern 4 6-10B	STRENGTH				1.2 x Self + 1.2 x Dead + 1.5 x Patt + 1.1 x Hype
ULS - favorable - pattern 4 6-10B	STRENGTH				1.2 x Self + 1.2 x Dead + 1.5 x Patt + 0.9 x Hype
SLS - longterm	Service Quasi-Permanent				Self + Dead + 0.6 x Live + Pres
steg1	CRACKED DEFLECTION	Sustained	20		Self + Pres
steg2	CRACKED DEFLECTION	Sustained	40		Self + Dead + Pres
steg3	CRACKED DEFLECTION	Sustained	180		Self + Dead + 0.6 x Live + Pres
ULS - unfavorable - pattern 5 6-10A	STRENGTH				1.35 x Self + 1.35 x Dead + 1.05 x Patt + 1.1 x Hype
ULS - favorable - pattern 5 6-10A	STRENGTH				1.35 x Self + 1.35 x Dead + 1.05 x Patt + 0.9 x Hype
ULS - unfavorable - pattern 5 6-10B	STRENGTH				1.2 x Self + 1.2 x Dead + 1.5 x Patt + 1.1 x Hype
ULS - favorable - pattern 5 6-10B	STRENGTH				1.2 x Self + 1.2 x Dead + 1.5 x Patt + 0.9 x Hype
ULS - unfavorable - pattern 6 6-10A	STRENGTH				1.35 x Self + 1.35 x Dead + 1.05 x Patt + 1.1 x Hype
ULS - favorable - pattern 6 6-10A	STRENGTH				1.35 x Self + 1.35 x Dead + 1.05 x Patt + 0.9 x Hype
ULS - unfavorable - pattern 6 6-10B	STRENGTH				1.2 x Self + 1.2 x Dead + 1.5 x Patt + 1.1 x Hype
ULS - favorable - pattern 6 6-10B	STRENGTH				1.2 x Self + 1.2 x Dead + 1.5 x Patt + 0.9 x Hype
ULS - unfavorable - pattern 7 6-10A	STRENGTH				1.35 x Self + 1.35 x Dead + 1.05 x Patt + 1.1 x Hype
ULS - favorable - pattern 7 6-10A	STRENGTH				1.35 x Self + 1.35 x Dead + 1.05 x Patt + 0.9 x Hype
ULS - unfavorable - pattern 7 6-10B	STRENGTH				1.2 x Self + 1.2 x Dead + 1.5 x Patt + 1.1 x Hype
ULS - favorable - pattern 7 6-10B	STRENGTH				1.2 x Self + 1.2 x Dead + 1.5 x Patt + 0.9 x Hype
Long_Term1	Long-Term Deflection	Auto		18250	0.14 x steg + 0.267 x steg + 2.375 x steg

Figure 4.8: *Set of load combinations modelled in ADAPT-Builder*

The total amount of load combinations modelled in ADAPT-Builder is illustrated in Figure 4.8. The amount of ULS combinations comes from applying a load combination that involves the different set of patterned loading for the live load. Since there is 7 patterned loading, in addition to a situation where the live load is applied as a full loading, equals a total of 16 different combinations. However, considering that the load factor for the prestressing is depending upon the prestressing acting in a favorable or unfavorable condition, the total set of load combinations for ULS equals 32 equations. "Live" and "Patt", as denoted in ADAPT-Builder, describes the scenarios where the live load is applied as a full load or as a patterned loading, respectively. Pattern 1 to pattern 4 is the recommended live load patterns given by Prab Bhatt, meanwhile pattern 5 to pattern 7 is the patterns recommended by Jan Arve Øverli. "Hype" stands for hyperstatic loading describes the load factor for the parasitic moment that comes along with indeterminate structures. Lastly "Pres" is the notation for the prestressing force acting as an external load. The hyperstatic moment are automatically calculated as the post-tensioned reinforcement is laid within the slab, and the analysis is executed (ADAPT Corporation, 2004).

For the long-term deflections in the SLS-state, ADAPT-Builder has the option to generate a long-term load combination based on the effects creep and shrinkage has on the model. This is a calculation method within ADAPT-Builder, denoted as Detailed Calculation (ACI 209). The values for creep and shrinkage that is used as input for this calculation method, is based on assumptions as such:

$$RH = 40\%\ Cementclass\ N$$

$$t_0 = 28\ days$$

Hand-calculations with the given assumptions, along with the known characteristics of our model, results in a creep- and shrinkage factor of $2{,}086$ and $4{,}275 * 10^{-4}$ respectively. The three load combinations denoted as steg1, steg2 and steg3, gives information to the calculation method when the different loads are applied within the model. Hence, we consider self-weight and prestressing to be applied and fully developed after a curing of 20 days. Furthermore, dead-weight is considered applied after 40 days, and lastly, live-load is applied at 180 days, with 60% of the load considered as a lasting long-term load. For the load-combination to be considered long-term, we input the observation day to be 18250 days after start. This is equivalent to assessing the deflection of slab after 50 years. This is consistent with evaluating the deflection of a building which is assumed to be dimensioned for 50 years lifespan. The last load combination within the set of load combinations in ADAPT-Builder is therefore generated with built-in factors, depending on the input of creep and shrinkage given.

4.6 Design strips & Element mesh

4.6.1 Design strips

During the modelling in ADAPT-Builder, the slab needs to be subdivided by support lines. These support lines were placed in both global x- and y-direction and follows the pattern of the columns. ADAPT-Builder will then subsequently develop design strips as illustrated below. The purpose of generating design strips is so the program can further subdivide strips into design sections to find properties of the slab during the analysis, such as capacity and necessary reinforcement. The support lines will help to determine the direction the reinforcement is to be placed within the slab. Furthermore, it provides the program with the information on how the loading is to be distributed (RISA Tech., 2023). The support lines will then generate design strips, which contains tributary regions and a certain number of design cuts. Tributary regions decide the loading width and the width of each cross section that will be checked for in terms of moment capacity. Design cuts will then be generated. These design cuts will have the width that is limited by the tributary regions. Each design cut in the slab gives the opportunity for the user to have a detailed analysis of the calculated moment capacity, amount of reinforcement, dimensioning moment etc. in the location for that design cut. It was chosen here to have a design cut at an interval of $300mm$. As mentioned in chapter 3, equivalent frame analysis gives that the loading width of each frame should be equivalent to half of the span width on each side of a column for concentrated cables. For distributed cables, the appropriate loading width should be set to 1m. As is shown in the illustrations below, the design strips are generated with a width corresponding of $\frac{L}{2}$. However, in the direction where the distributed cables lie, it will be manufactured manual design cuts of 1m width in the locations where it is most critical.

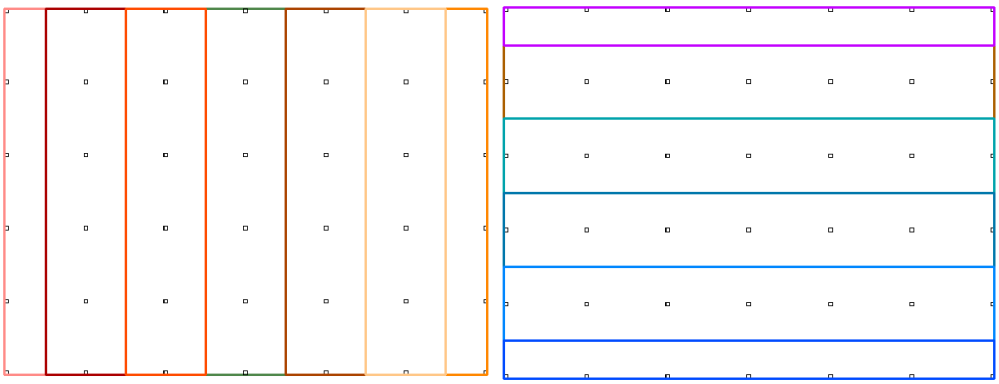

Figure 4.9: *Design strips in ADAPT-Builder*

Design strips in y-direction

Design strips in x-direction

4.6.2 Element mesh

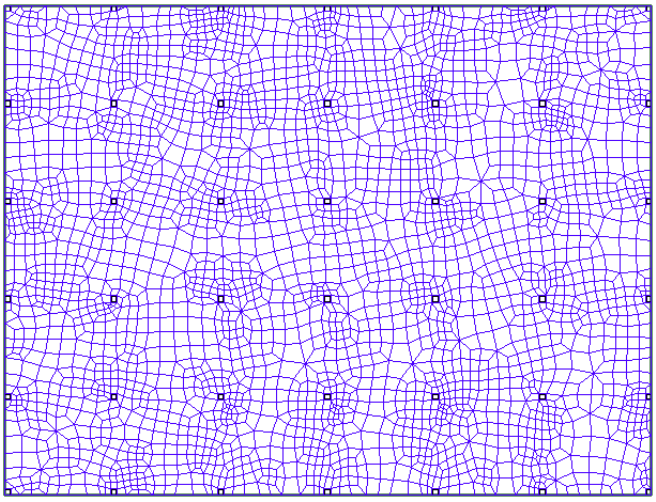

Figure 4.10: *Element mesh of slab in ADAPT-Builder*

Generating the design strips will enable the program to progress by either do the analysis with equivalent frame method or finite element method. Within the finite element method, you must discretize the slab into element of a size with a set of nodes that will accompany you with information of stresses, forces and displacements at the point of the nodes. ADAPT-Builder presents to you the option to choose element size, and whether you choose to let the program calculate a mesh distribution for you, make advanced adjustments to the original mesh or simply manually mesh it yourself. For the automatic mesh generation, ADAPT-Builder creates almost exclusively quadrilateral elements within the mesh. In most cases, $\frac{1}{6} - \frac{1}{8}$ division of the span length is a typical choice for element size. This will most commonly result in an accuracy of 98% to the results (RISA Tech., 2023). This equates to an element size of $1 - 1{,}37\ m$ for a mean span length of $\frac{8.5*5+8.6+7.8*5}{11} = 8{,}19\ m$. Furthermore, ADAPT-Builder recommends a node-distance within each element to be of 2-3 times the slab depth, which then equates to $0.64 - 0.96\ m$. Hence, it has been used the recommendations ADAPT-Builder has provided, which is element size of approximately $1.25\ m$ and maximum node-distance of $0.75\ m$. The program-generated element mesh is shown in the illustration above.

It is typical to do a finite element analysis first, in where ADAPT-Builder requires you to choose the load combinations that should undergo an analysis. After the finite element method, it is then possible to do a design of section, which is the equivalent frame method within ADAPT-Builder. It will

then take the set of load combinations chosen from the finite element method and calculate properties within each cross-section from the design cuts.

4.7 Base reinforcement

NA.9.2.2.1(1), EC2 gives following criteria for minimum reinforcement:

$$A_{s,min} = 0{,}26\frac{f_{ctm}}{f_{yk}} b_t d \geq 0{,}0013 b_t d$$

Where b_t denotes the mean width of the tension zone. This is the minimum required non-prestressed reinforcement for the reinforcement under tension. This is to ensure that the model has sufficient ductility. It is common to reinforce the slab with a reinforcement mesh of the type K 189 or K257, which is equivalent to $189\ \frac{mm^2}{m}$ and $257\ \frac{mm^2}{m}$, respectively. If this alone is not sufficient, it is common to further add reinforcement of bar size ø10 or ø12 (Trygstad, Etteroppspente uinjiserte betongdekker beregningseksempel, 2022). To meet the criteria for minimum reinforcement in the tension zones, it is common to reinforce both the upper- and lower edge of slab, as the tension zone exists in the lower edge of section within field, and upper edge of section by the supports. Furthermore, it is also practically beneficial, as it provides the on-site workers a reinforcement mesh to walk upon (Trygstad, Etteroppspente uinjiserte betongdekker beregningseksempel, 2022).

Considering the coverage of $60\ mm$, the presence of reinforcement in both x- and y-directions, and assumed bar size of ø10, the effective cross-section depth d_{mean} is approximately $250\ mm$.

the criterion for minimum reinforcement becomes:

$$A_{s,min} = 0{,}26 * \frac{3{,}2}{500} * 250 \geq 0{,}0013 * 250$$

$$A_{s,min} = 416\frac{mm^2}{m}$$

To meet with the criterion for minimum reinforcement, the slab is modelled with K 257, and supplemented further with $Ø10c450$, which results to $431{,}53\frac{mm^2}{m}$. This is a reinforcement mesh that is added in both upper- and lower edge of slab, so that all the areas within the tension meets within the criterion given.

Mesh Reinforcement

ID	Size 1	Spacing 1	As1	Size 2	Spacing 2	As2	Area	Weight	Unit cost	Total cost
		mm	mm2/m		mm	mm2/m	m 2	kg	Euro/kg	Euro
1			257.00			257.00	2008.50	8052.48	3.00	24157.43
2	10mm	450		10mm	450		2008.50	5465.80	3.00	16397.39
3	10mm	450		10mm	450		2008.50	5465.80	3.00	16397.39
4			257.00			257.00	2008.50	8052.48	3.00	24157.43
Total								27036.55		81109.66

Figure 4.11: *Report of the added mesh reinforcement within ADAPT-Builder*

4.8 Prestressing system within the slab

The cables defined as the prestressing system CCL XU2-15 is defined as cables used for unbonded post-tensioning. As this material product is utilized in this master, the cables in ADAPT-Builder have been modelled accordingly as an unbonded post-tensioning system. Furthermore, the tendon height has been set to $15\ mm$ in ADAPT-Builder as specified by the XU2-15 material properties.

4.8.1 Layout of post-tensioning reinforcement

For the post-tensioning system within the slab, it has been modelled as distributed strands in one direction and concentrated in the other. The concentrated strands are modelled along the longer side of the slab, more precisely $L = 51{,}500\ m$. Hence, the distributed cables are modelled along the shorter side, $L = 39\ m$. This gives the concentrated cables a loading consisting of a width of $7{,}8\ m$ and $3{,}9\ m$ as the design strips illustrates. Subsequently, the distributed cables will receive a loading of a width equivalent to $8.5\ m$, $8.55m$ and $4.25\ m$.

As mentioned in chapter 3, it is important to ensure that the concrete stress in tension is lower than the mean value of its strength in tension.

$$\sigma_{c,tension} \leq f_{ctm}$$

If this is sufficient, then we ensure that our model is considered in an uncracked state, and we can therefore calculate the concrete stresses within the slab according to state 1. However, if this is not sufficient, the slab must be considered as a cracked state, and the concrete stresses must be calculated within state 2 for cracked cross-sections. Furthermore, it is also stated how the concrete stresses should not exceed a certain level of stress in compression. This limitation is given below.

$$\sigma_{c,compression} \leq 0{,}6 f_{ck}(t)$$

Typically, the post-tensioned reinforcement is dimensioned after the criterions given in SLS. More precisely, these limitations to concrete stresses and deflection of slab. To ensure that the concrete stresses does not exceed the mean strength in tension for our concrete type ($f_{ctm} = 3{,}2\ Mpa$), it has

been deducted an approximate amount of post-tensioned reinforcement based on how big of a contribution the prestressing will have to the overall concrete stress. This is the formula that is applicable for uncracked cross-sections.

$$\sigma_c(t) = -\frac{P_0}{A_c} - \frac{M}{I}y$$

The distributed cables were modelled with a spacing of 1000 mm. For the concentrated cables, it was provided 14 cables for the bigger design strips and 6 cables for the design strips at the edges. Further analysis should provide more information on whether the amount of reinforcement is within the limit of $3{,}2\ Mpa$, when the contribution from the moment is fully established. This will in turn result to edits on the reinforcement, or alternatively the concrete type for the analysis to be with sufficient results according to the different standards. In another instance, it could be the case that the amount of reinforcement is insufficient in terms of design checks. Again, the need for edit of current reinforcement layout, slab thickness or concrete type needs reevaluated, so it is possible to find a design that meets both the criterions and design checks.

The initial post-tensioned layout was then analyzed according to the concrete stresses in the slab. This is done by using the SLS quasi-permanent load combination: $self + dead + 0{,}6Live + pres$. By editing the amount of post-tensioned reinforcement, the limitations to concrete stresses was met. The distributed cables were modelled with a spacing of 925 mm. The number of tendons within each design strip, and the resulting dimensioning concrete stresses are shown in the table below.

Table 4.9A: *number of tendons within each design strip and the resulting concrete stresses in ADAPT-Builder in y-direction*

Design strip	n_y	$\sigma_{c,tension}\ [Mpa]$	$\sigma_{c,compression}\ [Mpa]$
AF1	5	2,339	-3,627
AF2	9	3,157	-4,369
AF3	9	2,864	-4,152
AF4	9	3,092	-4,353
AF5	10	2,96	-4,202
AF6	9	3,158	-4,343
AF7	5	2,341	-3,697

ADAPT-Builder provides the option to represent one visual cable in the model as x actual strands. This has been done for the concentrated cables, as each cable in the longer direction of the slab then represents a certain number of tendons. These cables are modelled in ADAPT-Builder as 3-4 cables

per tendon visible in the model, and with a spacing of $400mm$. Hence, each strand is applied within a spacing of $100mm$. The number of concentrated cables varies between 3-18 cables per design strip. The number of tendons and the resulting dimensioning concrete stresses for each design strip is shown in the table below.

Table 4.9B: *number of tendons within each design strip and the resulting concrete stresses in ADAPT-Builder in x-direction*

Design strip	n_x	$\sigma_{c,tension}\ [Mpa]$	$\sigma_{c,compression}\ [Mpa]$
A17	4	3,044	-4,644
B17	16	3,149	-5,3
C17	14	3,035	-5,265
D17	12	3,02	-5,14
E17	18	3,036	-5,258
F17	3	3,094	-4,572

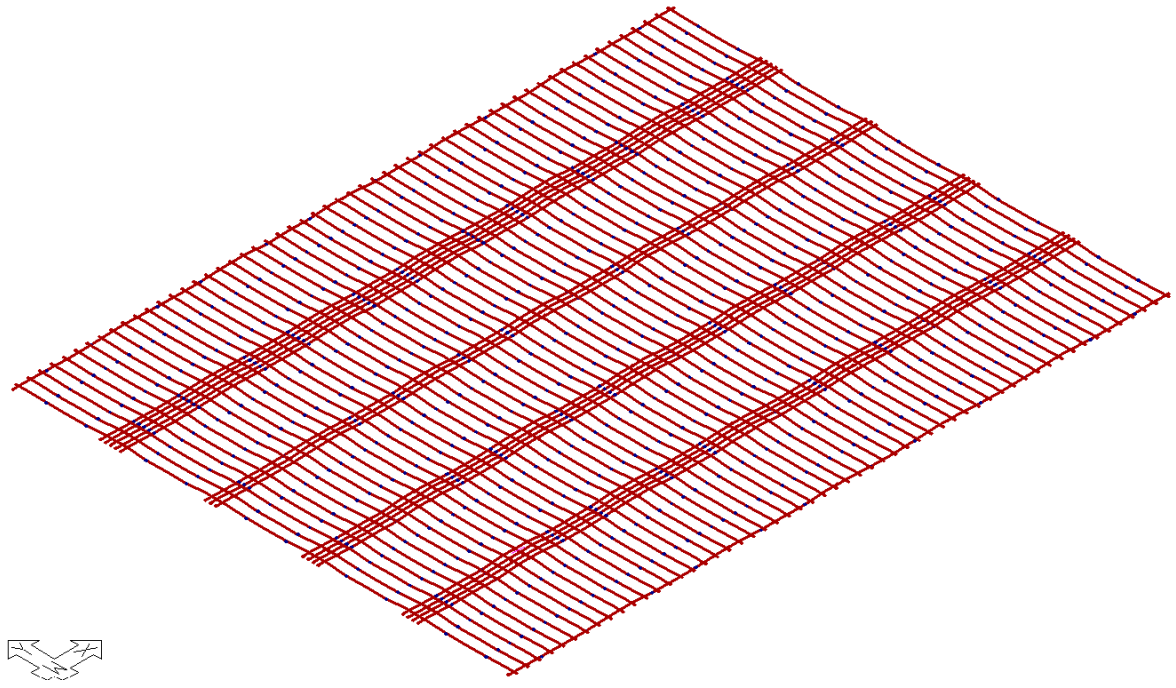

Figure 4.12: *Layout of the post-tensioned reinforcement: Equally distributed cables of spacing 925mm in the y-direction and concentrated cables, each with 3-4 cables, over the columns in x-direction*

Keep in mind that the PT-reinforcement was modelled to be within the limitations of EC2. As the slab is further modelled to be sufficient in terms of moment capacity, supplementary base reinforcement is needed at certain locations. The supplementary reinforcement will then contribute to decrease the concrete stresses further. This leads to a solution in where the concrete stresses are with a bit bigger margin in terms of the limitations.

4.8.2 Cable profile

For practical purposes, a harped cable profile is modelled in ADAPT-Builder. For the harped cable profile, the cables are assembled horizontally in the center of field areas, as well as over the support columns. Utilizing this type of cable profile results in an easier assembly at the workplace. Furthermore, a ratio of $\frac{A}{L} = 0{,}4$ will provide good results, in terms of higher uplift compared to a typical parabola shaped cable profile (Trygstad, Etteroppspente uinjiserte betongdekker beregningseksempel, 2022). Here, A describes the length of the segment of cable that is consistently horizontally assembled in the cable profile. L describes the length of each of the spans.

A typical layout of a cable profile is that it is placed on the upper- edge of slab over the supports, and lower-edge of slab at the field areas in between the supports. This is so it can create more efficient uplifts in accord with a typical moment pattern for a slab. Hence, so it counteracts the natural deflections within the slabs.

As the post-tensioning reinforcement in both directions collides over the supports, the eccentricity between the distributed- and concentrated reinforcement should be altered. In a practical aspect, the concentrated reinforcement is often the reinforcement that is placed firstly, and so it is natural to place the concentrated cables with a lower eccentricity than the distributed over the supports. In addition, it needs to be considered the need for supplementary reinforcement. Here it is chosen a recommended bar size of $16mm$, which should be accounted for when positioning the tendons. As a summation, it should be considered the minimum coverage of $60\ mm$, and the presence of XU2-15 in both directions, each with a $15\ mm$ diameter, slab thickness of $320\ mm$, base reinforcement mesh with 10 mm diameter and supplementary reinforcement of $16mm$ diameter. This results in a distance of $114{,}5\ mm$ from center of gravity of cable to upper edge of slab for concentrated cables. For the distributed tendons, the distance is correspondingly $99{,}5\ mm$. In ADAPT-Builder, it will be rounded up to $115mm$ and $100mm$ respectively.

For the lower edge at the field areas in between the supports, the cables are resting on top of a regular reinforcement mesh. Therefore, it should be considered the presence of reinforcement mesh in both directions with $10\ mm$ diameter, minimum coverage of $60\ mm$ and the supplementary reinforcement with $16mm$ diameter for the lower edge of slab. the distance between center of

gravity of tendon to lower edge of slab is approximately $100\ mm$. The various cable profiles are illustrated as shown below.

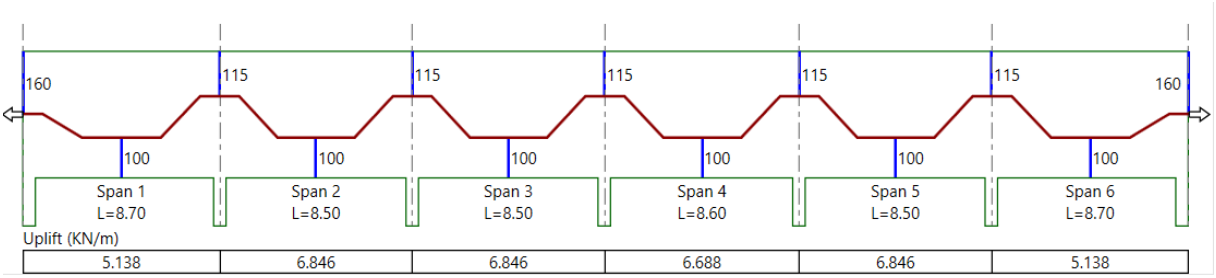

Figure 4.13A: *Cable profile of the concentrated tendons in ADAPT-Builder and the generated uplift per span length. This is cable profile of 4 tendons.*

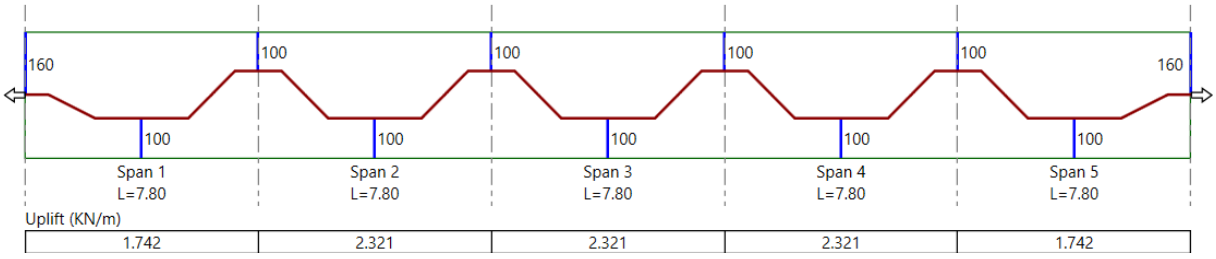

Figure 4.13B: *Cable profile of the distributed tendons in ADAPT-Builder and the generated uplift per span length. This is cable profile of one tendon.*

4.8.3 Prestressing force and prestress losses

Anchorage systems

In terms of anchorage system, it has been chosen to have active anchorages on both ends of each tendon in both directions. For tendons that exceeds $35\ m$, it is recommended to have active anchorage system on both ends (Trygstad, Etteroppspente uinjiserte betongdekker beregningseksempel, 2022). Since both the concentrated- and distributed tendons are placed within a slab of $51{,}5x39\ m^2$, the tendons have been modelled in ADAPT-Builder correspondingly.

Prestress force

The maximum jacking force allowed to be put into the system of XU2-15 is given to be $221\ KN$ (European Technical Assessment, 2020). As previously mentioned in chapter 3, EC2 5.10.2.1 (1) gives a criterion to the maximum possible jacking force. Utilizing the given material properties of our system, the resulting prestress P_{max} is given to be $221{,}4\ KN$.

$$P_{max} = A_p * \sigma_{p,max} = 150mm^2 * 1476\frac{N}{mm^2} = \mathbf{221{,}4\ KN}$$

$$\sigma_{p,max} = min\{0.8f_{pk}\ , 0.9f_{p0,1k}\} = min\{0.8 * 1860\ , 0.9 * 1640\} = 1476\ Mpa$$

As the limit for maximum jacking force in EC2 exceeds the provided jacking force for the XU2-15 system, $221\ KN$ has been modelled in ADAPT-Builder as the provided jacking force. Furthermore, EC2 5.10.3 gives the limitation to how big the prestress force should be after accounting for the immediate losses. Hence, with the provided material qualities for XU2-15, the initial prestress force P_{m0} is given as $209{,}1\ KN$.

$$P_{m0}(x) = A_p * \sigma_{pm0}(x) = 150mm^2 * 1394\frac{N}{mm^2} = \mathbf{209{,}1\ KN}$$

$$\sigma_{pm0}(x) = min\{0.75f_{pk}\ , 0.85f_{p0,1k}\} = min\{0.75 * 1860\ , 0.85 * 1640\} = 1394\ Mpa$$

Short-term prestress losses

ADAPT-Builder has the option to calculate the effective prestress force and long-term losses. In accord with the given material properties of the tendon system XU2-15, the seating loss is given as $6\ mm$. Furthermore, the wobble factor $k = 0{,}001\ \frac{rad}{m^{-1}}$ and the friction coefficient of $\mu = 0{,}07$ is also considered in ADAPT-Builder. This enables the program to accurately calculate the short-term losses, considering the friction losses and seating losses which are inevitable losses for post-tensioned tendons. The resulting forces and input in terms of prestress losses in ADAPT-Builder is given in the appendix.

Table 4.10A: *prestress force after immediate losses*

Tendons	$\boldsymbol{P_0}$ **ADAPT-Builder** $[\boldsymbol{KN/cable}]$	$\boldsymbol{P_0\ Hand\ calculated}\ [\frac{\boldsymbol{KN}}{\boldsymbol{cable}}]$
Distributed cables	205.32	206.32
Concentrates cables	206.81	206.35

As the table illustrates, the prestress force after immediate losses does not exceed the limitations of the initial prestress force, $P_{m0} = 209{,}1\ KN$, given by EC2.

Long-term prestress losses

ADAPT-Builder has the option to estimate long-term losses. This is assumed to be $75\ Mpa$ in the program. This is a reasonable value, as is often shown by hand-calculations according to Steinar Trygstad (Trygstad, Etteroppspente uinjiserte betongdekker beregningseksempel, 2022). For a

tendon with an area equivalent to $150\ mm^2$, this results into a loss of $11{,}25\ KN$ considering all forms of long-term losses.

Table 4.10B: *prestress force after long-term losses and immediate losses*

Tendons	P ADAPT-Builder $[\frac{KN}{cable}]$	$P\ Hand\ calculated\ [\frac{KN}{cable}]$
Distributed cables	194.07	183.89
Concentrated cables	195.56	196.45

The table above shows that the hand-calculated effective prestress force after time-dependent losses is close to the prediction by ADAPT-Builder, for concentrated cables. However, for distributed cables, the deviance is larger. This arises since the stresses in concrete for distributed cables is less counteracted by prestressing than for concentrated cables, as the spacing is $925\ mm$. This will in turn lead to relatively high stress-level at point of prestressing tendons in cross-section. Hence, the effect for time-dependent losses for distributed cables becomes much larger than for the concentrated cables.

Contribution from each type of prestress loss

The hand calculated resulting prestress losses comes from calculating how much loss each type of prestress loss has on the system. Below are the resulting data and corresponding prestress force after each type of prestress loss.

Table 4.11: *Table showing how much prestress force is lost by each type of mechanism, and the resulting effective prestress force*

Type of cable	Type of prestress loss	Loss [KN]	Corresponding prestress force after loss [KN]
Concentrated cables	Friction loss	≈ 10.465	
	Draw-in loss	16.89	
	Loss due to elastic deformation	0.968	
	Total		**206.35**
	Time-dependent losses	9.9	
	Total		**196.45**

Distributed cables	Friction loss	≈ 9.6825	
	Draw-in loss	18.67	
	Loss due to elastic deformation	0.43	
	Total		**206.32**
	Time-dependent losses	22.43	
	Total		**183.89**

4.9 Ultimate limit state

4.9.1 Moment capacity

The check of moment capacity has been done by analyzing the structure with the ULS combinations added in ADAPT-Builder. This then equals the 32 different set of load combinations, due to the various loud patterns and load factors.

The moment capacity in the structure will be sufficient if the dimensioning moment is lower than the capacity at the cross-section is evaluated.

$$\frac{M_{Ed}}{M_{Rd}} \leq 1$$

ADAPT-Builder will check the moment capacity by firstly use the finite element method to find the dimensioning forces at the different nodes in the slab. Secondly, it will analyze based on the defined design strips and generate cross-sections within these design strips. It is during this analysis that ADAPT-Builder will consider the amount of reinforcement added and calculate the moment capacity each cross-section has. As a result, it will compare the moment capacity to the dimensioning moment and give a graphical view which cross-section in which design strip does not pass the ULS check.

It is common to dimension the amount of PT-reinforcement based on SLS checks such as concrete stresses and deflection. Secondly, to ensure that moment capacity is sufficient, non-stressed reinforcement is added. ADAPT-Builder has the option to provide you a calculated rebar plan to create enough moment capacity in the sections where it is not sufficient. This solution has been added in the slab and is shown in the appendix.

Table 4.12: Dimensioning moment and capacity from ADAPT-Builder and verification by hand of moment capacity

ADAPT-Builder					
Type of moment	**Position**	$M_{Ed}\ [KNm]$	$M_{Rd}[KNm]$	$\frac{M_{Ed}}{M_{Rd}}$	**Load Combination**
$Field_{x-direction}$	D12	897.7	935.3	0.96	ULS unfavorable pattern 3 6-10A
$Support_{x-direction}$	B6	-998.7	-1007	0.992	ULS favorable pattern 7 6-10A
$Field_{y-direction}$	AB2	101.2	102.2	0.99	ULS unfavorable pattern 1 6-10A
$Support_{y-direction}$	E2	-198.1	-268	0.739	ULS favorable pattern 5 6-10A
Verification by hand					
Type of moment	**Position**	$M_{Ed}\ [KNm]$	$M_{Rd}\ [KNm]$	$\frac{M_{Ed}}{M_{Rd}}$	**Load combination**
$Field_{x-direction}$	D12	897.7	834.68	1.076	ULS unfavorable pattern 3 6-10A
$Support_{x-direction}$	B6	-998.7	-982.55	1.016	ULS favorable pattern 7 6-10A
$Field_{y-direction}$	AB2	101.2	103.4	0.979	ULS unfavorable pattern 1 6-10A
$Support_{y-direction}$	E2	-198.1	-271.8	0.729	ULS favorable pattern 5 6-10A

As the table shows, the dimensioning moment in the x-direction is much larger than in the y-direction. This is due to that the concentrated cables should be considered with a loading width equivalent to $\frac{L}{2}$. Meanwhile, distributed cables should be considered with a loading width of $1m$. Initially, the tributary regions are defined with a width of $\frac{L}{2}$. By finding the critical section in y-direction, a manual design section of width $1m$ was created to extract the appropriate dimensioning moment and moment capacity for the appropriate width for moment capacity and loading. For the x-direction, the moment capacity from ADAPT-Builder is based on a cross-section of width $\frac{L}{2}$. However, the moment capacity is conservatively based on a width of $\frac{L}{4}$ when calculated by hand. This is the proper moment capacity based on the recommendations given by Terje Kanstad for concentrated cables in equivalent frame method (Kanstad, Verifikasjon av resultater, håndregning. , 2022). ADAPT-Builder creates a supplementary rebar plan to achieve ratio under 1 for capacities based on a width of $\frac{L}{2}$. Hence, the actual moment capacity will not be sufficient when considering width of $\frac{L}{4}$ with a loading width of $\frac{L}{2}$, as the hand calculations show. However, this is considered a conservative moment verification approach, and adjusting the model for this requires manually supplementing with more rebars in many sections. The hand calculations for the moment capacities are given in the appendix.

As seen from table, the hand calculated moment capacity and the program-generated capacity by ADAPT-Builder varies slightly in the y-direction. The reasoning behind deviances may be due to rounding of reinforcement available within the critical section, in addition to α.

4.9.2 Shear capacity

It is also important to control for shear punching. The first control should be done for an internal column with the highest dimensioning normal force. Hence, the column that will be critical in terms of loadings. Another check is done for the end/edge columns where the area available u_1 is smaller, and so the dimensioning shear stress for such columns is higher. In addition, End/edge columns will also be limited in terms of contribution from prestressing cables σ_{cp}, as mentioned in section 3.7.2.

As mentioned previously in chapter 3, EC2 6.4.3(2) gives the following checks for shear punching:

a) $\upsilon_{Ed} \leq \upsilon_{Rd,max}$
b) $\upsilon_{Ed} \leq \upsilon_{Rd,c}$
c) $\upsilon_{Rd,cs} \geq \upsilon_{Ed}$

Here, the last check is applicable if check in b) is not passed, so there is a need for reinforcement to prevent shear punching failure.

Internal Column

Column E2 was found as the column with the highest dimensioning forces. The normal force within the column was found to be $V_{Ed} = 1672{,}1\ KN$. There is a presence of moment around both axis, and so the β value was taken from the recommended values in EC2 for internal columns (Figure 6.21N in EC2). The columns are with the dimensions $c_1 * c_2 = 550 * 550\ mm^2$ and the effective depth d_{eff} is estimated when considering the presence of base reinforcement, supplementary reinforcement, presence of shear reinforcement and post-tensioned reinforcement along both directions. ADAPT-Builder here informs that the $d_{eff} = 244\ mm$. The resulting circumferences are then $u_1 \approxeq 5266.19\ mm$ and $u_0 = 2200\ mm$. This leads to a dimensioning shear stress of:

$$\upsilon_{Ed} = 1.496\ Mpa \text{ for check at } u_1$$

$$\upsilon_{Ed} = 3.582\ Mpa \text{ for check at } u_0$$

$\upsilon_{Rd,max}$ is given as $4{,}09\ Mpa$, such that check a) is sufficient against the appropriate $\upsilon_{Ed} = 3.582\ Mpa$. This is considering the mentioned effective depth and the concrete type B35.

The capacity check without necessary reinforcement for shear punching was proven to be not sufficient. As mentioned previously in section 3.7.2, for concentrated cables, the affected area in terms of σ_{cp} follows a distribution at an angle 45° until it reaches $\frac{L}{2}$. In this case, column E2 is placed $8.5\ m$ from edge, which means the entire affected area b_x equals the entire loading width ($b_x = 7.8\ m$). Furthermore, the base reinforcement that is considered in this calculation is only the reinforcement that is assumed to be in tension. It is assumed that the base reinforcement that contributes to the capacity for shear punching is the reinforcement that lies within the span of column width plus $3d$ on each side. As a result, $\upsilon_{Rd,c}$ is calculated to be $0.843\ Mpa$. Since this is checked against the dimensioning shear stress at the critical circumference u_1, the shear capacity is not sufficient without additional shear reinforcement.

Necessary shear reinforcement has then been calculated, with an assumption of radial distance $\mathrm{S_r} = 160\ \mathrm{mm}$. The necessary shear reinforcement can be calculated when the shear capacity with shear reinforcement $\upsilon_{\mathrm{Rd,cs}}$ equals the dimensioning shear stress $\upsilon_{\mathrm{Ed}} = 1.496\ \mathrm{Mpa}$. The necessary reinforcement was calculated to be $\mathrm{A_{sw}} = 1560.1\ \mathrm{mm^2}$. As a result, it was chosen to reinforce the columns with 20Ø10, which equals $\mathrm{A_{sw}} = 1570.8\ \mathrm{mm^2}$. With this choice of shear reinforcement, the capacity $\upsilon_{\mathrm{Rd,cs}}$ is calculated to be $1.5\ \mathrm{Mpa}$. Hence, the shear capacity is sufficient with given shear reinforcement, as the dimensioning stress is given as $\upsilon_{\mathrm{Ed}} = 1.496\ \mathrm{Mpa}$.

EC2 6.4.5(1) gives limitation to how big contribution the shear reinforcement can have to the shear capacity. This limitation is given as $\mathrm{k_{max}}\upsilon_{\mathrm{Rd,c}}$. Here, $\mathrm{k_{max}}$ is dependent on the type of shear reinforcement used in the design. Terje Kanstad recommends the use of a T-headed studs as shear reinforcement type on prestressed slabs (Kanstad, Verifikasjon av resultater, håndregning. , 2022). This leads to $\mathrm{k_{max}} = 1.8$, which gives the limitation to be $\mathrm{k_{max}}\upsilon_{\mathrm{Rd,c}} = 1.517\ \mathrm{Mpa}$. In other words, the calculated shear capacity $\upsilon_{\mathrm{Rd,cs}}$ is ultimately $1.5\ \mathrm{Mpa}$, which is sufficient in terms of the dimensioning shear stress.

End/Edge column

Column E7 was found as the column with the highest dimensioning forces. The normal force within the column was found to be $V_{Ed} = 691.2\ KN$. There is a presence of moment around both axis, and so the β value was taken from the recommended values in EC2 for edge columns (Figure 6.21N in

EC2). The columns are with the dimensions $c_1 * c_2 = 550 * 550\ mm^2$ and the effective depth d_{eff} is $244\ mm$. The resulting circumferences are then $u_1 \approxeq 3183\ mm$ and $u_0 = 1282\ mm$. This leads to a dimensioning shear stress of:

$$\upsilon_{Ed} = 1{,}246\ Mpa \text{ for check at } u_1$$

$$\upsilon_{Ed} = 3{,}093\ Mpa \text{ for check at } u_0$$

$\upsilon_{Rd,max}$ is given as $4{,}09\ Mpa$, such that check a) is sufficient against the appropriate $\upsilon_{Ed} = 3{,}093\ Mpa$.

The capacity check without necessary reinforcement for shear punching was proven to be not sufficient. In this case, column E7 is placed $0\ m$ from edge of slab.

This means that the entire affected area b_x equals the width of critical cross-section $(2d)$ from column face, which expands $45°$ out to critical cross-section $2d$ from column face. In this case, the width at column face is originally $c_1 + 2 * 2d$ along the slab edge (y-direction), and the resulting width is evaluated at $488mm$ from column face (x-direction), which results in $b_x = 3676\ mm$. Furthermore, the reinforcement ratio $\rho_{l,y}$ is restricted in distribution as this is an edge column. In this case, the width for the reinforcement ratio can only extend $3d$ outside the column on only one side. As a result, $\upsilon_{Rd,c}$ is calculated to be $0.87\ Mpa$. Since this is checked against the dimensioning shear stress at the critical circumference u_1, the shear capacity is not sufficient without additional shear reinforcement.

Necessary shear reinforcement has then been calculated, with an assumption of radial distance $\mathrm{S_r} = 160\ \mathrm{mm}$. The necessary shear reinforcement can be calculated when the shear capacity with shear reinforcement $\upsilon_{\mathrm{Rd,cs}}$ equals the dimensioning shear stress $\upsilon_{\mathrm{Ed}} = 1.246\ \mathrm{Mpa}$. The necessary reinforcement was calculated to be $\mathrm{A_{sw}} = 648\ \mathrm{mm^2}$. As a result, it was chosen to reinforce the columns with 9Ø10, which equals $\mathrm{A_{sw}} = 706.9\ \mathrm{mm^2}$. With this choice of shear reinforcement, the capacity $\upsilon_{\mathrm{Rd,cs}}$ is calculated to be $1.3\ \mathrm{Mpa}$. The upper limitation is calculated to be $\mathrm{k_{max}}\upsilon_{\mathrm{Rd,c}} = 1.566\ \mathrm{Mpa}$. In other words, the calculated shear capacity $\upsilon_{\mathrm{Rd,cs}}$ is ultimately $1.3\ \mathrm{Mpa}$, which is sufficient in terms of the dimensioning shear stress.

ADAPT-Builder

ADAPT-Builder presents solutions in terms of shear reinforcement against shear punching failure. The program informs that our columns in the model needs to be sufficient, and so it does not pass the check $\upsilon_{Ed} \leq \upsilon_{Rd,c}$. ADAPT-Builder confirms that the most critical columns for an internal and edge/end column are the column mentioned previously. A report file shows the calculated shear stresses at different critical sections and the allowable stresses $\upsilon_{Rd,c}$ without shear reinforcement. A summary of the hand-calculated results and the design solution from ADAPT-Builder is presented below.

Table 4.13: *Hand calculated design solution and calculations from ADAPT-Builder for critical load combination*

Hand calculated results						
Label	$\boldsymbol{v_{Ed,0}\ [Mpa]}$	$\boldsymbol{v_{Ed,1}\ [Mpa]}$	$\boldsymbol{v_{Rd,c}\ [Mpa]}$	$\boldsymbol{A_{sw}\ [mm^2]}$ $\boldsymbol{Necessary}$	$\boldsymbol{A_{sw}\ [mm^2]}$ $\boldsymbol{Chosen}$	$\boldsymbol{v_{Rd,cs}\ [Mpa]}$
E2	3.582	1.496	0.843	1560	20Ø10@160	1.5
E7	3.093	1.246	0.87	648	9Ø10@160	1.3
ADAPT-Builder						
Label	$\boldsymbol{v_{Ed,0}\ [Mpa]}$	$\boldsymbol{v_{Ed,1}\ [Mpa]}$	$\boldsymbol{v_{Rd,c}\ [Mpa]}$			
E2	3.582	1.497	0.841			
E7	3.093	1.246	0.731			

The deviance between the shear capacity from ADAPT-Builder to hand calculated results for the edge/end column E7 can be since the ADAPT-Builder utilizes finite element method. Since the edge column is close to slab edge, the width b_x in question is an estimated effective width as recommended by Terje Kanstad. It will in other words, not be fully utilized width as is the case for the internal column E2. With the finite element method, ADAPT-builder chooses the node that reveals the actual prestress $\sigma_{c,x}$ in the point of the effective width. Hence, my calculation follows an approximation of prestress $\sigma_{c,x}$, meanwhile ADAPT-Builder can pick the prestress $\sigma_{c,x}$ more accurately.

4.10 Serviceability limit state

4.10.1 Control of stresses

As mentioned previously in chapter 4.7, there are certain limitations to the concrete stresses within the slab that needs to be met. For concrete stresses in tension, this is then given as:

$$\sigma_{c,tension} \leq f_{ctm} \Rightarrow \sigma_{c,tension} \leq 3{,}2\ Mpa$$

For concrete stresses in compression, this limitation is dependent on how developed the strength in concrete is at the day where prestress is applied to the slab. If it is assumed that the prestressing is applied 3 days after casting of concrete and that the concrete is has a cement class N, the following limitation is given:

$$\sigma_{c,compression} \leq 0{,}6 f_{ck}(t) \Rightarrow \sigma_{c,compression} \leq 10{,}62\ Mpa$$

Table 4.14: *Maximum concrete stresses in tension and compression within the model*

ADAPT-Builder		**Hand calculated results**	
$\boldsymbol{\sigma_{c,tension}}$ $\boldsymbol{[Mpa]}$	$\boldsymbol{\sigma_{c,compression}}$ $\boldsymbol{[Mpa]}$	$\boldsymbol{\sigma_{c,tension}}$ $\boldsymbol{[Mpa]}$	$\boldsymbol{\sigma_{c,compression}}$ $\boldsymbol{[Mpa]}$
3,158	-5,3	3,11	-5,55

As mentioned previously in chapter 4.7, the concrete stresses are evaluated for the quasi-permanent load combination: $self + dead + 0{,}6Live + pres$. The table above highlights the critical concrete stresses that can be found within our model. It can therefore be concluded that the concrete stresses within the slab does not exceed the limitation of concrete stresses given by EC2. This means that our slab is considered an uncracked cross-section, such that the concrete stresses can be found by calculation according to the state 1 as given in chapter 2. A verification of these results by hand calculation is provided in the appendix. However, this calculation will deviate about 10% as it is not considered the effect of reinforcement onto the calculation of concrete stresses, as recommended by Terje Kanstad (Kanstad, Kontroll i bruks- og bruddgrensetilstand, 2022).

The maximum concrete stress in compression, $\sigma_{c,compression} = -5{,}3\ Mpa$ can be found on the lower edge of column B6. More specifically when it is evaluated along the x-direction (design strip B17). Column B2 is the critical point when evaluating the compression along the y-direction (design strip AF2). Here it is approximately $\sigma_{c,compression} = -4{,}369\ Mpa$ at the lower edge of cross-section. In summary, column B6 is the critical point within the slab in terms of stresses in compression.

The maximum concrete stress in tension, $\sigma_{c,tension} = 3{,}158\ Mpa$ can be found on the upper edge of column E6. In addition, $\sigma_{c,tension} = 3{,}157\ Mpa$ can be found on the upper edge of column B2. More specifically when it is evaluated along the y-direction (design strip AF6 & AF2). However, when evaluating stresses in x-direction (design strip B17), the maximum stress can be found at column B6.

Here it is approximately $\sigma_{c,tension} = 3{,}149\ Mpa$ at the upper edge. Hence, the critical point for stresses in tension is at column E6.

Since the stresses within the slab is below the limits given for an uncracked cross-section, it is not necessary to view and perform an analysis of crack-width limitations.

4.10.2 Critical moment of cracking

A check for critical moment of cracking M_{cr} has been executed. The purpose of this check is to ensure that the construction has appropriate ductility. As mentioned previously in chapter 3, M_{cr} defines the necessary moment for the cross-section to go from state I to state II in SLS state. This is at the point where $\sigma_{c,tension} = f_{ctm}$. The critical moment of cracking is therefore:

$$M_{cr} = f_{ctm}\frac{I}{y} + \frac{P_0}{A_c}\frac{I}{y}$$

Furthermore, EC2 9.2.1.1 (4) gives recommendations for minimum capacity in comparison to the critical moment of cracking. This limitation applies to prestressed un-grouted cables, and is set to:

$$M_{Rd} \geq 1.15 M_{cr}$$

In essence, ADAPT-Builder shows the distribution of moment capacities along each design strip. This is then moment capacities based on $\frac{L}{2}$. Since the moment capacities should be based on width of $\frac{L}{4}$ for concentrated and $1m$ for distributed cables, comparing these moment capacities to the critical moment of cracking is not applicable. Hence, it was chosen to compare the critical moment of cracking to the 4 hand-calculated moment capacities that was shown in section 4.9.1 in the table below. This is then the moment capacities according to the appropriate width as recommended by Terje Kanstad for distributed- and concentrated cables.

Table 4.15: *Comparison with critical moment of cracking for design strip to the hand-calculated moment capacities analyzed in section 4.9.1*

Type of moment	Position	$M_{Rd}\ [KNm]$	Design strip	$M_{cr}\ [KNm]$	$\frac{M_{Rd}}{M_{cr}} \geq 1.15$
$Field_{x-direction}$	D12	834.68	D17	558.36	1.495
$Support_{x-direction}$	B6	-982.55	B17	-602.48	1.63
$Field_{y-direction}$	AB2	103.4	AF2	65.56	1.577

$Support_{y-direction}$	E2	-271.8	AF2	65.56	4.146

Realistically speaking, the sections that are most prone to cracking is for the sections above columns and middle of field. By comparing with the sections that contains the largest dimensioning moment and compare the corresponding capacities to the corresponding critical moment of cracking, we can conclude that it should be sufficient over each column and field within each design strip.

However, in theory, the criteria given by EC2 should be sufficient for all design sections within all design strips. This is shown to not be sufficient in certain design sections where the dimensioning moments are approximately zero. In other words, the sections between middle of field to columns. Since the dimensioning moments are low here, the need for moment capacity is very small in these sections. Hence, ADAPT-Builder has not generated supplementary reinforcement, as there is no need. The moment capacities in these sections are therefore smaller than over support and field. What it means in essence is that the mesh reinforcement that is calculated in section 4.7 and modelled in ADAPT-Builder is not sufficient even though it is in accord with EC2. However, it can be discussed whether these sections should be sufficient in terms of this check. These are not sections that are prone to cracking as there is very little presence of dimensioning moment, and so it is not areas that needs to have great ductility.

4.10.3 Deflection

It is necessary to check whether the deflection within the slab is within the limits specified in EC2. As mentioned before the limitations in EC2 is suggested as such:

$$\delta \leq \frac{L}{250}$$

This results in the given limitations for the different span lengths existing within the slab:

$$\delta \leq \frac{8.5 * 10^3 mm}{250} = 34\ mm$$

$$\delta \leq \frac{8.6 * 10^3 mm}{250} = 34.4\ mm$$

$$\delta \leq \frac{7.6 * 10^3 mm}{250} = 30.4\ mm$$

$$\delta \leq \frac{7.8 * 10^3 mm}{250} = 31.2\ mm$$

Which limitation is applicable is dependent on which point within the slab is evaluated. For instance, a point that is enclosed by the gridlines 1, 2, E and F (which gives span lengths of $8.5\ m$ and $7.6\ m$, in each respective directions): the limits should then be set as $30.4\ mm$.

The deflection needs to be evaluated for a long-term deflection that considers the effect of shrinkage and creep over time. As mentioned previously in chapter 4.5, ADAPT-Builder has automatically generated a load combination that is applicable for this purpose. Hence, the load combination $LongTerm1\colon 0{,}14Steg + 0{,}267Steg + 2{,}375Steg$ is utilized when analyzing the deflection of this structure. This considers the deflection of the slab after 50 years.

The point with the biggest deflection can be found in the middle of the gridlines 6,7, A and B. Since this area has span length of $8.5\ m$ and $7.6\ m$ in their respective directions, the limit is set to $30.4\ mm$. ADAPT-Builder shows a maximum deflection at this point to be given as:

$$\delta = 16{,}21\ mm$$

Hence, the deflection within the slab meets the criterions given by EC2 for deflection.

A 3D model of the overall deflection in the slab is illustrated below. This is significantly scaled so it can give the viewer the perception of where the highest deflection areas within the slab is located.

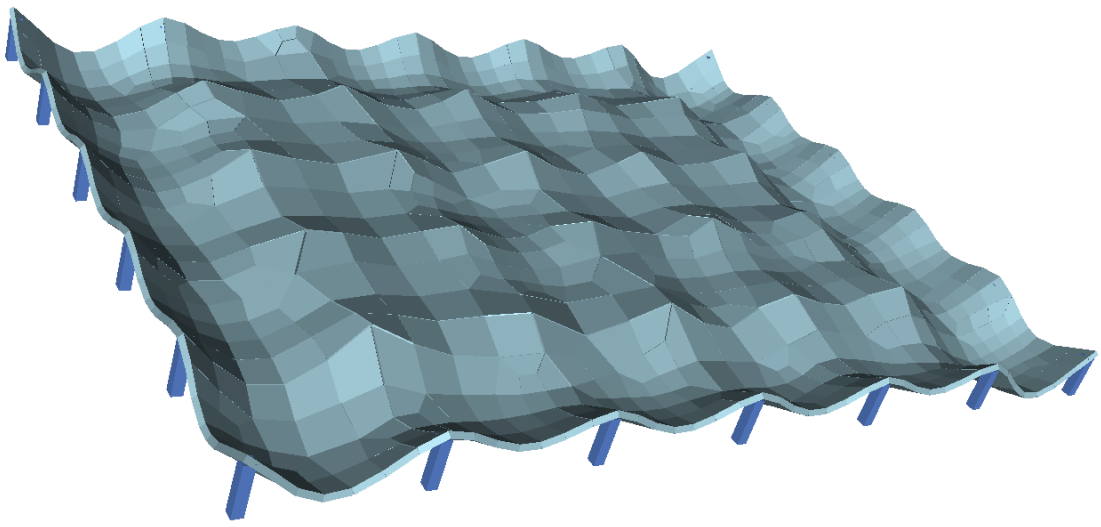

Figure 4.14: *A significantly scaled 3D model in ADAPT-Builder of the deflection.*

5. Discussion

5.1 Discussion of results between ADAPT-Builder and by hand

5.1.1 Prestress force and loss of prestress

The calculations for prestress force after immediate losses is very similar to the results displayed in ADAPT-builder. For distributed cables, the deviance between the hand-calculated to that of the program calculated results is 0.48%. For concentrated cables, the deviance is $0{,}22\%$. ADAPT-builder calculates a loss of applied jacking force to be of 7.1% and 6.42% for distributed- and concentrated cables, respectively. Meanwhile the hand calculated results display a loss of 6.64% and 6.63% for the distributed- and concentrated cables.

The calculations in ADAPT-Builder compared to that of hand calculations for long-term prestress force shows a slightly bigger deviance. Here, the distributed cables show a deviance in results of 5.54%. The deviance for concentrated cables is 0.455%. This means that ADAPT-Builder calculated a total loss of 12.19% and 11.51% from initial jacking force, for distributed- and concentrated cables respectively. However, my hand calculations shows that the total loss is 16.79% and 11.1%. The biggest difference can be seen by comparing the contribution long-term losses has in comparison to the immediate losses. ADAPT-Builder shows a loss in prestress force due to long-term losses to be about 5.4%. My hand calculated results show a loss for concentrated- and distributed cables to be 4.8% and 10.87%. We can therefore conclude that the biggest deviance seems to be for the long-term losses for the distributed cables.

The reason as to why the calculation of immediate losses is accurately represented to that of ADAPT-Builder is simply because the calculations is based on the same calculation principles. The slight deviance for the immediate losses can be due to rounding results during the calculations.

For the long-term prestress losses, ADAPT-Builder assumes a long-term loss of prestress force to be $75\ Mpa$. This is also as mentioned in section 4.8.3, a reasonable assumption according to Steinar Trygstad (Trygstad, Etteroppspente uinjiserte betongdekker beregningseksempel, 2022). However, when hand-calculated, we make assumptions to calculate the contribution for relaxation, shrinkage and creep. For instance, we assume a class 2 relaxation for the prestressing steel. As this is inputs that is not considered for the long-term losses in ADAPT-Builder, we increase the risk of higher deviance in the results.

Even though the hand calculated, absolute long term prestress force (ΔP_{c+s+r}) only deviates slightly between distributed- and concentrated cables, there is still a big difference in the resulting effective prestress force per cable. The reason for this stems from how much prestress loss is designated to each cable. Since the spacing between distributed cables is large, each cable takes a higher

percentage of the absolute long term prestress force than the concentrated cables. As seen in Appendix 1, Section A, each distributed cable takes a loss of $22.43\ KN$, meanwhile the concentrated looses $9.9\ KN$ per cable.

As mentioned in section 2.1, Prab Bhatt explains how constructions with tensioned reinforcement needs to have higher strength concrete types as it is important to have better deformational properties. Having better deformational properties is an important aspect, as it will influence how much of the prestress force is retained in the long term (Bhatt, 2011). It can be discussed if the assumption of $75\ Mpa$ for long term losses is not applicable since the choice of my concrete type may not be of high enough strength for it to be a reasonable assumption.

5.1.2 Moment capacity

The results for the moment capacity check varies mostly in the x-direction when comparing the results from ADAPT-builder to the hand calculated results. The highest deviance is for the critical field moment in x-direction, where the deviance between results of ADAPT-Builder to the hand calculated results is correspondingly 11.6%. For the critical moment at support in x-direction, this gave a deviance of 2.4%. However, for the y-direction, the deviance is significantly smaller as it is held within 1%.

The difference in deviance between evaluation the results in x- and y-direction can be explained due to how the program chooses to calculate the moment capacity. ADAPT-Builder considers a cross-section of equal size to that of loading width when calculating the moment capacity. This calculation procedure is similarly done by hand for the distributed cables. However, when calculating by hand the moment capacity for the concentrated cables, the width of cross-section is considered smaller than that of ADAPT-Builder. This calculation procedure is in line by the recommendations given by Terje Kanstad in section 3.6.1.

5.1.3 Shear punching

The only significant deviance between ADAPT-Builder to the hand calculated results for shear capacity check arises when the shear capacity is calculated for the edge/end column E7. Here, the hand calculated result displays a capacity of $\upsilon_{Rd,c} = 0.87$, meanwhile ADAPT-Builder displays a capacity of $\upsilon_{Rd,c} = 0.731$. In other words, this accords to a deviance of approximately 16%. However, the deviance in capacity for the internal column E2 is negligible.

This can be explained by the contribution prestressed reinforcement has to the shear capacity. As Terje Kanstad recommended in section 3.7.2, the applicable width when calculating the contribution of prestress for concentrated cables expands $45°$ from edge of slab until loading width $\frac{L}{2}$. When we consider the internal column, the applicable width is equal to that of the loading width $\frac{L}{2}$. However, for the edge/end column, the applicable width is an approximation as it lies on edge of slab. What is then considered correct contribution for prestress for concentrated cables is dependent on the recommendation by Terje Kanstad, when calculated by hand.

In addition, ADAPT-Builder uses finite element method, such that the approximation of prestress for concentrated cables is more accurately represented as it can read results from node at point of evaluation. While for the hand calculated results, it must assume a linear distribution for the prestress, as the prestress lowers in relation to the increased effective depth.

The difference in how ADAPT-Builder obtains relevant value for contribution of prestress in x-direction to the hand calculations is what may be the biggest reason for the cause of deviance for shear capacities of column E7.

5.1.4 Concrete stresses

The deviance between hand verified concrete stresses and concrete stresses by ADAPT-Builder is 1.52% and 4.5% for stresses in tension and compression, respectively. This deviance is seen as significantly small as it equates to a difference of $0.25\ Mpa$ at most. Therefore, it is assumed that the only reason for deviance in this case is due to rounding of inputs in formula and consequently the result.

5.2 Possible changes to optimize solution further

I chose to dimension the amount of post-tensioned reinforcement based on achieving concrete stresses that is below what is defined as an uncracked state in SLS. This means that the highest stresses the slab could have in tension was limited to $f_{ctm} = 3{,}2\ Mpa$. Dimensioning the amount of PT reinforcement is often dependent on the concrete stresses, deflection, and prestress force. As described in section 2.1, Sørensen and Bhatt explains the benefits of having crack-free slabs. Sørensen explains how the decrease in deflection due to the use of PT reinforcement leads to a slab with less cracks (Sørensen, 2013). Bhatt explains how crack-free slabs is especially beneficial in the case of car parks, as less cracks limits the damage due to seepage of water with de-icing salts from

melting snow (Bhatt, 2011). This led to that the restrictive measurement in terms of amount of PT reinforcement was greatly impacted by the level of concrete stresses in SLS.

However, calculating amount of PT reinforcement based on this limitation is not a necessity. It is perfectly possible to dimension the PT reinforcement in a way that leads to the concrete stresses in tension being higher than this limitation. This will only mean that the cross-section is considered in a cracked state during SLS analysis. My solution can therefore be viewed upon as an over-dimensioned solution. My solution utilizes less of the benefits of PT reinforcement than possible, as I have chosen to increase slab depth and decrease spans for the solution to give concrete stresses in tension below an uncracked state.

The results from analysis of show a margin between limitation given by EC2 to the results from ADAPT-Builder, when considering the deflections. The highest deflection in slab is given to be $\delta = 16.21\ mm$, meanwhile the limitation is approximately $\delta \approx 32\ mm$ by EC2, depending on the spans considered. This also implies it is possible to optimize the slab such that the deflection is closer to the limitation. In other words, decreasing the slab depth, increase spans or lower the PT reinforcement.

The highest number of concentrated cables in my slab is 18 cables, which resides in design strip E17. There is no maximum number of how many cables should be within each concentrated design strip, but other projects have considered 20-24 cables to be in the upper limitation of common practice (Hojem, 2022). This implies I have an opportunity to increase PT and decrease other geometric features of my slab.

In addition, during the analysis, the coverage seemed to limit the effect each cable had to the uplift. Since the coverage was given to be $60\ \mathrm{mm}$, this led to a limitation on the maximum possible eccentricity for each cable in both directions. This will consequently lead to less effect out of each tendon, as it creates less moment due to prestressing, to counteract the dimensioning moments. This will then ultimately lead to higher concrete stresses. As a solution, I chose to increase slab depth to increase the efficiency of each cable, so that it was possible to have a reasonable number of concentrated cables within each design strip.

A possible optimalization would therefore be to dimension the slab by the limitation of deflection. Which means applying a mixture of changes such as decreasing slab depth, increasing span width, and increasing the PT reinforcement until a maximum number between 20-24 cables, without consideration of concrete stresses in tension.

All things considered; I have managed to produce a solution with PT reinforced slab which exceeds the expected dimensions of unstressed slabs. As mentioned in chapter 2.5.1, a typical design of an

unstressed flat slab contains a maximum span length up to $7{,}2\ m$ between each column. My solution therefore proves the benefits of utilizing PT in slab in comparison to unstressed slabs.

Although the slab thickness exceeds the recommendation given by Prab Bhatt in section 4.2 for PT reinforced slabs, the choice of thickness is in this case, highly influenced by a larger coverage than what is usually considered for buildings. If the coverage was $35 - 45\ mm$, it is possible that the slab thickness would have been within the recommendations from Prab Bhatt.

6. Conclusion

This master has shown the potential benefits which arises from utilizing PT reinforcement in slabs compared to regular reinforcement. Section 5.2 highlights the potential aspects in where my solution could have been improved. It touches on the fact that the solution can be viewed upon as an over-dimensioned solution for use of PT in slabs. How the deflection is considered remarkably low, and the stresses are conservatively considered, and that the number of concentrated cables is lower than what is considered a practical limitation. Regardless, the slab still illustrates a solution in where the spans are higher than what is considered common for slabs with no PT reinforcement. As previously mentioned, unstressed flat slabs contain a maximum span length up to $7{,}2\ m$ between each column. If the solution were optimized even further as explained in the discussion, the possible spans could have been higher.

As mentioned previously in section 2.2, the biggest asset by introducing tensioned reinforcement, is how it lowers the predicted deflection. As seen from results in ADAPT-Builder, my slab is a solution in where the deflection is much lower than criteria given by EC2. The results from ADAPT-Builder displays a low deflection, which implies a possibility to lower the chosen thickness of slab even further. Deflection was, in this case, not the determining variable that decided the choice of PT reinforcement and design of slab. The determining variable in terms of PT reinforcement was the choice to construct a solution in where the concrete stresses were lower than f_{ctm}, such that it can be considered an uncracked solution. However, as this is not a necessity, the opportunity to lower thickness of slab, or increasing span width even further is possible.

Steinar Trygstad also explains the potential environmental benefits of utilizing PT reinforcement. This is in large, due to the possibility of utilizing smaller slab thickness since the deflection is largely improved by using PT reinforcement. This subsequently leads to less use of concrete, which then will

resolve into a solution that in more environmentally beneficial. My choice of thickness of slab was given to be $320\ mm$, which can be considered quite large. However, the reasoning for this choice was not due to the presence of PT reinforcement over non-stressed reinforcement, but largely influenced by the high loading and high coverage requirements. This led to a need for a larger depth in order to have good effect of use of PT reinforcement. If the loading and coverage were lower, it would have been possible to lower the depth thickness further.

7. References

ADAPT Corporation. (2004, November 13). DESIGN PROCESS USING ADAPT-BUILDER PLATFORM. Redwood City, California, USA.

Balázs, G., Farkas, G., & Kovács, T. (2016). *Reinforced and prestressed concrete bridges.* Budapest: Budapest University of Technology and Economics.

Bhatt, P. (2011). *Prestressed concrete design to eurocodes.* Abingdon: Spon press.

CCL Scandinavia. (n.d.). *XU Unbonded system*. Retrieved from CCL Scandinavia: https://en.cclscan.dk/xu-system

Collins, M. P., & Mitchell, D. (1991). *Prestressed concrete structures.* Prentice Hall.

European Technical Assessment. (2020). *ETA 19/0733.* European Technical Assessment.

Hojem, P. (2022). *Prosjektering og analyse av etteroppspent flatdekke med konsentrerte spennkabler.* Trondheim: NTNU.

Jacobsen, S. (2022). *Concrete Technology.* Trondheim: Norwegian University of Science and Technology.

Kalland, K. (Director). (2022). *Forankringer, faste og bevegelige skjøtekoblinger* [Motion Picture].

Kanstad, T. (Director). (2022). *Kontroll i bruks- og bruddgrensetilstand* [Motion Picture].

Kanstad, T. (Director). (2022). *Verifikasjon av resultater, håndregning.* [Motion Picture].

Norsk betongforening. (2022, September 20). *Flatdekker - Beregning og konstruktiv utforming.* Retrieved from Norsk betongforening: https://betong.net/publikasjoner-2/historisk-arkiv/

NTNU - Department of structural engineering. (2021). *Concrete structures 3 - Compendium.* Trondheim: NTNU.

Obrien, E., Dixon, A., & Shiels, E. (2012). *Reinforced and prestressed concrete design to EC2.* Abingdon: Spon Press.

RISA Tech. (2023, 1 12). *Welcome to ADAPT-Builder*. Retrieved from https://risa.com/risahelp/adaptbuilder/index.html

Spennteknikk. (2022, September 12). *Brosjyrer/kataloger om spennteknikk.* Retrieved from Spennteknikk: https://www.spennteknikk.no/wp-content/uploads/2018/05/BBR-VT-CONA-Single-spenntausystem-24022011.pdf

Standard Norge. (2016). *NS EN 1990.*

Standard Norge. (2019). *NS-EN 1991-1-1.*

Standard Online AS. (2021). *NS-EN 1992-1-1.* Lysaker: Standard Norge.

Sørensen, S. I. (2013). *Betongkonstruksjoner - Beregning og dimensjonering etter Eurocode 2.* Bergen: Fagbokforlaget.

Trygstad, S. (Director). (2022). *Etteroppspente uinjiserte betongdekker beregningseksempel* [Motion Picture].

Trygstad, S. (Writer), & Trygstad, S. (Director). (2022). *Generelt om spennarmeringens fortrinn* [Motion Picture].

Øverli, J. A. (Director). (2022). *Analyse av spennarmerte konstruksjoner* [Motion Picture].

Appendix 1: verification of result through hand calculation

A Prestress force and prestress losses

A.1 Prestress force

$P_{max} = 221\ KN$	EC2, section 5.10.2.1(1), equation (5.41)
$P_{m0} = 209.1\ KN$	EC2, section 5.10.3(2), equation (5.43)

A.2 Immediate prestress losses

A.2.1 Prestress losses in x-direction: concentrated cables

Calculation basis

$L = 51.5\ m$	The whole length of each distributed cable
$L_{span} = \{8.7, 8.5, 8.5, 8.6, 8.5, 8.7\}\ m$	Length of each span, so that $L_{span1} = 8.7\ m$
Active-Active	Type of anchorages at each end of cable
$E_p = 195\ 000\ \frac{N}{mm^2}$	E-module for prestressing tendons
$E_{cm} = 34\ 000\ \frac{N}{mm^2}$	Mean E-module for concrete type B35
$b = 1000\ mm$	Evaluating a cross-section with 1m width
$h = 320\ mm$	Height of slab
$A_p = 150\ mm^2$	Cross-sectional area of one tendon
$n_{x,1m} = \frac{18}{7.8\ m} = 2.307$	Number of tendons per meter based off the design strip with highest amount of concentrated cables (E17)
$e = 60\ mm$	Maximum eccentricity from half of slab height

Friction loss

$\theta_1 = \tan^{-1}\left(\frac{60}{0.15*8.7*10^3}\right) = 0.046\ rad$	Change in angle from jacking end to field. Cable starts with eccentricity 0 mm and reaches eccentricity 60mm over the length of $0.15L_{span1}$
$\theta_2 = \tan^{-1}\left(\frac{105}{0.15*8.7*10^3}\right) = 0.08\ rad$	Change in angle from field to top of support. Cable starts with eccentricity 60 mm below and reaches eccentricity 45 mm above, over the length of $0.15\ L_{span1}$

$\theta_3 = \tan^{-1}\left(\frac{105}{0.15*8.5*10^3}\right) = 0.082\ rad$ — Change in angle from field to top of support. Cable starts with eccentricity 60 mm below and reaches eccentricity 45 mm above, over the length of 0.15 L_{span2}

$\theta_4 = \tan^{-1}\left(\frac{105}{0.15*8.6*10^3}\right) = 0.0812\ rad$ — Change in angle from field to top of support. Cable starts with eccentricity 60 mm below and reaches eccentricity 45 mm above, over the length of 0.15 L_{span4}

$\sum\theta = 2\theta_1 + 2\theta_2 + 6\theta_3 + 2\theta_4 = 0.9064\ rad$ — Sum of total changes in angles over the whole cable profile

$\mu = 0.07\ rad^{-1}$ — friction coefficient

$x = 51.5m$ — Length of cable from one jacking end to another

$k = 0.01\ m^{-1}$ — Wobble factor

$$\boldsymbol{\Delta P_{\mu}(x) = P_{max}\left(1 - e^{-\mu(\theta+kx)}\right) = 20.93\ KN}$$

Draw-in loss

$\Delta_{lås} = 6\ mm$ — Seating loss.

$a = \frac{\Delta P_{\mu}}{L} = \frac{20.93}{51.5} = 0.4064\ \frac{KN}{m}$ — Assuming the slope of effect from draw-in loss is like the slope of friction loss

$l_{lås} = \sqrt{\frac{\Delta_{lås}*E_p*A_p}{a}} = \sqrt{\frac{6*195000*150}{0.4604}} = 20.78\ m$ — Length that is impacted by the draw-in loss

$$\boldsymbol{\Delta P_{lås,a} = 2 * a * l_{lås} = 2 * 0.4064 * 20.78 = 16.89\ KN}$$

Elastic deformation loss due to stressing tendons

Since the anchorages are effective on both ends, the prestress force after immediate losses is estimated by calculating an average prestress force at center of cable profile and at one active end.

At center of cable profile, the friction losses are approximately half of ΔP_μ since x is $\frac{51.5}{2}\ m$, and the deviance between each span is small. For draw-in loss, the effected length $20.78\ m$ is less than half of the length of cable. This means that in the center of cable-profile, this will be unaffected by the draw-in losses. For the active end, the friction loss is zero. This gives:

$$P_0 = \frac{P_{max} - \Delta P_{lås,a} + P_{max} - \frac{\Delta P_\mu}{2}}{2} = 207.32\ KN$$

$\eta = \frac{E_p}{E_{cm}} = 5.735$	E-module ratio
$j = 0.5$	Factor provided by EC2, 5.10.5.1(2)
$A_t = bh + (\eta - 1)A_p n_{x,1m} = 321638\ mm^2$	Transformed cross-sectional area
$y_t = \frac{(\eta-1)A_p e}{A_t} n_{x,1m} = 0.306\ mm$	Distance between center of gravity for concrete section alone to the center of gravity for section with reinforcement present
$I_t = \frac{bh^3}{12} + bhy_t^2 + (\eta - 1)A_p n_{x,1m}(e - y_t)^2 = 2.736 * 10^9\ mm^4$	Transformed second moment of area of cross-section
$\Delta\sigma_c = \left(\frac{P_0}{A_t} + \frac{P_0(e-y_t)^2}{I_t}\right) n_{y,1m} = 2.25\ Mpa$	Stress in concrete at center of gravity for prestressing tendons

$$\boldsymbol{\Delta P_{el} = A_p E_p \frac{j\Delta\sigma_c}{E_{cm}} = 0.968\ KN}$$

Average prestress force after immediate losses

$P_{0,draw-in+friction} = 207.32\ KN$

$\Delta P_{el} = 0.968\ KN$

$$\boldsymbol{P_0 = 207.32 - 0.968 = 206.35\ KN}$$

A.2.2 Prestress losses in y-direction: distributed cables

Calculation basis

$L = 39\ m$	The whole length of each distributed cable
$L_{span} = 7.8\ m$	Length of each span

Active-Active	Type of anchorages at each end of cable
$E_p = 195\,000\ \frac{N}{mm^2}$	E-module for prestressing tendons
$E_{cm} = 34\,000\ \frac{N}{mm^2}$	Mean E-module for concrete type B35
$b = 1000\ mm$	Evaluating a cross-section with 1m width
$h = 320\ mm$	Height of slab
$A_p = 150\ mm^2$	Cross-sectional area of one tendon
$n_{y,1m} = \frac{1000\ mm}{925\ mm}$	Number of tendons within the cross-section based on spacing 925 mm for distributed cables
$e = 60\ mm$	Maximum eccentricity from half of slab height

Friction loss

$\theta_1 = \tan^{-1}\left(\frac{60}{0.15*7.8*10^3}\right) = 0.05123\ rad$	Change in angle from jacking end to field. Cable starts with eccentricity 0 mm and reaches eccentricity 60mm over the length of $0.15L_{span}$
$\theta_2 = \tan^{-1}\left(\frac{120}{0.15*7.8*10^3}\right) = 0.1022\ rad$	Change in angle from field to top of support. Cable starts with eccentricity 60 mm below and reaches eccentricity 60 mm above, over the length of $0.15L_{span}$
$\sum\theta = 2*\theta_1 + 8*\theta_2 = 0.92006\ rad$	Sum of total changes in angles over the whole cable profile
$\mu = 0.07\ rad^{-1}$	friction coefficient
$x = 39m$	Length of cable from one jacking end to another
$k = 0.01\ m^{-1}$	Wobble factor

$$\boldsymbol{\Delta P_\mu(x) = P_{max}\left(1 - e^{-\mu(\theta+kx)}\right) = 19.365\ KN}$$

Draw-in loss

$\Delta_{låsa} = 6\ mm$	Seating loss
$a = \frac{\Delta P_\mu}{L} = \frac{19.365}{39} = 0.4965\ \frac{KN}{m}$	Assuming the slope of effect from draw-in loss is like the slope of friction loss
$l_{låsa} = \sqrt{\frac{\Delta_{låsa} * E_p * A_p}{a}} = \sqrt{\frac{6*195000*150}{0.4965}} = 18.8\ m$	Length that is impacted by the draw-in loss

$$\boldsymbol{\Delta P_{låsa,a} = 2 * a * l_{låsa} = 2 * 0.4965 * 18.8 = 18.67\ KN}$$

Elastic deformation loss due to stressing tendons

Since the anchorages are effective on both ends, the prestress force after immediate losses is estimated by calculating an average prestress force at center of cable profile and at one active end. At center of cable profile, the friction losses are half of ΔP_μ since x is $\frac{39}{2}\ m$. For draw-in loss, the effected length $18.8\ m$ is less than half of the length of cable. This means that in the center of cable-profile, this will be unaffected by the draw-in losses. For the active end, the friction loss is zero. This gives:

$$P_0 = \frac{P_{max} - \Delta P_{låsa,a} + P_{max} - \frac{\Delta P_\mu}{2}}{2} = 206.75\ KN$$

$\eta = \frac{E_p}{E_{cm}} = 5.735$	E-module ratio
$j = 0.5$	Factor provided by EC2, 5.10.5.1(2)
$A_t = bh + (\eta - 1)A_p n_{y,1m} = 320767\ mm^2$	Transformed cross-sectional area
$y_t = \frac{(\eta-1)A_p e}{A_t} n_{y,1m} = 0.1436\ mm$	Distance between center of gravity for concrete section alone to the center of gravity for section with reinforcement present
$I_t = \frac{bh^3}{12} + bhy_t^2 + (\eta - 1)A_p n_{y,1m}(e - y_t)^2 = 2.733 * 10^9\ mm^4$	Transformed second moment of area of cross-section
$\Delta\sigma_c = \left(\frac{P_0}{A_t} + \frac{P_0(e-y_t)^2}{I_t}\right) n_{y,1m} = 0.99\ Mpa$	Stress in concrete at center of gravity for prestressing tendons

$$\boldsymbol{\Delta P_{el} = A_p E_p \frac{j\Delta\sigma_c}{E_{cm}} = 0.43\ KN}$$

Average prestress force after immediate losses

$P_{0,draw-in+friction} = 206.75\ KN$

$\Delta P_{el} = 0.43\ KN$

$$\boldsymbol{P_0 = 206.75 - 0.43 = 206.32\ KN}$$

A.3 Time-dependent prestress losses

A.2.1 Prestress losses in y-direction: distributed cables

Calculation basis

$b = 1000\ mm$

$h = 320\ mm$

$RH = 40\%$	Assuming a relative humidity of 40%
$t_0 = 28\ days$	Assuming that permanent loads are applied after 28 days of casting
$t = 18250\ days$	Evaluated at 18250 days as the construction is dimensioned for 50 years life span
$f_{cm} = 43\ Mpa$	Mean strength in concrete type B35
$f_{pk} = 1860\ Mpa$	Characteristic strength in tension for prestressing tendons
$\sigma_{pm0}(x) = 1394\ Mpa$	Initial stress in prestressing tendons

Assumed class 2 for relaxation

Cement class N

$P_0 = 206.32\ KN$	Prestress force after immediate losses as calculated above
$e = 60\ mm$	Maximum eccentricity
$y_t = 0.1436\ mm$	Distance between center of gravity for concrete section to center of gravity for concrete section with reinforcement considered, as calculated above
$A_t = 320767\ mm^2$	Transformed cross-sectional area
$I_t = 2{,}733 * 10^9\ mm^4$	Transformed second moment of area of cross-section
$n_{y,1m} = \frac{1000}{925}$	Number of tendons considering 1m width and spacing 925 mm as shown above

---

Creep

$u = 2b = 2000\ mm$

$h_0 = \frac{2A_c}{u} = h = 320\ mm$ — EC2, equation (B.6) – Effective slab thickness

$\alpha_1 = (\frac{35}{f_{cm}})^{0.7} = 0.8658$ — EC2, equation (B.8c)

$\alpha_2 = (\frac{35}{f_{cm}})^{0.2} = 0.95966$ — EC2, equation (B.8c)

$\alpha_3 = (\frac{35}{f_{cm}})^{0.5} = 0.902$ — EC2, equation (B.8c)

$\varphi_{RH} = \left[1 + \frac{1-\frac{RH}{100}}{0.1*h_0^{\frac{1}{3}}}\alpha_1\right]\alpha_2 = 1.6885$ — EC2, equation (B.3b) for $f_{cm} > 35\ Mpa$

$\beta(f_{cm}) = \frac{16.8}{\sqrt{f_{cm}}} = 2.5619$ — EC2, equation (B.4)

$\beta(t_0) = \frac{1}{0.1+t_0^{0.2}} = 0.488$ — EC2, equation (B.5)

$\varphi_0 = \varphi_{RH} * \beta(f_{cm}) * \beta(t_0) = 2.11$ — EC2, equation (B.2)

$\beta_H = 1.5[1 + (0.012RH)^{18}]h_0 + 250\alpha_3 \leq 1500\alpha_3$ — EC2, equation (B.8b) for $f_{cm} \geq 35\ Mpa$

$= 705.5$

$\beta_c(t, t_0) = [\frac{(t-t_0)}{(\beta_H+t-t_0)}]^{0.3} = 0.98866$ — EC2, equation (B.7)

$$\boldsymbol{\varphi(t, t_0) = \varphi_0 * \beta_c(t, t_0) = 2.086}$$

Shrinkage

$k_h = 0.745$ — EC2, table 3.3 – Interpolated value

$\varepsilon_{cd,0} = 0.00049$ — EC2, table 3.2 – Interpolated value

$\beta_{ds}(t, t_s) = \frac{(t-t_s)}{(t-t_s)+0.04h_0^{\frac{1}{3}}} \approx 1$ — EC2, equation (3.10) – When t is so high the value will go towards 1

$\varepsilon_{cd}(t) = k_h\beta_{ds}(t, t_s)\varepsilon_{cd,0} = 3.65 * 10^{-4}$ — EC2, equation (3.9)

$\varepsilon_{ca}(\infty) = 2.5(f_{ck} - 10) * 10^{-6} = 6.25 * 10^{-5}$ — EC2, equation (3.12)

$\beta_{as}(t) = 1 - e^{-0.2t^{0.5}} \approx 1$ — EC2, equation (3.13) – When t is so high the value will go towards 1

$\varepsilon_{ca}(t) = \beta_{as}(t)\varepsilon_{ca}(\infty) = 6.25 * 10^{-5}$ — EC2, equation (3.11)

$$\boldsymbol{\varepsilon_{cs}(t) = \varepsilon_{cd}(t)\varepsilon_{ca}(t) = 4.275 * 10^{-4}}$$

Relaxation

$\rho_{1000} = 2.5\%$	EC2, section 3.3.2(6)
$\sigma_{pi} = \sigma_{pm0}(x) = 1394\ Mpa$	EC2, section 3.3.2(7)
$\mu = \frac{\sigma_{pi}}{f_{pk}} = 0.75$	EC2, section 3.3.2(7)
$t = 500\ 000\ hours$	EC2, section 3.3.2(8) for long-term effects of relaxation. Equals 57 years.

EC2, equation (3.29) in section 3.3.2(7) for class 2 relaxation:

$$\boldsymbol{\Delta\sigma_{pr} = 0.66\rho_{1000}e^{9.1\mu}(\frac{t}{1000})^{0.75(1-\mu)}\sigma_{pi} * 10^{-5} = 67.9\ Mpa}$$

Stress in concrete section at level of the prestressing tendons

$M_{g+0.6q} = 143\ KNm$	Biggest moment in y-direction for slab, considering a cross section of 1m. This is for a quasi-permanent load combination without the addition of prestress force. Happens at column E2, so the cable profile has eccentricity 60mm.
$M_t = -P_0(e - y_t)n_{y,1m} + M_{g+0.6q} = 129.65\ KNm$	Moment that is occurring at the center of gravity for concrete section. Here the cable profile is placed so it counteracts the moment over the support.
$\sigma_{c,QP} = \frac{P_0}{A_t}n_{y,1m} + \frac{M_t}{I_t}(e - y_t) = 2.14\ Mpa$	Resulting stresses at location of prestressing tendons in cross-section. Considering that moment M_t and moment due to prestressing works in opposite directions. In addition, y-direction here is negative.

Time-dependent prestress loss, simplified formula

$$\Delta P_{c+s+r} = A_p \frac{\varepsilon_{cs}E_p + 0.8\Delta\sigma_{pr} + \frac{E_p}{E_{cm}}\varphi(t,t_0)\sigma_{c,QP}}{1 + \frac{E_p}{E_{cm}}\frac{A_p}{A_c}\left(1 + \frac{A_c}{I_c}z_{cp}^2\right)[1 + 0.8\varphi(t,t_0)} = 24.25\ KN$$

$$\frac{\Delta P_{c+s+r}}{n_{y,1m}} = 22.43\ KN\ per\ cable$$

Resulting effective prestress force after immediate and time-dependent prestress losses:

$$\boldsymbol{P_0' = P_0 - 22.43\ KN = 183.89\ KN}$$

A.2.2 Prestress losses in x-direction: concentrated cables

Calculation basis

$b = 1000\ mm$	
$h = 320\ mm$	
$RH = 40\%$	Assuming a relative humidity of 40%
$t_0 = 28\ days$	Assuming that permanent loads are applied after 28 days of casting
$t = 18250\ days$	Evaluated at 18250 days as the construction is dimensioned for 50 years life span
$f_{cm} = 43\ Mpa$	Mean strength in concrete type B35
$f_{pk} = 1860\ Mpa$	Characteristic strength in tension for prestressing tendons
$\sigma_{pm0}(x) = 1394\ Mpa$	Initial stress in prestressing tendons
Assumed class 2 for relaxation	
Cement class N	
$P_0 = 206.35\ KN$	Prestress force after immediate losses as calculated above
$e = 60\ mm$	Maximum eccentricity
$y_t = 0.306\ mm$	Distance between center of gravity for concrete section to center of gravity for concrete section with reinforcement considered, as calculated above
$A_t = 321638\ mm^2$	Transformed cross-sectional area
$I_t = 2{,}736 * 10^9\ mm^4$	Transformed second moment of area of cross-section
$n_{x,1m} = \frac{18}{7.8\ m} = 2.307$	Number of tendons considering 1m width and the highest number of concentrated cables in x-direction

Creep

$$\boldsymbol{\varphi(t, t_0) = \varphi_0 * \beta_c(t, t_0) = 2.086}$$

Shrinkage

$\boldsymbol{\varepsilon_{cs}(t) = \varepsilon_{cd}(t)\varepsilon_{ca}(t) = 4.275 * 10^{-4}}$

See section A.2.1 for calculation of creep, shrinkage and relaxation effects on slab

Relaxation

$$\boldsymbol{\Delta\sigma_{pr} = 0.66\rho_{1000}e^{9.1\mu}(\frac{t}{1000})^{0.75(1-\mu)}\sigma_{pi} * 10^{-5} = 67.9\ Mpa}$$

Stress in concrete section at level of the prestressing tendons

$M_{g+0.6q} = 157.95\ KNm$

Biggest moment in x-direction for slab, considering a cross section of 1m. This is for a quasi-permanent load combination without the addition of prestress force. Happens at column B6, so the cable profile has eccentricity 60mm.

$M_t = -P_0(e - y_t)n_{y,1m} + M_{g+0.6q} = 129.53\ KNm$

Moment that is occurring at the center of gravity for concrete section. Here the cable profile is placed so it counteracts the moment over the support.

$\sigma_{c,QP} = \frac{P_0}{A_t}n_{y,1m} + \frac{M_t}{I_t}(e - y_t) = 1.346\ Mpa$

Resulting stresses at location of prestressing tendons in cross-section. Considering that moment M_t and moment due to prestressing works in opposite directions. In addition, y-direction here is negative.

Time-dependent prestress loss, simplified formula

$$\Delta P_{c+s+r} = A_p \frac{\varepsilon_{cs}E_p + 0.8\Delta\sigma_{pr} + \frac{E_p}{E_{cm}}\varphi(t,t_0)\sigma_{c,QP}}{1 + \frac{E_p}{E_{cm}}\frac{A_p}{A_c}\left(1 + \frac{A_c}{I_c}z_{cp}^2\right)[1 + 0.8\varphi(t,t_0)}} = 22.84\ KN$$

$$\frac{\Delta P_{c+s+r}}{n_{y,1m}} = 9.9\ KN\ per\ cable$$

Resulting effective prestress force after immediate and time-dependent prestress losses:

$$\boldsymbol{P_0' = P_0 - 9.9\ KN = 196.45\ KN}$$

B Ultimate Limit State

B.1 Moment Capacity check

B.1.1 Field moment y-direction: distributed cables

Calculation basis

Biggest field moment in y-direction can be found in cross-section: “Section_ID_749”.

This is located at the positioning AB2 with load combination: ULS unfavorable pattern 1 6-10A.

$B = 1m$	Width of cross-section evaluated for moment capacity and loading
$d = 238\,mm$	Evaluated effective depth based on orientation of base mesh, supplementary reinforcement and tendons in both directions
$f_{cd} = 0.85\frac{35}{1.5}\,Mpa$	Dimensioning strength for concrete type B35
$f_{yd} = \frac{500}{1.15}\,Mpa$	Dimensioning strength for non-stressed steel
$A_p = 150mm^2$	cross-sectional area of one tendon

Dimensioning moment:

$M_{g,Ed} = 1.35Self + 1.35Dead = 84.73\,KNm$	Dimensioning moment for static load at critical field section in y-direction
$M_{q,Ed} = 1.05Pattern1 = 13.84\,KNm$	Dimensioning moment for live load at critical field section in y-direction
$M_1 = 1.1Hype = 2.64\,KNm$	Parasitic moment due to indeterminate structure
$\boldsymbol{M_{Ed} = 101.21\,KNm}$	Resulting dimensioning moment for critical cross-section

Moment capacity:

$P_0' = 194.07\,KN$	Effective prestress force as assumed by ADAPT-Builder for distributed cables
$P_y = P_0' + 100\,Mpa * A_p = 209.07\,KN$	Applicable prestress force for moment capacity
$n_y = 1$	Number of tendons within 1m of the critical cross-section as shown by ADAPT-Builder
$S_p = \frac{P_y * n_y}{\gamma_s} = 181.8\,KN$	Contribution of force due to existence of tendons in cross-section

$A_{s,mesh} = K\ 257 + \pi * 5^2 * \frac{1000}{450} = 431.53\ mm^2$	Base reinforcement at cross-section
$A_{s,supplementary} = \pi * 8^2 * 1 = 200.96\ mm^2$	Supplementary reinforcement at cross-section
$A_{s,total} = 632.4929\ mm^2$	Total non-stressed reinforcement at cross-section
$\alpha = \frac{S_p + f_{yd} A_s}{0.8 f_{cd} bd} = 0.1209$	balanced factor

$$\boldsymbol{M_{Rd}} = 0.8(1 - 0.4\alpha)\alpha b d^2 f_{cd} = \mathbf{103.4\ KNm} > M_{Ed}$$

B.1.2 Support moment y-direction: distributed cables

Calculation basis

Biggest support moment in y-direction can be found in cross-section: “Section_ID_750”.

This is located at the positioning E2 with load combination: ULS favorable pattern 5 6-10A.

$B = 1m$	Width of cross-section evaluated for moment capacity and loading
$d = 238\ mm$	Evaluated effective depth based on orientation of base mesh, supplementary reinforcement and tendons in both directions
$f_{cd} = 0.85 \frac{35}{1.5}\ Mpa$	Dimensioning strength for concrete type B35
$f_{yd} = \frac{500}{1.15}\ Mpa$	Dimensioning strength for non-stressed steel
$A_p = 150 mm^2$	cross-sectional area of one tendon

Dimensioning moment:

$M_{g,Ed} = 1.35 Self + 1.35 Dead = -174.76\ KNm$	Dimensioning moment for static load at critical support section in y-direction
$M_{q,Ed} = 1.05 Pattern5 = -25.72\ KNm$	Dimensioning moment for live load at critical support section in y-direction
$M_1 = 0.9 Hype = 2.38\ KNm$	Parasitic moment due to indeterminate structure
$\boldsymbol{M_{Ed}} = \mathbf{-198.1\ KNm}$	Resulting dimensioning moment for critical cross-section

Moment capacity:

$P_0' = 194.07\ KN$	Effective prestress force as assumed by ADAPT-Builder for distributed cables
$P_y = P_0' + 100\ Mpa * A_p = 209.07\ KN$	Applicable prestress force for moment capacity
$n_y = 1$	Number of tendons within 1m of the critical cross-section as shown by ADAPT-Builder
$S_p = \frac{P_y * n_y}{\gamma_s} = 181.8\ KN$	Contribution of force due to existence of tendons in cross-section
$A_{s,mesh} = k\ 257 + \pi * 5^2 * \frac{1000}{450} = 431.5329\ mm^2$	Base reinforcement at cross-section
$A_{s,supplementary} = \pi * 8^2 * 11 = 2211.681\ mm^2$	Supplementary reinforcement at cross-section
$A_{s,total} = 2643.21\ mm^2$	Total non-stressed reinforcement at cross-section
$\alpha = \frac{S_p + f_{yd} A_s}{0.8 f_{cd} bd} = 0.352$	balanced factor

$$\boldsymbol{M_{Rd}} = 0.8(1 - 0.4\alpha)\alpha b d^2 f_{cd} = \mathbf{271.8\ KNm} > M_{Ed}$$

B.1.3 Field moment x-direction: concentrated cables

Calculation basis

Biggest field moment in x-direction can be found in cross-section: “Section_ID_1501012”.

This is located at the positioning D12 with load combination: ULS unfavorable pattern 3 6-10A.

$L = 7.8m$	Loading width of cross-section for dimensioning moment
$B = 3.9m$	Width of cross-section evaluated for moment capacity
$d = 253.5\ mm$	Evaluated effective depth based on orientation of base mesh, supplementary reinforcement and tendons in both directions
$f_{cd} = 0.85 \frac{35}{1.5}\ Mpa$	Dimensioning strength for concrete type B35
$f_{yd} = \frac{500}{1.15}\ Mpa$	Dimensioning strength for non-stressed steel

$A_p = 150mm^2$	cross-sectional area of one tendon

Dimensioning moment:

$M_{g,Ed} = 1.35Self + 1.35Dead = 723.92\ KNm$	Dimensioning moment for static load at critical field section in x-direction
$M_{q,Ed} = 1.05Pattern3 = 127.04\ KNm$	Dimensioning moment for live load at critical field section in x-direction
$M_1 = 1.1Hype = 46.74\ KNm$	Parasitic moment due to indeterminate structure
$\boldsymbol{M_{Ed} = 897.7\ KNm}$	Resulting dimensioning moment for critical cross-section

Moment capacity:

$P_0' = 195.56\ KN$	Effective prestress force as assumed by ADAPT-Builder for concentrated cables
$P_x = P_0' + 100\ Mpa * A_p = 210.56\ KN$	Applicable prestress force for moment capacity
$n_x = 12$	Number of tendons within 3.9m of the critical cross-section as shown by ADAPT-Builder
$S_p = \frac{P_x * n_x}{\gamma_s} = 2197.15\ KN$	Contribution of force due to existence of tendons in cross-section
$A_{s,mesh} = K\ 257 + \pi * 5^2 * \frac{3900}{450} = 1682.98\ mm^2$	Base reinforcement at cross-section
$A_{s,supplementary} = \pi * 8^2 * 8 = 1608.5\ mm^2$	Supplementary reinforcement at cross-section
$A_{s,total} = 3291.48\ mm^2$	Total non-stressed reinforcement at cross-section
$\alpha = \frac{S_p + f_{yd}A_s}{0.8 f_{cd} bd} = 0.2313$	balanced factor

$$\boldsymbol{M_{Rd}} = 0.8(1 - 0.4\alpha)\alpha bd^2 f_{cd} = \mathbf{834.68\ KNm} < M_{Ed}$$

B.1.4 Support moment x-direction: concentrated cables

Calculation basis

Biggest support moment in x-direction can be found in cross-section: “Section_ID_1706000”.

This is located at the positioning B6 with load combination: ULS favorable pattern 7 6-10A.

$L = 7.8m$	Loading width of cross-section for dimensioning moment
$B = 3.9m$	Width of cross-section evaluated for moment capacity
$d = 253.5\ mm$	Evaluated effective depth based on orientation of base mesh, supplementary reinforcement and tendons in both directions
$f_{cd} = 0.85\frac{35}{1.5}\ Mpa$	Dimensioning strength for concrete type B35
$f_{yd} = \frac{500}{1.15}\ Mpa$	Dimensioning strength for non-stressed steel
$A_p = 150mm^2$	cross-sectional area of one tendon

Dimensioning moment:

$M_{g,Ed} = 1.35Self + 1.35Dead = -910.82\ KNm$	Dimensioning moment for static load at critical support section in x-direction
$M_{q,Ed} = 1.05Pattern7 = -138.08\ KNm$	Dimensioning moment for live load at critical support section in x-direction
$M_1 = 0.9Hype = 50.22\ KNm$	Parasitic moment due to indeterminate structure
$\boldsymbol{M_{Ed} = -998.7\ KNm}$	Resulting dimensioning moment for critical cross-section

Moment capacity:

$P_0' = 195.56\ KN$	Effective prestress force as assumed by ADAPT-Builder for concentrated cables
$P_x = P_0' + 100\ Mpa * A_p = 210.56\ KN$	Applicable prestress force for moment capacity
$n_x = 16$	Number of tendons within 3.9m of the critical cross-section as shown by ADAPT-Builder
$S_p = \frac{P_x * n_x}{\gamma_s} = 2929.53\ KN$	Contribution of force due to existence of tendons in cross-section
$A_{s,mesh} = K\ 257 + \pi * 5^2 * \frac{3900}{450} = 1682.98\ mm^2$	Base reinforcement at cross-section
$A_{s,supplementary} = \pi * 8^2 * 8 = 1608.5\ mm^2$	Supplementary reinforcement at cross-section
$A_{s,total} = 3291.48\ mm^2$	Total non-stressed reinforcement at cross-section

$\alpha = \frac{S_p + f_{yd} A_s}{0.8 f_{cd} bd} = 0.278$	balanced factor

$$\boldsymbol{M_{Rd}} = 0.8(1 - 0.4\alpha)\alpha bd^2 f_{cd} = \mathbf{982.55\ KNm} < M_{Ed}$$

B.2 Shear capacity check

Internal column

Calculation basis

Biggest dimensioning forces in ULS for an internal column can be found at column E2.

$c_1 = c_2 = 550\ mm$	Dimensions of each side of rectangular column
$V_{Ed} = 1672{,}1\ KN$	Dimensioning shear force in slab by critical column
$b_x = 7.8\ m$	Applicable width for cross-section
$b_y = 8.5\ m$	Applicable width for cross-section
$h = 320\ mm$	slab thickness
$f_{ck} = 35\ Mpa$	characteristic strength for concrete type B35
$A_{s,mesh,x} = K\ 257 + Ø10c450$	Base reinforcement evaluated for cross-section with width b_x
$A_{s,mesh,y} = K\ 257 + Ø10c450$	Base reinforcement evaluated for cross-section with width b_y
$A_{s,supplementary,x} = 4Ø16$	Supplementary reinforcement evaluated for cross-section with width b_x
$A_{s,supplementary,y} = 12Ø16$	Supplementary reinforcement evaluated for cross-section with width b_y
$P_{max} = 221\ KN$	Applied maximum prestress force utilized in ADAPT-Builder
$n_x = 18$	Number of concentrated cables (x-direction) within the width b_x
$n_y = 9$	Number of distributed cables (y-direction) within the width b_y

Dimensioning shear stress:

$d_{eff} = \frac{d_y + d_z}{2} = 244\ mm$	EC2, section 6.4.2(1), equation (6.32). Effective depth utilized here is the suggested effective depth by ADAPT-Builder. By hand: $\frac{238+253.5}{2} = 245.75\ mm\ \approx 244\ mm$
$\beta = 1.15$	EC2, section 6.4.3(6), Figure 6.21N
$u_1 = 2c_1 + 2c_2 + 4\pi d = 5266.19\ mm$	Critical circumference around internal column, at a distance 2d from face of column
$u_0 = 2c_1 + 2c_2 = 2200\ mm$	Critical circumference around internal column, at face of column
$v_{Ed} = \beta \frac{V_{Ed}}{u_1 d} = 1.496\ Mpa$	EC2, section 6.4.3(3), equation (6.38). Dimensioning shear stress at critical circumference u_1
$v_{Ed} = \beta \frac{V_{Ed}}{u_0 d} = 3.582\ Mpa$	EC2, section 6.4.3(3), equation (6.38). Dimensioning shear stress at critical circumference u_0

Maximum shear capacity $v_{Rd,max}$:

$v = 0.6\left(1 - \frac{f_{ck}}{250}\right) = 0.516$	EC2, section NA.6.2.2(6), equation (NA.6.6N)
$v_{Rd,max} = 0.4 v f_{cd} = 4.09\ Mpa$	EC2, section NA.6.4.5(3)

$$\boldsymbol{v_{Ed} = 3.582\ Mpa\ \leq\ v_{Rd,max} = 4.09\ Mpa}\ \textbf{OK}$$

Shear capacity without necessary reinforcement for shear punching, $v_{Rd,c}$:

$v_{Rd,c} = C_{Rd,c} k (100 \rho_l f_{ck})^{\frac{1}{3}} + k_1 \sigma_{cp}$	EC2, section 6.4.4(1), equation (6.47)
$v_{Rd,c} \geq (v_{min} + k_1 \sigma_{cp})$	EC2, section 6.4.4(1), equation (6.47)
$k = 1 + \sqrt{\frac{200}{d}} \leq 2 = 1.905$	
$C_{Rd,c} = \frac{0.18}{\gamma_c} = 0.12$	EC2, section NA.6.4.4(1)
$A_{s,mesh,x} = K\ 257 + \pi * 5^2 * \frac{b_x}{450\ mm} = 3366\ mm^2$	Base reinforcement in tension calculated for width b_x
$A_{s,supplementary,x} = 4 * \pi * 8^2 = 804\ mm^2$	Supplementary reinforcement calculated for width b_x

$A_{s,x} = A_{s,mesh,x} + A_{s,supplementary,x} = 4170\ mm^2$ Total non-stressed reinforcement in tension for cross-section evaluated at x-direction

$\rho_{l,x} = \frac{A_{s,x}}{d(c_1+2*3d)} = 0.0085$ Contribution from reinforcement in x-direction divided over recommended spacing by EC2

$A_{s,mesh,y} = K\ 257 + \pi * 5^2 * \frac{b_y}{450\ mm} = 3668\ mm^2$ Base reinforcement in tension calculated for width b_y

$A_{s,supplementary,y} = 12 * \pi * 8^2 = 2413\ mm^2$ Supplementary reinforcement calculated for width b_y

$A_{s,y} = A_{s,mesh,y} + A_{s,supplementary,y} = 6081\ mm^2$ Total non-stressed reinforcement in tension for cross-section evaluated at y-direction

$\rho_{l,y} = \frac{A_{s,y}}{d(c_2+2*3d)} = 0.0124$ Contribution from reinforcement in y-direction divided over recommended spacing by EC2

$\rho_l = \sqrt{\rho_{l,x} * \rho_{l,y}} = 0.010266$

$k_1 = 0.1$ EC2, section NA.6.4.4

$A_{c,x} = b_x * h = 2496 * 10^3\ mm^2$ Width of the affected area for concentrated cables equals the entire width b_x as the internal column is placed far enough from edge of slab. This is as recommended by Terje kanstad in section 3.7.2

$\sigma_{c,x} = \frac{0.85*0.9*P_{max}*n_x}{A_{c,x}} = 1.22\ Mpa$

$A_{c,y} = b_y * h = 2720 * 10^3\ mm^2$

$\sigma_{c,y} = \frac{0.85 * 0.9 * P_{max} * n_y}{A_{c,y}} = 0.56\ Mpa$

$\sigma_{cp} = \frac{\sigma_{c,x} + \sigma_{c,y}}{2} = 0.89\ Mpa$

$v_{min} = 0.035 k^{\frac{3}{2}} f_{ck}^{\frac{1}{2}} = 0.544\ Mpa$ EC2, section NA.6.4.4, equation (NA.6.3N)

$C_{Rd,c} k (100 \rho_l f_{ck})^{\frac{1}{3}} + k_1 \sigma_{cp} = 0.843\ Mpa$

$v_{min} + k_1 \sigma_{cp} = 0.6334\ Mpa$

$$\boldsymbol{v_{Rd,c} = 0.843\ Mpa \leq v_{Ed} = 1.496\ Mpa}$$ **NOT OK**

Shear capacity with necessary reinforcement for shear punching $v_{Rd,cs}$:

$v_{Rd,cs} = 0.75v_{Rd,c} + 1.5(\frac{d}{S_r})A_{sw}f_{ywd,ef}\frac{1}{u_1 d}\sin\alpha$	EC2, section 6.4.5(1), equation (6.52)
$v_{Rd,cs} \leq k_{max}v_{Rd,c}$	
$\alpha = 90^{\circ}$	Assumed orientation of shear reinforcement
$f_{ywd,ef} = 250 + 0.25d = 311\ Mpa$	Effective dimensioning shear strength of reinforcement
$S_r = 160\ mm$	Spacing between each section with shear reinforcement
$A_{sw} = \frac{v_{Ed} - 0.75v_{Rd,c}}{1.5\frac{d}{S_r}f_{ywd,ef}\frac{1}{u_1 d}\sin\alpha} = 1560.1\ mm^2$	Necessary reinforcement as $v_{Rd,cs} = v_{Ed} = 1.496\ Mpa$:
$A_{sw} = 1570.8\ mm^2$	Choice of reinforcement to meet criteria of necessary reinforcement (20Ø10)
$k_{max} = 1.8$	EC2, section NA.6.4.5(1)
$0.75v_{Rd,c} + 1.5\left(\frac{d}{S_r}\right)A_{sw}f_{ywd,ef}\frac{1}{u_1 d}\sin\alpha = 1.5\ Mpa$	Capacity with appropriate shear reinforcement included
$k_{max}v_{Rd,c} = 1.517\ Mpa$	

$$\boldsymbol{v_{Rd,cs} = 1.5 \geq v_{Ed} = 1.496\ Mpa} \quad \textbf{OK}$$

End/Edge column

Calculation basis

Biggest dimensioning forces in ULS for an edge/end column can be found at column E7.

$c_1 = c_2 = 550\ mm$	Dimensions of each side of rectangular column
$V_{Ed} = 691.2\ KN$	Dimensioning shear force in slab by critical column
$b_x = 3.676\ m$	Effective width for concentrated cables in accord with recommendation by Terje kanstad, as explained in section 3.7.2
$L_x = 7.8\ m$	Applicable width for cross-section
$b_y = 4.25\ m$	Applicable width for cross-section
$h = 320\ mm$	slab thickness
$f_{ck} = 35\ Mpa$	characteristic strength for concrete type B35

$A_{s,mesh,x} = K\ 257 + Ø10c450$	Base reinforcement evaluated for cross-section with width L_x
$A_{s,mesh,y} = K\ 257 + Ø10c450$	Base reinforcement evaluated for cross-section with width b_y
$P_{max} = 221\ KN$	Applied maximum prestress force utilized in ADAPT-Builder
$n_x = 18$	Number of concentrated cables (x-direction) within the width L_x
$n_y = 5$	Number of distributed cables (y-direction) within the width b_y

Dimensioning shear stress:

$d_{eff} = \frac{d_y + d_z}{2} = 244\ mm$	EC2, section 6.4.2(1), equation (6.32). Effective depth utilized here is the suggested effective depth by ADAPT-Builder. By hand: $\frac{238+253.5}{2} = 245.75\ mm\ \approx 244\ mm$
$\beta = 1.4$	EC2, section 6.4.3(6), Figure 6.21N
$u_1 = 2c_1 + 2c_2 + 2\pi d = 3183.1\ mm$	Critical circumference around internal column, at a distance 2d from face of column
$u_0 = c_2 + 3d \leq 2c_1 + c_2 = 1282\ mm$	EC2, section 6.4.5(3). Critical circumference around internal column, at face of column.
$\upsilon_{Ed} = \beta \frac{V_{Ed}}{u_1 d} = 1.246\ Mpa$	EC2, section 6.4.3(3), equation (6.38). Dimensioning shear stress at critical circumference u_1
$\upsilon_{Ed} = \beta \frac{V_{Ed}}{u_0 d} = 3.093\ Mpa$	EC2, section 6.4.3(3), equation (6.38). Dimensioning shear stress at critical circumference u_0

Maximum shear capacity $\boldsymbol{\upsilon_{Rd,max}}$:

$\upsilon = 0.6\left(1 - \frac{f_{ck}}{250}\right) = 0.516$	EC2, section NA.6.2.2(6), equation (NA.6.6N)
$\upsilon_{Rd,max} = 0.4\upsilon f_{cd} = 4.09\ Mpa$	EC2, section NA.6.4.5(3)

$$\boldsymbol{\upsilon_{Ed} = 3.093\ Mpa\ \leq\ \upsilon_{Rd,max} = 4.09\ Mpa}\ \textbf{OK}$$

Shear capacity without necessary reinforcement for shear punching, $\upsilon_{Rd,c}$:

$\upsilon_{Rd,c} = C_{Rd,c}k(100\rho_l f_{ck})^{\frac{1}{3}} + k_1\sigma_{cp}$ EC2, section 6.4.4(1), equation (6.47)

$\upsilon_{Rd,c} \geq (\upsilon_{min} + k_1\sigma_{cp})$ EC2, section 6.4.4(1), equation (6.47)

$k = 1 + \sqrt{\frac{200}{d}} \leq 2 = 1.905$

$C_{Rd,c} = \frac{0.18}{\gamma_c} = 0.12$ EC2, section NA.6.4.4(1)

$A_{s,mesh,x} = K\ 257 + \pi * 5^2 * \frac{L_x}{450\ mm} = 3366\ mm^2$ Base reinforcement in tension calculated for width L_x

$A_{s,x} = A_{s,mesh,x} = 3366\ mm^2$ Total non-stressed reinforcement in tension for cross-section evaluated at x-direction

$\rho_{l,x} = \frac{A_{s,x}}{d(c_1+2*3d)} = 0.0068$ Contribution from reinforcement in x-direction divided over recommended spacing by EC2

$A_{s,mesh,y} = K\ 257 + \pi * 5^2 * \frac{b_y}{450\ mm} = 3366\ mm^2$ Base reinforcement in tension calculated for width b_y

$A_{s,y} = A_{s,mesh,y} = 3366\ mm^2$ Total non-stressed reinforcement in tension for cross-section evaluated at y-direction

$\rho_{l,y} = \frac{A_{s,y}}{d(c_2+3d)} = 0.01076$ Contribution from reinforcement in y-direction divided over recommended spacing by EC2. Notice how this spacing is limited as column E7 is an edge column

$\rho_l = \sqrt{\rho_{l,x} * \rho_{l,y}} = 0.00855$

$k_1 = 0.1$ EC2, section NA.6.4.4

$A_{c,x} = b_x * h = 1176.32 * 10^3\ mm^2$ Width of the affected area for concentrated cables equals the width b_x as the edge column has limited distributed width. This is an approximate affected width at the critical circumference u_1

$$\sigma_{c,x} = \frac{0.85 * 0.9 * P_{max} * n_x}{A_{c,x}} = 2.587\ Mpa$$

$A_{c,y} = b_y * h = 1360 * 10^3\ mm^2$

$$\sigma_{c,y} = \frac{0.85 * 0.9 * P_{max} * n_y}{A_{c,y}} = 0.622\ Mpa$$

$$\sigma_{cp} = \frac{\sigma_{c,x} + \sigma_{c,y}}{2} = 1.6405\ Mpa$$

$$v_{min} = 0.035 k^{\frac{3}{2}} f_{ck}^{\frac{1}{2}} = 0.544\ Mpa$$ EC2, section NA.6.4.4, equation (NA.6.3N)

$$C_{Rd,c} k (100 \rho_l f_{ck})^{\frac{1}{3}} + k_1 \sigma_{cp} = 0.87\ Mpa$$

$$v_{min} + k_1 \sigma_{cp} = 0.70445\ Mpa$$

$$\boldsymbol{v_{Rd,c} = 0.87\ Mpa \leq v_{Ed} = 1.246\ Mpa}$$ **NOT OK**

Shear capacity with necessary reinforcement for shear punching $\boldsymbol{v_{Rd,cs}}$:

$$v_{Rd,cs} = 0.75 v_{Rd,c} + 1.5 (\frac{d}{S_r}) A_{sw} f_{ywd,ef} \frac{1}{u_1 d} \sin \alpha$$ EC2, section 6.4.5(1), equation (6.52)

$$v_{Rd,cs} \leq k_{max} v_{Rd,c}$$

$\alpha = 90^{\circ}$ Assumed orientation of shear reinforcement

$f_{ywd,ef} = 250 + 0.25d = 311\ Mpa$ Effective dimensioning shear strength of reinforcement

$S_r = 160\ mm$ Spacing between each section with shear reinforcement

$A_{sw} = \frac{v_{Ed} - 0.75 v_{Rd,c}}{1.5 \frac{d}{S_r} f_{ywd,ef} \frac{1}{u_1 d} \sin \alpha} = 647.95\ mm^2$ Necessary reinforcement as $v_{Rd,cs} = v_{Ed} = 1.246\ Mpa$:

$A_{sw} = 706.86\ mm^2$ Choice of reinforcement to meet criteria of necessary reinforcement (9Ø10)

$k_{max} = 1.8$ EC2, section NA.6.4.5(1)

$0.75 v_{Rd,c} + 1.5 \left(\frac{d}{S_r}\right) A_{sw} f_{ywd,ef} \frac{1}{u_1 d} \sin \alpha = 1.3\ Mpa$ Capacity with appropriate shear reinforcement included

$k_{max} v_{Rd,c} = 1.566\ Mpa$

$$\boldsymbol{v_{Rd,cs} = 1.3 \geq v_{Ed} = 1.246\ Mpa}$$ **OK**

C Serviceability limit state

C.1 Check of Concrete stresses

C.1.1 Biggest stress in compression in slab

Calculation basis

The biggest stress in compression in slab can as previously mentioned to be found at lower edge of slab at column B6. This is evaluated in the x-direction, so it is for the design strip B17. ADAPT-Builder found it to be $-5.3\ Mpa$.

$n_x = 16$	Number of cables within design strip B17
$P_0 = 206.81\ KN$	Calculated prestress force after immediate losses for concentrated cables (x-direction) by ADAPT-Builder.
$b = 7.8\ m$	Width of design strip B17
$h = 320\ mm$	
$y = 160\ mm$	Positive direction downwards
$A_c = bh = 2496 * 10^3\ mm^2$	
$I = \frac{bh^3}{12} = 2.13 * 10^{10}\ mm^4$	

Dimensioning moment & resulting concrete stress:

$M_{g+q} = -747.77\ KNm$	Moment due to static and live load at the critical cross-section with highest stress in compression, in accord with ADAPT-Builder
$M_p = 185.38\ KNm$	Moment due to prestressing at the critical cross-section with highest stress in compression, in accord with ADAPT-Builder
$M = M_{g+q} + M_p = -562.39\ KNm$	Resulting moment at critical-cross section

$$\boldsymbol{\sigma_{c,min} = -\frac{P_0}{A_c} n_x + \frac{M}{I} y = -5.55\ Mpa}$$

C.1.2 Biggest stress in tension in slab

Calculation basis

The biggest stress in tension in slab can as previously mentioned to be found at upper edge of slab at column E6. This is evaluated in the y-direction, so it is for the design strip AF6. ADAPT-Builder found it to be $3.158\ Mpa$.

$n_y = 9$	Number of cables within design strip AF6
$P_0 = 205.32\ KN$	Calculated prestress force after immediate losses for distributed cables (y-direction) by ADAPT-Builder.
$b = 8.5\ m$	Width of design strip AF6
$h = 320\ mm$	
$y = -160\ mm$	Positive direction downwards
$A_c = bh = 2720 * 10^3\ mm^2$	
$I = \frac{bh^3}{12} = 2.321 * 10^{10}\ mm^4$	

Dimensioning moment & resulting concrete stress:

$M_{g+q} = -649.6\ KNm$	Moment due to static and live load at the critical cross-section with highest stress in tension, in accord with ADAPT-Builder
$M_p = 99.15\ KNm$	Moment due to prestressing at the critical cross-section with highest stress in tension, in accord with ADAPT-Builder
$M = M_{g+q} + M_p = -550.45\ KNm$	Resulting moment at critical-cross section

$$\boldsymbol{\sigma_{c,min} = -\frac{P_0}{A_c} n_y + \frac{M}{I} y = 3.11\ Mpa}$$

C.2 Critical moment of cracking M_{cr}

C.2.1 Field moment capacity in x-direction: concentrated cables

Calculation basis

This is located at the positioning D12, within design strip D17. The capacity here is found to be $M_{Rd} = 834.68\ KNm$

$P_0 = 206.81\ KN$	Calculated prestress force after immediate losses for concentrated cables (x-direction) by ADAPT-Builder.

$n_x = 12$ Number of concentrated cables (x-direction) within the design strip D17

$b = 7800\ mm$

$h = 320\ mm$

$A_c = 7800 * 320 = 2496 * 10^3\ mm^2$

$I = \frac{7800 * 320^3}{12} = 2.13 * 10^{10}\ mm^4$

$y = 160\ mm$

$f_{ctm} = 3.2\ Mpa$

Critical moment of cracking & utilization ratio:

$$\boldsymbol{M_{cr}} = \frac{P_0 * n_x}{A_c} * \frac{I}{y} + f_{ctm} * \frac{I}{y} = \boldsymbol{558.36\ KNm}$$

$$\frac{\boldsymbol{M_{Rd}}}{\boldsymbol{M_{cr}}} = \boldsymbol{1.495 \geq 1.15 \quad OK}$$

C.2.2 support moment capacity in x-direction: concentrated cables

Calculation basis

This is located at the positioning B6, within design strip B17. The capacity here is found to be $M_{Rd} = -982.55\ KNm$

$P_0 = 206.81\ KN$ Calculated prestress force after immediate losses for concentrated cables (x-direction) by ADAPT-Builder.

$n_x = 16$ Number of concentrated cables (x-direction) within the design strip B17

$b = 7800\ mm$

$h = 320\ mm$

$A_c = 7800 * 320 = 2496 * 10^3\ mm^2$

$I = \frac{7800 * 320^3}{12} = 2.13 * 10^{10}\ mm^4$

$y = -160\ mm$

$f_{ctm} = 3.2\ Mpa$

Critical moment of cracking & utilization ratio:

$$\boldsymbol{M_{cr}} = \frac{P_0 * n_x}{A_c} * \frac{I}{y} + f_{ctm} * \frac{I}{y} = \boldsymbol{-602.48\ KNm}$$

$$\frac{\boldsymbol{M_{Rd}}}{\boldsymbol{M_{cr}}} = \boldsymbol{1.63\ \geq 1.15\quad OK}$$

C.2.3 field- and support moment capacity in y-direction: distributed cables

Calculation basis

Field moment capacity is located at the positioning AB2, within design strip AF2. The capacity here is found to be $M_{Rd-field} = 103.4\ KNm$**.**

Support moment capacity is located at the positioning E2, within design strip AF2. The capacity here is found to be $M_{Rd-support} = -271.8\ KNm$

$P_0 = 205.32\ KN$ — Calculated prestress force after immediate losses for distributed cables (y-direction) by ADAPT-Builder.

$n_x = 1$ — Number of distributed cables (y-direction) within the width b

$b = 1000\ mm$

$h = 320\ mm$

$A_c = 1000 * 320 = 320 * 10^3\ mm^2$

$I = \frac{1000 * 320^3}{12} = 2730.67 * 10^6\ mm^4$

$y = 160\ mm$

$f_{ctm} = 3.2\ Mpa$

Critical moment of cracking & utilization ratio:

$$\boldsymbol{M_{cr}} = \frac{P_0 * n_x}{A_c} * \frac{I}{y} + f_{ctm} * \frac{I}{y} = \boldsymbol{65.56\ KNm}$$

$$\frac{\boldsymbol{M_{Rd-field}}}{\boldsymbol{M_{cr}}} = \boldsymbol{1.577\ \geq 1.15\quad OK} \qquad \frac{\boldsymbol{M_{Rd-support}}}{\boldsymbol{M_{cr}}} = \boldsymbol{4.146 \geq 1.15\ OK}$$

Appendix 2: Results from ADAPT-Builder

D Sketches of orientation of tendons and reinforcement within slab

D.1 Tendon plan

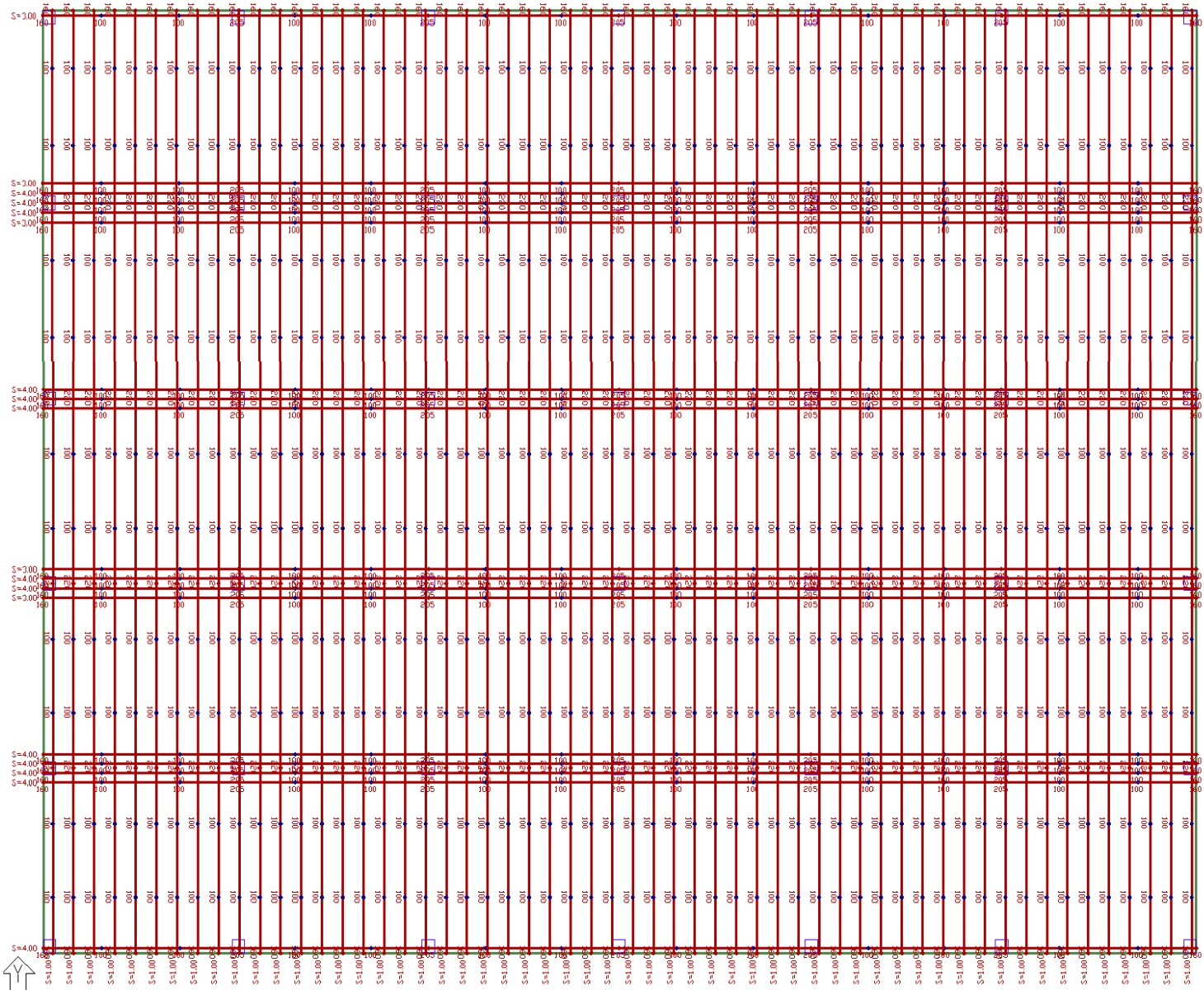

D.2 Rebar plan upper edge

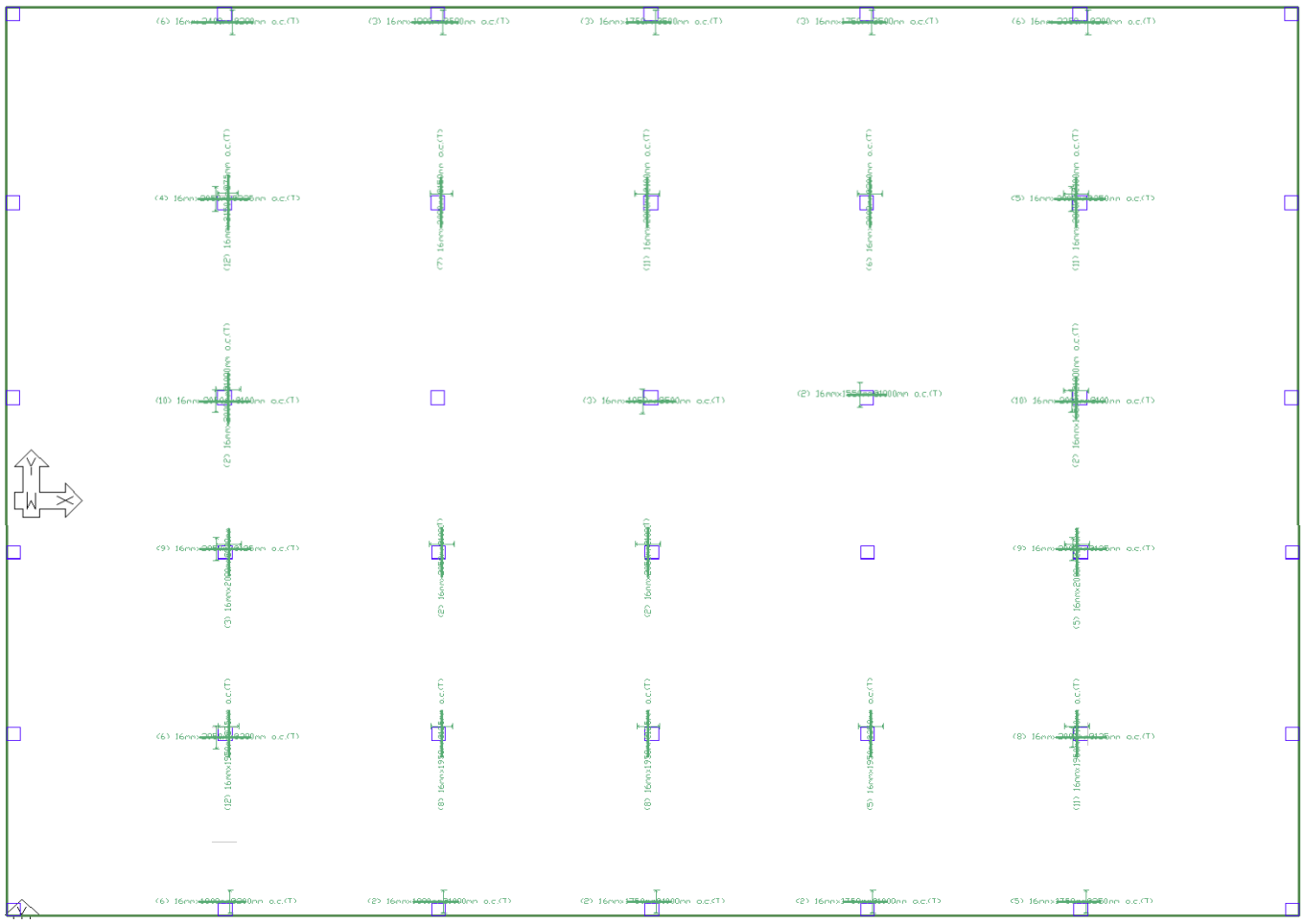

D.3 Rebar plan lower edge

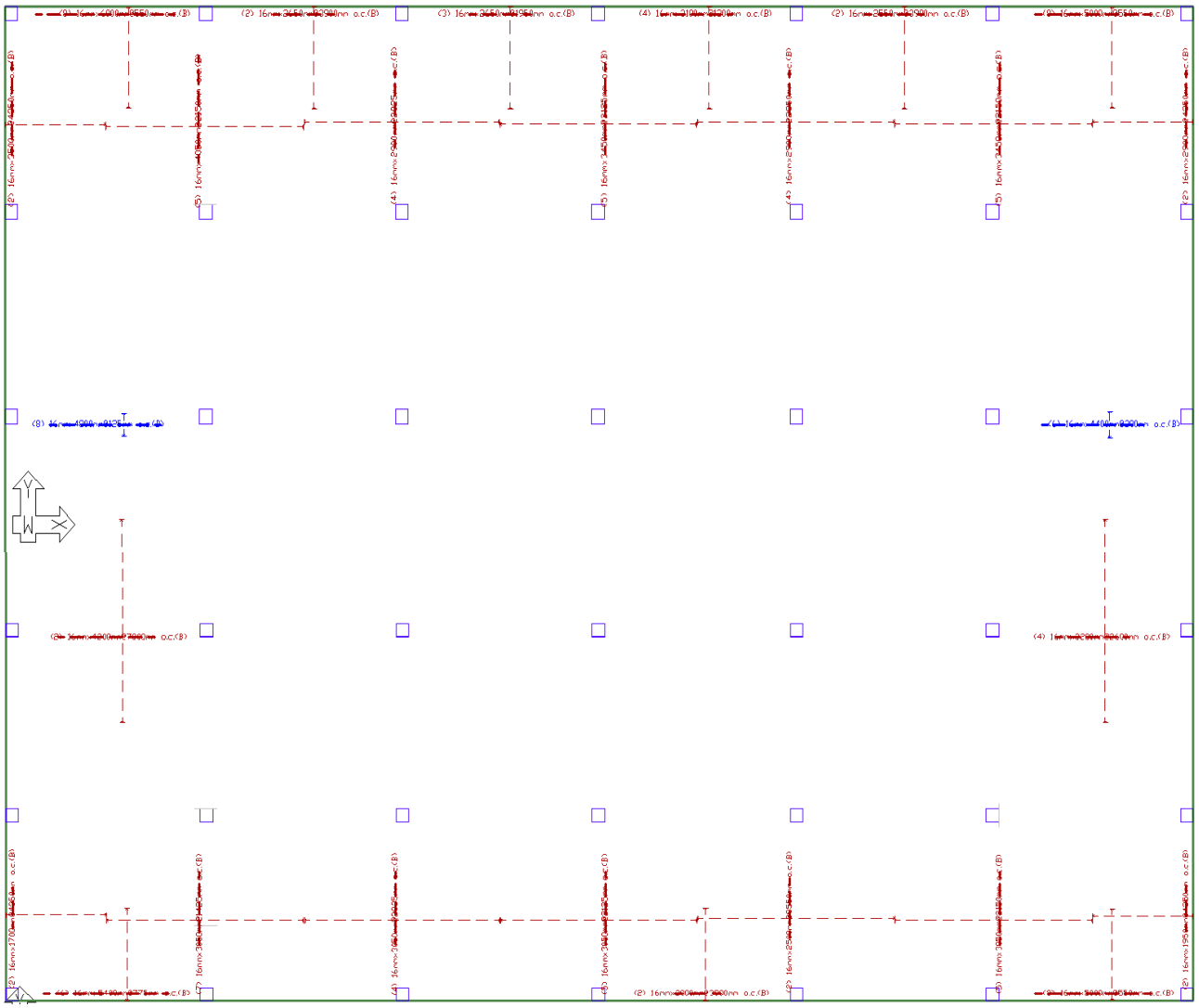

E Amount of base- and supplementary reinforcement

210.00 REBAR TOTALS

Bar Reinforcement (calculated and user defined base reinforcement)

Type	Quantity	Size	Length/ bar	Length	Weight	Unit cost	Total cost
	bars		m	m	kg	Euro/kg	Euro
1	8	16mm	6.00	48.00	75.24	3.00	225.72
2	6	16mm	5.40	32.40	50.79	3.00	152.36
3	16	16mm	5.00	80.00	125.40	3.00	376.20
4	8	16mm	4.80	38.40	60.19	3.00	180.57
5	6	16mm	4.40	26.40	41.38	3.00	124.15
6	2	16mm	4.20	8.40	13.17	3.00	39.50
7	5	16mm	4.05	20.25	31.74	3.00	95.22
8	2	16mm	3.50	7.00	10.97	3.00	32.92
9	10	16mm	3.45	34.50	54.08	3.00	162.24
10	4	16mm	3.20	12.80	20.06	3.00	60.19
11	4	16mm	3.10	12.40	19.44	3.00	58.31
12	21	16mm	3.05	64.05	100.40	3.00	301.19
13	10	16mm	2.90	29.00	45.46	3.00	136.37
14	5	16mm	2.65	13.25	20.77	3.00	62.31
15	2	16mm	2.55	5.10	7.99	3.00	23.98
16	2	16mm	2.50	5.00	7.84	3.00	23.51
17	6	16mm	2.40	14.40	22.57	3.00	67.72
18	6	16mm	2.35	14.10	22.10	3.00	66.30
19	12	16mm	2.15	25.80	40.44	3.00	121.32
20	33	16mm	2.05	67.65	106.04	3.00	318.12
21	79	16mm	2.00	158.00	247.66	3.00	742.99
22	49	16mm	1.95	95.55	149.77	3.00	449.32
23	11	16mm	1.80	19.80	31.04	3.00	93.11
24	15	16mm	1.75	26.25	41.15	3.00	123.44
25	2	16mm	1.70	3.40	5.33	3.00	15.99
26	2	16mm	1.65	3.30	5.17	3.00	15.52
27	2	16mm	1.55	3.10	4.86	3.00	14.58
Total				868.30	1361.05		4083.15

Note:
Type = Identification assigned to a group of bars with the same diameter and length.

Mesh Reinforcement

ID	Size 1	Spacing 1	As1	Size 2	Spacing 2	As2	Area	Weight	Unit cost	Total cost
		mm	mm2/m		mm	mm2/m	m 2	kg	Euro/kg	Euro
1			257.00			257.00	2008.50	8052.48	3.00	24157.43
2	10mm	450		10mm	450		2008.50	5465.80	3.00	16397.39
3	10mm	450		10mm	450		2008.50	5465.80	3.00	16397.39
4			257.00			257.00	2008.50	8052.48	3.00	24157.43
Total								27036.55		81109.66

Architectural Beam Reinforcement

Beam label	Quantity	Size	Length/ bar	Length	Weight	Unit cost	Total cost
	bars		m	m	kg	Euro/kg	Euro

Total				0.00	0.00		0.00

Summary

Reference Plane	Floor Area	Floor Volume	Weight	Rate	Rate	Cost
	m2	m3	kg	kg/m2	kg/m3	Euro
Current plane	2008.50	642.72	28397.60	14.14	44.18	85192.81
Total	2008.50	642.72	28397.60	14.14	44.18	85192.81

Unit weight of mild steel = 7800.00 kg/m3

F Loss of prestress force

F.1 Distributed tendon

ADAPT-FELT 3D (Version: Builder 22)
POST-TENSIONING STRESS LOSS & ELONGATION CALCULATIONS

File Name: ModelOFSLAB.adm
Tendon Label, ID: "Tendon 2241", 2241
Project Title: General name
Specific Title: Specific name
Date: 02-14-23 Time: 18:40

Fu = 1860.00 MPa
Es = 195000.00 MPa
System = Unbonded
K = 0.0010 rad/m
Num of Strands = 1.00
L = 39.04 m

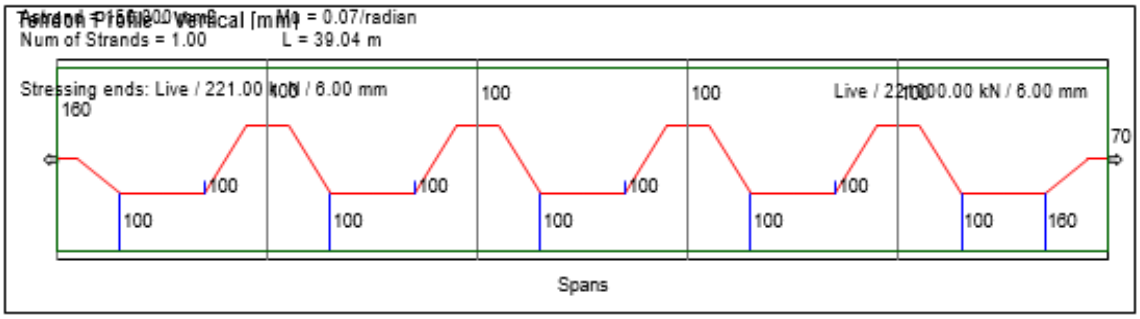

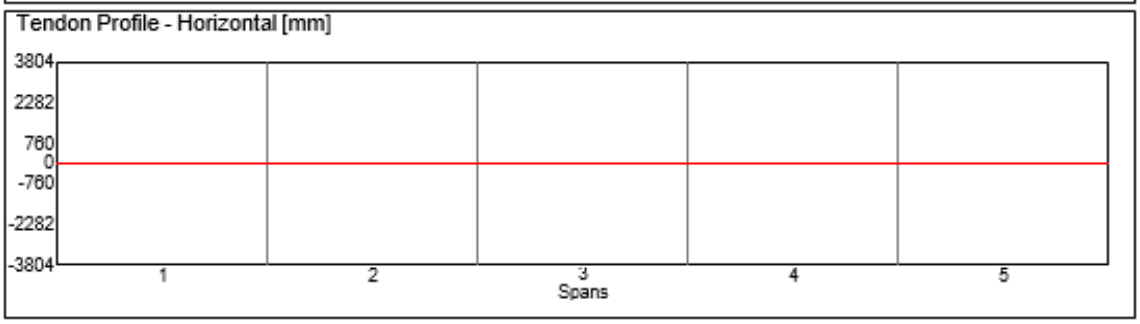

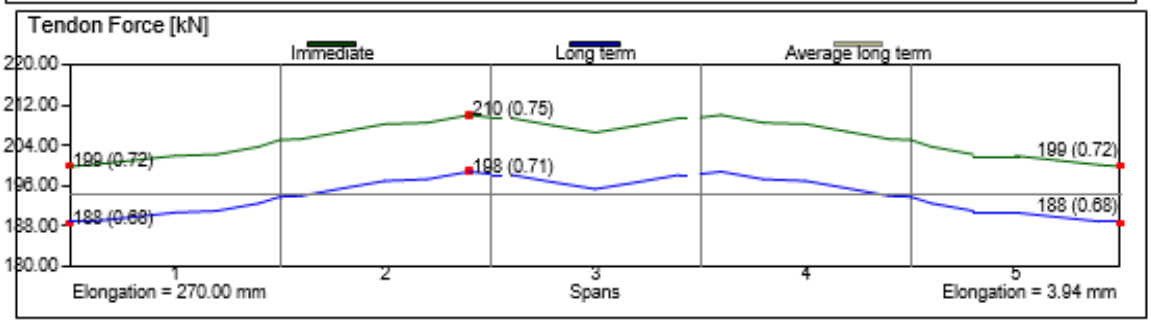

Average values (after release/final)
Force = 205.32 / 194.07 kN
Stress = 1368.81 / 1293.81 MPa

Long-term loses (Lump Sum)
Total Losses = 75.00 MPa

Jacking Force / Stress
Left pull = 221.00 kN / 1473.33 MPa
Right pull = 221.00 kN / 1473.33 MPa

Anchor set influence (corresponding stress/ratio)
Left pull = 15.60 m (1400 MPa / 0.75)
Right pull = 14.05 m (1400 MPa / 0.75)

Elongation (before/after anchor set)
Left pull = 276.00 mm / 270.00 mm
Right pull = 9.94 mm / 3.94 mm
Total after anchor set = 273.94 mm
Total after anchor set/L = 0.01 mm/m

Critical Stress Ratios (at stressing/at anchorage)
Left pull = 0.79 / 0.72
Right pull = 0.79 / 0.72
Maximum along tendon = 0.75
Minimum along tendon = 0.72

ADAPT Structural Concrete Software
adaptsupport@RISA.com | www.RISA.com | +1 (800) 332-RISA

F.2 Concentrated tendon

ADAPT-FELT 3D (Version: Builder 22)
POST-TENSIONING STRESS LOSS & ELONGATION CALCULATIONS

File Name: ModelOFSLAB.adm
Tendon Label, ID: "Tendon 2270", 2270
Project Title: General name
Specific Title: Specific name
Date: 02-14-23 Time: 18:47

Fu = 1860.00 MPa
Es = 195000.00 MPa
Area = 150.00 mm²
Num of Strands = 1.00
System = Unbonded
K = 0.0010 rad/m
Mu = 0.07/radian
L = 51.53 m

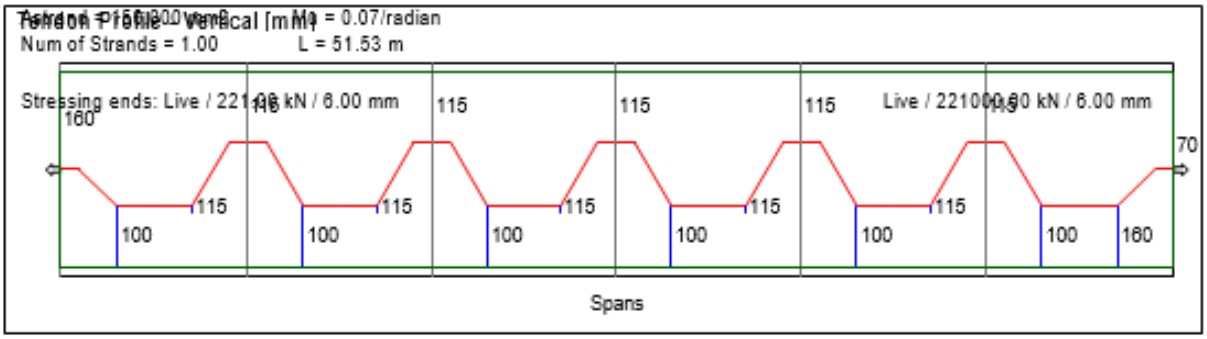

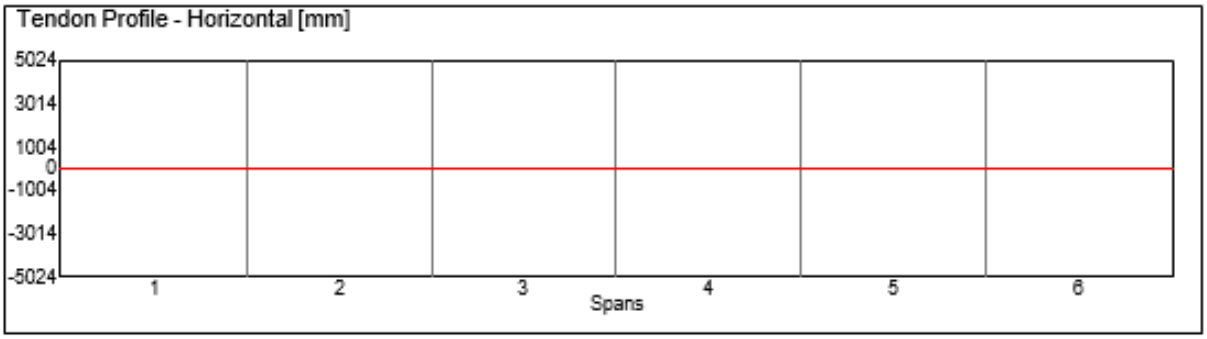

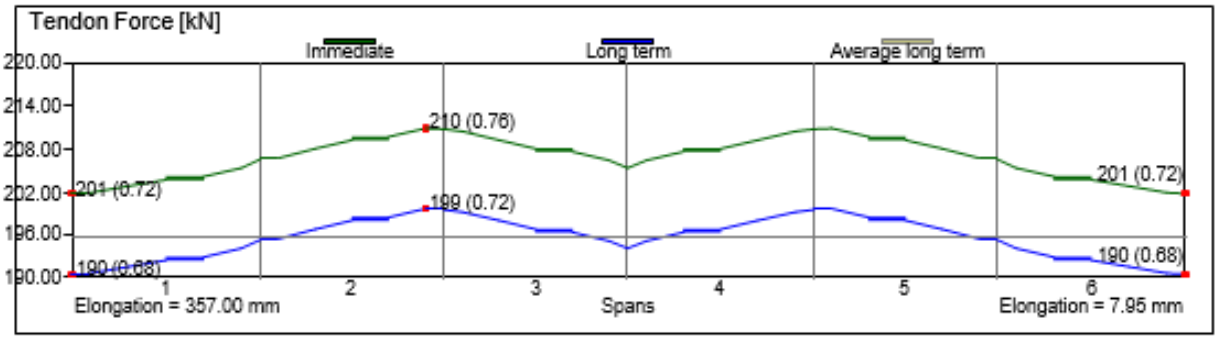

Average values (after release/final)
Force = 206.81 / 195.56 kN
Stress = 1378.73 / 1303.73 MPa

Long-term loses (Lump Sum)
Total Losses = 75.00 MPa

Jacking Force / Stress
Left pull = 221.00 kN / 1473.33 MPa
Right pull = 221.00 kN / 1473.33 MPa

Anchor set influence (corresponding stress/ratio)
Left pull = 17.20 m (1406 MPa / 0.76)
Right pull = 15.46 m (1406 MPa / 0.76)

Elongation (before/after anchor set)
Left pull = 363.00 mm / 357.00 mm
Right pull = 13.95 mm / 7.95 mm
Total after anchor set = 364.95 mm
Total after anchor set/L = 0.01 mm/m

Critical Stress Ratios (at stressing/at anchorage)
Left pull = 0.79 / 0.72
Right pull = 0.79 / 0.72
Maximum along tendon = 0.76
Minimum along tendon = 0.72

Appendix 3: Geometry tables provided by Verkís

G Prefabricated waffle element

Label	Length $[mm]$	Width $[mm]$	Cutout $[mm^2]$
1	5480	2000	-
2	5860	2000	-
3	5480	1680	-
4	5860	1680	-
5	5860	2000	1450x70
6	4410	2000	-
7	4410	1680	-
8	2365	650	-
9	5480	1455	-
10	5480	1680	-
11	5860	2000	550x70
12	5860	2000	3495x545
13	5860	1680	-
14	5860	2000	397x844 R=4135
15	5860	2000	R=4135
16	5860	2000	560x1494 R=4135
17	5860	650	-
18	5860	2000	1450x570
19	4410	2000	-
20	4410	1680	-
21	5860	2000	3090x545
22	5860	1455	-
23	5860	2000	550x570
24	5310	2000	-

H Band beams and columns

Structural beam with post-tensioning reinforcement	Width $[mm]$
Biti B1	1800
Biti B2	1800
Biti B3	1800
Biti B4	1800
Biti B5	1800
Biti B6	1800
Biti B7	1500
Biti B8	1500

Column	Type	Size
B2/3	Circular	R = 310
B7	Circular	R = 310
C2	Circular	R = 320
C3	Circular	R = 320
C4	Circular	R = 320
C5	Circular	R = 320
C6	Circular	R = 320

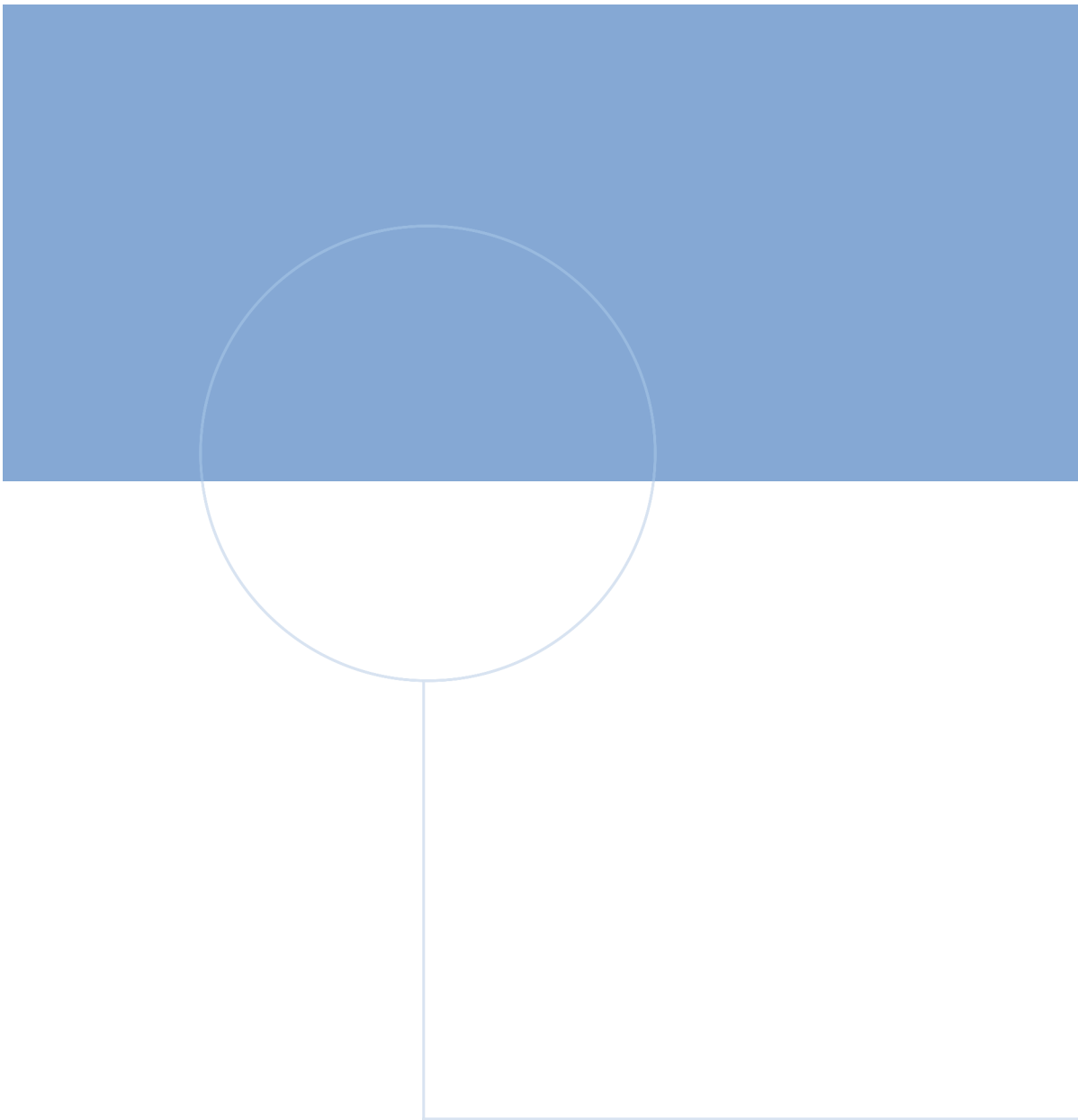

NTNU

Norwegian University of
Science and Technology